DESIGN AND DEVELOPMENT OF A MECHANICALLY ADJUSTABLE LINEAR TORSION SPRING USING CAMS

A THESIS SUBMITTED TO
THE GRADUATE SCHOOL OF NATURAL AND APPLIED SCIENCES
OF
MIDDLE EAST TECHNICAL UNIVERSITY

BY

MEHMET KILIÇ

IN PARTIAL FULFILLMENT OF THE REQUIREMENTS
FOR
THE DEGREE OF MASTER OF SCIENCE
IN
MECHANICAL ENGINEERING

SEPTEMBER 2009

Approval of the thesis:

DESIGN AND DEVELOPMENT OF A MECHANICALLY ADJUSTABLE LINEAR TORSION SPRING USING CAMS

submitted by **MEHMET KILIÇ** in partial fulfillment of the requirements for the degree of **Master of Science in Mechanical Engineering Department, Middle East Technical University** by,

Prof. Dr. Canan Özgen _____
Dean, Graduate School of **Natural and Applied Sciences**

Prof. Dr. Suha Oral _____
Head of Department, **Mechanical Engineering**

Asst. Prof. Dr. Yiğit Yazıcıoğlu _____
Supervisor, **Mechanical Engineering Dept., METU**

Asst. Prof. Dr. Dilek Funda Kurtuluş _____
Co-Supervisor, **Aerospace Engineering Dept., METU**

Examining Committee Members:

Prof. Dr. Eres Söylemez _____
Mechanical Engineering Dept., METU

Asst. Prof. Dr. Yiğit Yazıcıoğlu _____
Mechanical Engineering Dept., METU

Prof. Dr. Sıtkı Kemal İder _____
Mechanical Engineering Dept., METU

Prof. Dr. Reşit Soylu _____
Mechanical Engineering Dept., METU

Asst. Prof. Afşar Saranlı _____
Electrical and Electronics Engineering Dept., METU

Date: _____

I hereby declare that all information in this document has been obtained and presented in accordance with academic rules and ethical conduct. I also declare that, as required by these rules and conduct, I have fully cited and referenced all material and results that are not original to this work.

Name, Last name : Mehmet Kılıç

Signature :

ABSTRACT

DESIGN AND DEVELOPMENT OF A MECHANICALLY ADJUSTABLE LINEAR TORSION SPRING USING CAMS

Kılıç, Mehmet
M. Sc., Department of Mechanical Engineering
Supervisor : Asst. Prof. Dr. Yiğit Yazıcıoğlu
Co-Supervisor: Asst. Prof. Dr. Dilek Funda Kurtuluş

September 2009, 82 pages

Linear springs with variable stiffnesses find some key roles in robotic applications. They are implemented into robotic devices for two main reasons, to increase energy efficiency of walking-running robots and prosthesis, and to get safe human-robot interaction at industrial robots. Being inspired from the human actuation system, a mathematical method to get mechanically adjustable linear springs is noted in the literature; antagonistically working two quadratic springs method. But the proposed solution requires two non-linear springs with quadratic spring characteristics and they are not readily available. Several solutions have been noted in the literature for the acquisition of such non-linear springs. At this thesis work, the solution is realized with a string wrapping around cam mechanism. Two different prototypes were designed and constructed and the second one was physically tested to validate the linear spring behavior. The results displayed good linear spring characteristics with different levels of adjustable spring stiffness. Beside the antagonistically working two quadratic springs method, three novel methods to get mechanically adjustable linear springs are introduced at this thesis. They are based on using hanging weights,

an exponential characteristic spring and a linear translation spring respectively. The real prototypes were not manufactured but sample designs using string wrapping around cam mechanisms are made.

Keywords: Variable Stiffness, Non-Linear Springs, String Wrapping Around Cam Mechanism, Antagonistic Actuation

ÖZ

YAY SABİTİ AYARLANABİLİR LİNEER BURMALI YAYIN KAM ÜZERİNE SARILAN İP MEKANİZMASI İLE TASARIMI VE İMALATI

Kılıç, Mehmet
M. Sc., Makina Mühendisliği Bölümü
Tez Yöneticisi : Asst. Prof. Dr. Yiğit Yazıcıoğlu
Ortak Tez Yöneticisi: Asst. Prof. Dr. Dilek Funda Kurtuluş

Eylül 2009, 82 sayfa

Yay sabiti ayarlanabilir lineer yaylar robotik çalışmalarında önemli kullanım alanları bulmaktadır. Ayarlanabilir yaylar robotlara iki temel amaç için uygulanmaktadır; yürüyen-koşan robotlar ve uzuv protezlerinde enerji verimini artırmak ve endüstriyel robotlarda güvenli insan-robot etkileşimi sağlamak. Bu konuda iskelet-kas sisteminden esinlenen ve düşman olarak çalışan yaylar metodu diye isimlendirilen matematiksel bir metot bulunmaktadır. Fakat bu çözüm, yay karakteristiği parabolik olan iki tane lineer olmayan yay gerektirmektedir ve bu tür yaylar piyasada kolaylıkla bulunamamaktadır. Literatürde bu yaylar için çeşitli çözümler sunulmuştur. Bu tez çalışmasında, problem kam üzerine sarılan ip mekanizması ile çözülmektedir. Bu şekilde çalışan iki değişik ayarlanabilir yay tasarlanmış, imal edilmiş ve elde edilen yaya karakteristiklerinin doğrusallığı fiziksel olarak test edilmiştir. Deney sonuçları imal edilen yayın değişik yay sertliklerinde lineer yay davranışı sergilediğini göstermiştir. Bu tezde, birbirine düşman çalışan yaylar metodunun dışında ayarlanabilir lineer yay elde etmek için üç yeni metot daha sunulmaktadır. Bu üç yeni metot sırasıyla asılı ağırlıklar, üstel karakteristikli yay ve

lineer yay kullanmaya dayanmaktadır. Tez kapsamında, bu üç yeni metot için ilk örnekler imal edilmemiş fakat kam üstüne sarılan ip mekanizması ile örnek tasarımları yapılmıştır.

Anahtar Kelimeler: Değişebilen Yay Sabiti, Lineer Olmayan Yaylar, Kam Üstüne Sarılan İp Mekanizması, Düşman Çalışan Yaylar

ACKNOWLEDGEMENTS

Below I give the history of this thesis work and you will find some acknowledgements in within. But keep in mind that this is a real story!

When I first started to pursue master's education, I was planning to work on Micro Air Vehicles; hand size flying vehicles. Unfortunately, there were not anyone involved in this topic in Mechanical Engineering Department but I still needed to find a supervisor to continue education. Then, Yiğit Yazıcıoğlu took the risk and accepted me as his thesis student although he was neither involved in Aerodynamics nor in Micro Air Vehicles. Of course none of us could know where this relation would lead us at that time but soon after he made me attend the meetings of a research group, the Rhex group or the six leg walking-running robot group. The date was November 2007. Although I attended those meetings for 5 months only, the lectures that I listened at those meetings were the first snowball that eventually leaded me to this thesis report. You wonder what happened to Micro Air Vehicle topic. I save it for the Ph. D. studies.

At one of such Rhex meetings, a student named Ömür Arslan happened to talk about the abstracts of some papers that he thought that it worth to discuss at the meetings. Then the word came to Jonathon Hurst's 2007 paper [6]. Ömür said, "And at this paper, the guy claims that he have designed a mechanically adjustable linear spring for his robot leg". I took out my antennas immediately because it sounded so magical to me; tuning the stiffness mechanically, is it really possible? I asked Ömür how that researcher had realized that. But he had only read the abstract but not the paper so we opened the paper himself and tried to understand the idea from the schematics. Funny, we could not understand it at that time but I would understand its details at the following week and would lecture it at the meeting two weeks later. This was the first time that I had heard of antagonistically working two quadratic springs method.

Thus, I would like to specifically thank to Ömür Arslan that he was the reason how I became aware of this method. Meanwhile, the date was February 2008.

So, I had understood the antagonistically working two quadratic springs method in detail and now knew that the only thing that stands between me and the success was the acquisition of two quadratic springs. This problem stayed on the shelf until I bought and read the book "İstanbul'un Son Nişan Taşları" or in translation "İstanbul's Last Sign Stones" written by Şinasi Acar. At the first chapter, the author was discussing the Ottoman Bows. It was exactly after reading it that I started to quest for the bows. I already knew that there were two kinds of bows; the classic bow and the compound bow, but what was special to the compound bow? In short, I understood that the compound bows were designed to change the force-draw curves of the arrow so that it becomes a concave down curve instead of being an increasing function. Then, the archer withstands a small force when he is just about to aim the target yet the arrow is loaded with a reasonable potential energy. The compound bows were making this possible with their non-circular cams. This gave me the invaluable idea; a string could wrap around a non-circular cam and I came up with the simplest form of string wrapping around cam mechanism. I realized that the cam surface could be specifically designed to get any non-linear characteristics we want. Now everything was clear; I had found a way to obtain parabolic characteristic torsion spring. The date was May 2008. I remember myself telling this idea to my friend Ferhat Sağlam when we were trekking near Kızılcahamam. I had explained him the string wrapping around cam mechanism by drawing it on a flattened molehill. I thank Ferhat that he listened to me with an interest.

Solving the cam profile problem was not easy. I had several fruitless attempts. The interesting thing is after getting a wrong solution; it used to take me one week to realize it. Finally in July 2008, I solved the problem. It was a numerical solution and was based on solving five coupled differential equations together. I used this solution for one year. But in 15 July 2009, I realized that there was also a stepwise analytical solution available. Thanks to God that it was me who noticed that first. Then I threw away the numerical solution.

I manufactured two prototypes for mechanically adjustable linear torsion spring. The first one was finished on 31 December 2008 and the second one was finished in May 2009. I manufactured all the parts by myself with my small lathe and milling machine at home. Right at this point, the greatest thank goes to TÜBİTAK. I pursued all my graduate work with the scholarship that I took from TÜBİTAK. I never started to work at any company and TÜBİTAK's scholarship made me concentrate on the thesis work only and this was what I really wanted. If it were not for that scholarship, I would not able to buy that lathe and milling machine and there would not be this work. By the way, the lathe and the milling machine cost 1200TL in September 2008.

How can I miss the night 26 June 2009? At that night, I had an illumination and found two different ways of getting mechanically adjustable linear spring; the method with an exponential characteristic spring and the method with a linear translation spring. This illumination was so strong that by cooking those ideas more, I also found a stepwise analytical solution to the cam profile problem (this was also referred two paragraphs ago). In short, the appearance of this thesis changed significantly. I can certainly say that these are the best ideas that I have ever had. Then who is acknowledged here? Surely the God.

I would like to thank my best friend Taylan Karaağaçlı. He listened to my ideas in patience when we were on long strolls along Ankara streets. Exchanging ideas with Taylan still have not ended so does the streets of Ankara.

I also would like to thank my supervisor Yiğit Yazıcıoğlu and co-supervisor Dilek Funda Kurtuluş for their valuable revisions on the thesis text.

This work is supported by TÜBİTAK 2210 Yurtiçi Yüksek Lisans Burs Programı.

Dedim: artık bilgiden yana eksiğim yok;
Şu dünyanın sırrına ermişim az çok.
Derken aklım geldi başıma, bir de baktım:
Ömrüm gelip geçmiş, hiç bir şey bildiğim yok.

Ömer Hayyam

TABLE OF CONTENTS

CHAPTER 1

INTRODUCTION

1.1 Applications of mechanically adjustable springs

In real life, mechanically adjustable springs find their main uses in robotic applications. They are embedded into robotic devices for two different purposes; to increase energy efficiency of walking-running robots and prosthesis, and to get safe human-robot interaction at industrial robots. These fields are explained briefly at the following subsections and the necessity of mechanically adjustable springs is expressed.

1.1.1 Walking-running robots

When it is first said “walking-running robots”, the first robots come to the minds are the ASIMO of Honda and QRIO of Sony (Figure 1.1). These robots have demonstrated smooth and versatile motions and have proven themselves with their interesting abilities like dancing, serving food to people at a restaurant and playing violin. Besides their astonishing capabilities, these robots suffer from energy inefficiency. They actuate their limbs with continuously controlled electric motors. When the limb is going to accelerate, the electric motor provides power. When the limb is going to decelerate, the electric motor again provides power to stop the limb. Thus, the electric gear motors continuously consume power. This type of walking strategy is named as active dynamic walking. As an alternative to active dynamic walking, a new design and control paradigm, passive dynamic walking, was proposed [3]. Several passive dynamic walkers have been designed (Figure 1.2).

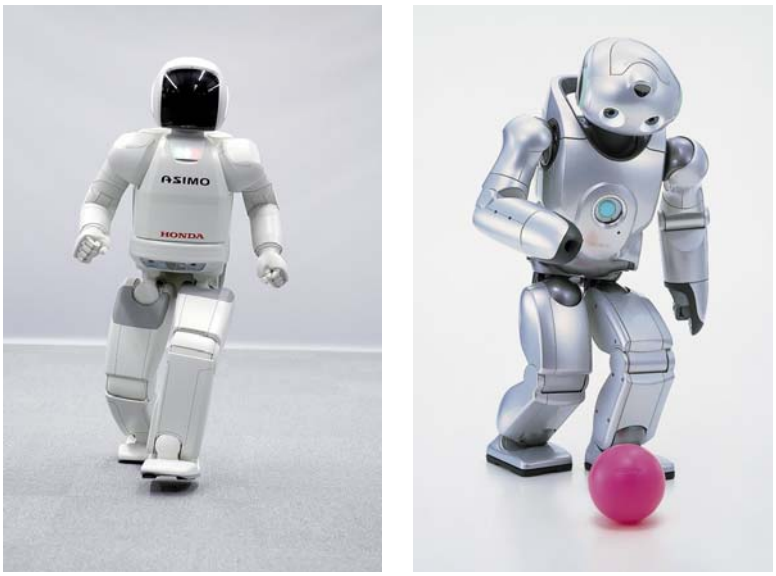

Fig.1.1: ASIMO (Honda) [1] and QRIO (Sony) [2].

These walkers have neither an actuation nor a control on them but able to perform stable walking with the aid of their special dynamics. It should be mentioned here that they still need a slight actuation to overcome the friction at their joints and that is given to the walkers by making them walk down a slight slope. As the passive dynamic walkers are observed (Figure 1.2), they include nothing but some swinging pendulums.

Fig.1.2: The walker of A. Sano [4] and the walker of Garcia [5].

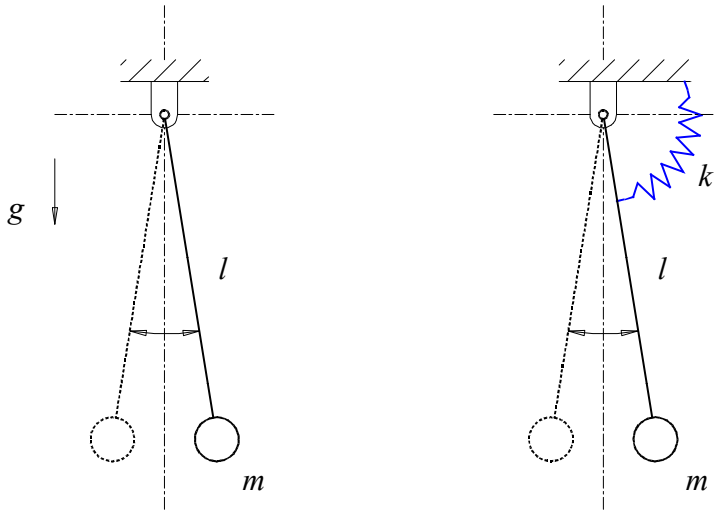

Fig.1.3: Pendulum swinging due to gravity (Left) and due to torsion spring (Right).

A simple swinging pendulum under the effect of gravity swings with the natural frequency given in Equation (1.1) (Figure 1.3 – Left).

$$\omega = \sqrt{\frac{g}{l}} \tag{1.1}$$

A passive dynamic walker is designed for a specific step frequency, strike length and the stiffness of the ground. To change any of these parameters requires changing the natural dynamics of the pendulum links and as Equation (1.1) suggests, this can be realized changing the link lengths only. A robot with changing link lengths is not that logical. On the other hand, the pendulum links of a passive dynamic walker do not necessarily rely on the gravity to swing but can rely on a torsion spring that works on the pendulum (Figure 1.3 – Right). The new pendulum system then has the following natural frequency,

$$\omega = \sqrt{\frac{k}{ml^2}} \tag{1.2}$$

This time not only l but also m and k can be played with. With the same reasoning to l, it is not logical to play with m, then the spring constant k remains as a

valuable control parameter to change the step frequency or the strike length of the passive dynamic walker.

Starting from these principles, several walking running robots have been built (Figure 1.4). The main idea in minds is; the passive dynamic walkers are able to make stable walks even without actuation or control. Then, instead of continuously controlled actuators, using slight control and actuation into the system, like changing the spring constant or setting the touch down angle of the leg before touching the ground, it may be possible for these passive dynamic walkers to make more versatile motions and they still stay energy efficient. The research on the topic still goes on and the passive dynamic walkers as satisfactory as the active dynamic walkers have not been noted yet. But they highlight the necessity of adjustable springs.

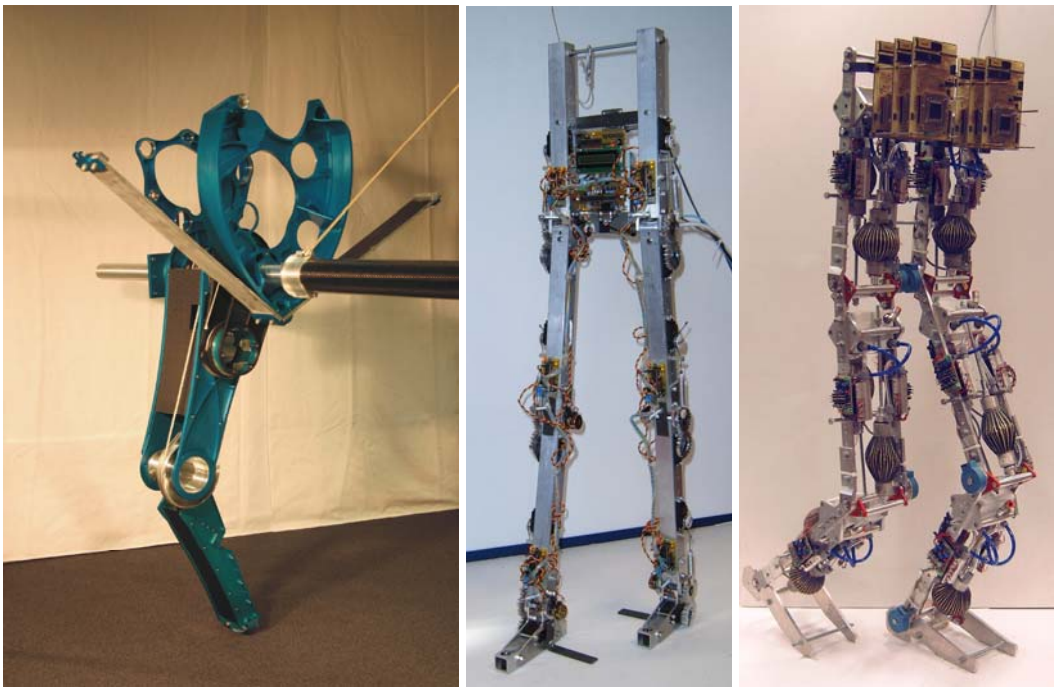

Fig.1.4: BiMASC [6], Veronica [7] and Lucy [8].

1.1.2 Prosthesis and orthesis

Prosthesis and orthesis are another area that the adjustable springs have a use. Nowadays, most prostheses are still passive, that is, they include only an elastic element (Figure 1.5). But the more advanced ones have a spring element and plus an actuator (Figure 1.6). The stiffness of these prostheses is fixed during the design phase and set to an average value, such that the natural frequency of the device is fixed. Thus only for a certain stiffness of the ground and walking speed the user will feel comfortable walk. When the walking conditions change, the user will not only have an uncomfortable walk but also consume more power. To overcome these problems, novel designs are proposed by several researchers (Figure 1.7). Hollander et al. have introduced the Jack Spring Actuator, an actuator with an adjustable spring

Fig.1.5: Constant stiffness foot prosthesis [9].

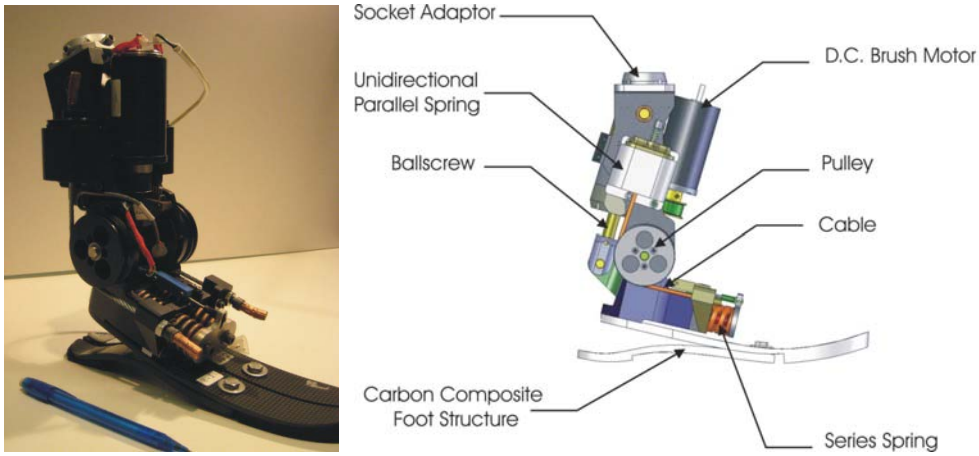

Fig.1.6: Powered ankle-foot prosthesis with an actuator and spring element [10].

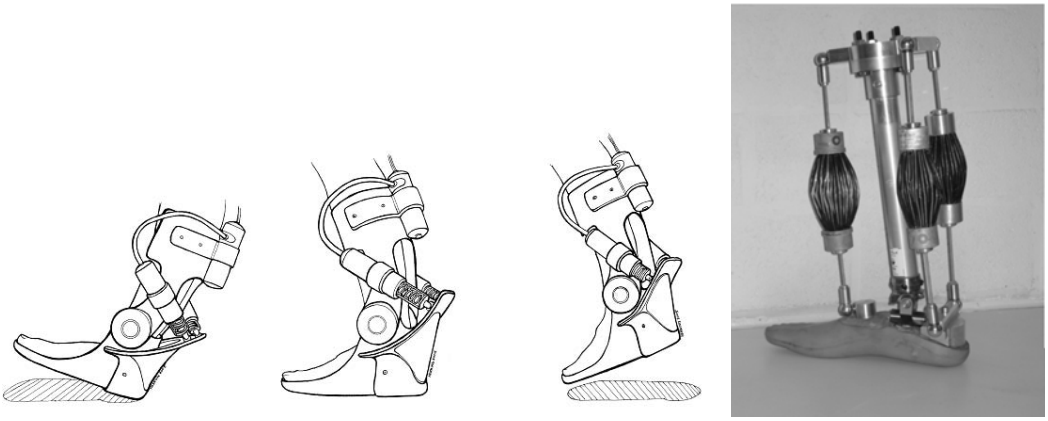

Fig.1.7: The adjustable robotic tendon concept (Left) [11] and Intelligent Prosthesis actuated by pleated Pneumatic Artificial Muscles: IPPAM (Right) [12].

in series with it, to use it in the adjustable robotic tendon concept (Figure 1.7) [11]. They also proved it with simulations that by tuning the adjustable spring at the prosthesis, both the highest power needed during walk and the total energy consumed per step is lowered [11]. Similarly, Versluys et al. develops foot prosthesis actuated with pneumatic artificial muscles (Figure 1.7) [12]. These devices are still under development and are not commercially available yet.

1.1.3 Safe human-robot interaction

An industrial robot is expected to be fast and accurate while working. To fulfill these requirements, these robots are actuated with stiff actuators. But stiff actuators do not comply with impacts and are a threat to humans in working environment so they are placed in human free environments. But, for some applications it is useful to have robots and humans fulfilling tasks together. Machines that interact with humans must be safe against all possible accidents. One solution to the problem is to use actuators with adjustable compliance. A machine that moves fast is typically more dangerous than a slow moving machine. The idea is; the stiffness is adjusted to be high at low speeds, allowing for high positional accuracy, and low at high speeds, resulting in a softer impact. Tonietti et al. have introduced the Variable Stiffness Actuator for robotic manipulators concerning the safe human-robot interaction (Figure 1.8) [13].

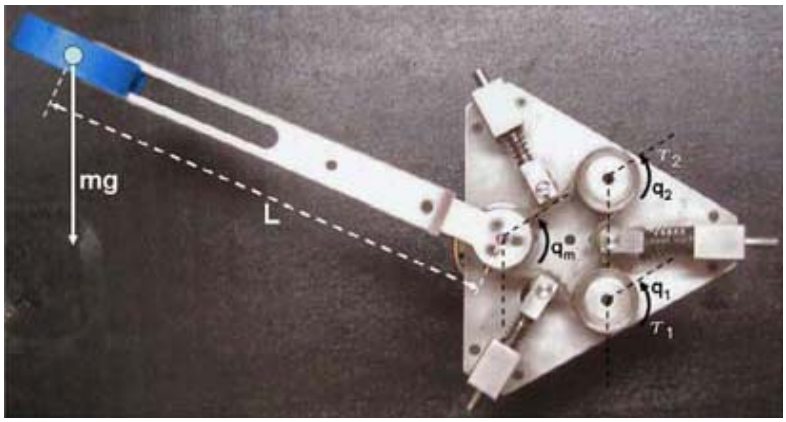

Fig.1.8: A robotic arm prototype actuated with Variable Stiffness Actuator [13]

1.2 Contributions

Three contributions have been made to the subject and explained in this thesis. The discussion begins with the examination of the Mechanically Adjustable Springs appeared in the literature in Chapter 2. The samples seen in the literature are first divided into two; the ones that rely on the antagonistically working two non-linear springs concept and the ones besides these. The antagonistically working two non-linear springs concept is a powerful mathematical tool that guaranties mechanically adjustable springs with perfect linearity. In the literature, it is a well known fact that these non-linear springs must be quadratic springs and this is always shown by inserting a quadratic spring equation into the antagonistic set-up equations and the adjustable linear spring equation is seen in return. But in Chapter2, it was proven mathematically that those non-linear springs must be quadratic springs if this set-up is to give linear behaviors and it is in fact the unique solution to the problem. This is the first contribution to the subject. Quadratic springs are a kind of non-linear springs and they are not easily available. In Chapter 3, the general method to realize any non-linear spring characteristic by using a mechanism is explained. And it was introduced there that the string wrapping around cam mechanism is a possible and powerful candidate for this purpose. At the following subsections, the design of the cam surface is explained in detail. This is the second contribution to the subject. In Chapter 4, four different methods to obtain mechanically adjustable linear springs

have been discussed. The first method is the well known method; the antagonistically working two quadratic springs method. In Chapter 4.1, it was explained how to get quadratic springs by using string wrapping around cam mechanism and how to embed them into an antagonistic set-up to get mechanically adjustable linear torsion springs. A prototype was also manufactured and tested for linearity and spring constant adjustment. In Chapters 4.2, 4.3 and 4.4, three new methods to get adjustable springs have been described. These three methods are as powerful as the antagonistically working two quadratic springs method and they are the third contribution to the subject. The common thing at these four different works is that all of them use cams and gives mechanically adjustable torsion springs in return. Something important should be mentioned here; the antagonistically working two quadratic springs method only gives adjustable linear springs but the remaining three works can also be designed for any kind of adjustable spring characteristics. There is nothing comparable to these works in the literature and the author thinks that this is in fact the most important contribution to the subject among the ones cited above.

CHAPTER 2

MECHANICALLY ADJUSTABLE SPRINGS

In literature, several different mechanically adjustable springs have been designed and constructed. In all applications, the demand is for adjustable linear springs because linear springs are mathematically simple to express and they simplify the equations of motion. Acquiring perfect linear behaviors for all spring constants is not always possible so most works that will be discussed at this chapter are just approximations to linear behavior. Here, the works appeared in the literature are categorized into two groups; the ones that rely on antagonistically working two non-linear springs and the ones beside these. This division is fair because antagonistically working two non-linear springs concept guaranties adjustable springs with perfect linearity whereas the ones that will be discussed under the other methods are just approximations to linear behavior (except the very last one).

2.1 Antagonistically working two non-linear springs method

Interestingly, everything has started observing human actuation system. It is a well known fact that human muscles can only pull but not push. So at least two muscles

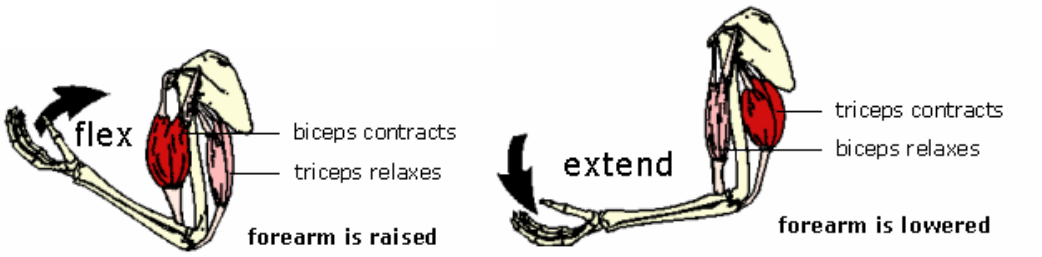

Fig.2.1: Antagonistic setup of biceps and triceps in human arm [14].

are required to actuate a rotational joint and they work antagonistically (Figure 2.1). When the biceps contracts and the triceps relax, the arm is flexed. When the triceps contracts and the biceps relax, the arm extends. However, this set-up achieves something more mystic than that. When both muscles contract, the arm orientation does not change but the stiffness of the elbow joint increases and when both relaxes, the stiffness of the elbow joint decreases. This fact have been experimentally verified

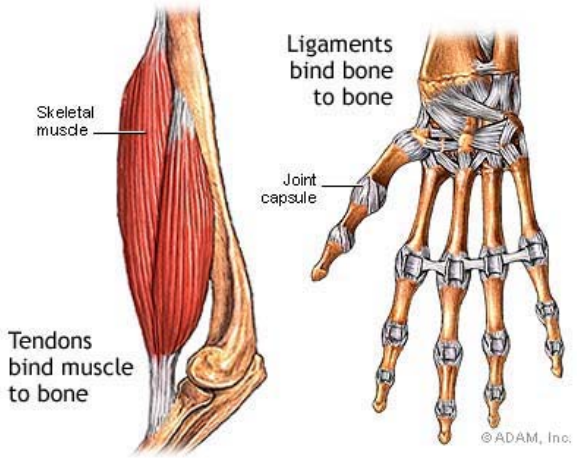

Fig.2.2: Tendons and Ligaments [15].

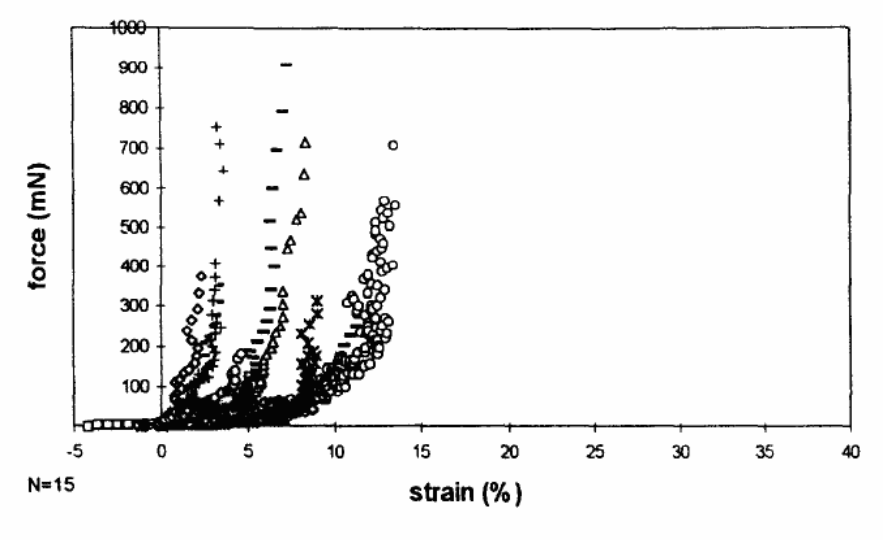

Fig.2.3: The passive stress-strain curves for the tendons [18]. (test results of the tibialis anterior muscle tendon complex of 15 female Holtzman rats).

at numerous publications [16]-[19]. The explanation to the phenomena hides behind the muscle-tendon units (Figure 2.2). The muscles are not attached to the bones directly but via tendons. Besides attaching muscles to bones, tendons serve as excellent elastic energy stores during motions thus behave like springs. But their spring characteristics have a strong non-linear behavior (Figure 2.3) and it is this property that makes them able to change the joint stiffness when either muscles contract or relax [18], [19].

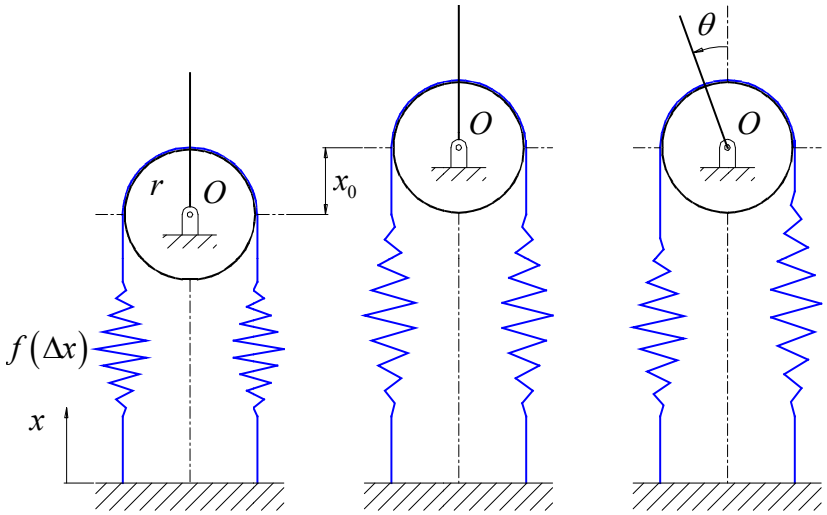

Fig.2.4: Two springs working antagonistically.

Being inspired from the human actuation system and its capabilities, researchers have noticed that in fact with a similar mechanical set-up, it may be possible to obtain adjustable linear springs mathematically and came up with the pulley spring system shown in Figure 2.4. Two identical springs with an arbitrary spring characteristic are attached to a pulley with a string wrapping around it. A handle on the pulley can rotate it with respect to point O. Then a torsion spring behavior is obtained at the handle. At this point, a critical question is asked; with what kind of springs do the torsion spring behavior becomes a linear one and is it possible that the pretension given to the springs can change the stiffness of this torsion spring? The answer is that a quadratic spring satisfies the two requirements together. This can

easily be shown by putting the quadratic spring equation into the calculations and have been made like that at numerous publications. But at this work, the necessary spring function will be found directly and it will be proven that no other springs can satisfy the two requirements together but the quadratic one.

Let $f(\Delta x)$ be the force displacement characteristic of the translational springs and r be the radius of the pulley. Let the pulley be pulled in x direction by an amount of x_0 and rotated in CCW direction by an angle of θ (Figure 2.4). Then the resulting moment acting on the pulley with respect to point O is,

$$M(\theta) = r\left[f(x_0 - r\theta) - f(x_0 + r\theta) \right] \tag{2.1}$$

Let $M(\theta)$ be a linear function of θ and the stiffness of it be a function of x_0. Then,

$$r\left[f(x_0 - r\theta) - f(x_0 + r\theta) \right] = -k(x_0)\theta \tag{2.2}$$

At this point, the possible f functions that will satisfy Equation (2.2) are sought. However Equation (2.2) can not say anything meaningful about the nature of the f function. But, if it were not for the right hand side of the Equation (2.2), it would say something meaningful. Then, to eliminate the right hand side of the equation, take its derivative with respect to θ two times.

$$\rightarrow\ r^2\left[-f'(x_0 - r\theta) - f'(x_0 + r\theta) \right] = -k(x_0)$$

$$\rightarrow\ r^3\left[f''(x_0 - r\theta) - f''(x_0 + r\theta) \right] = 0$$

$$\rightarrow\ f''(x_0 - r\theta) = f''(x_0 + r\theta) \tag{2.3}$$

Now Equation (2.3) tells something meaningful. It includes the second derivative of the f function and states that, f'' function is symmetric with respect to $\Delta x = x_0$ line (Figure 2.5.a). However x_0 is not a fixed value and f'' function must be symmetric with respect to every $\Delta x = x_0$ line regardless of what x_0 is.

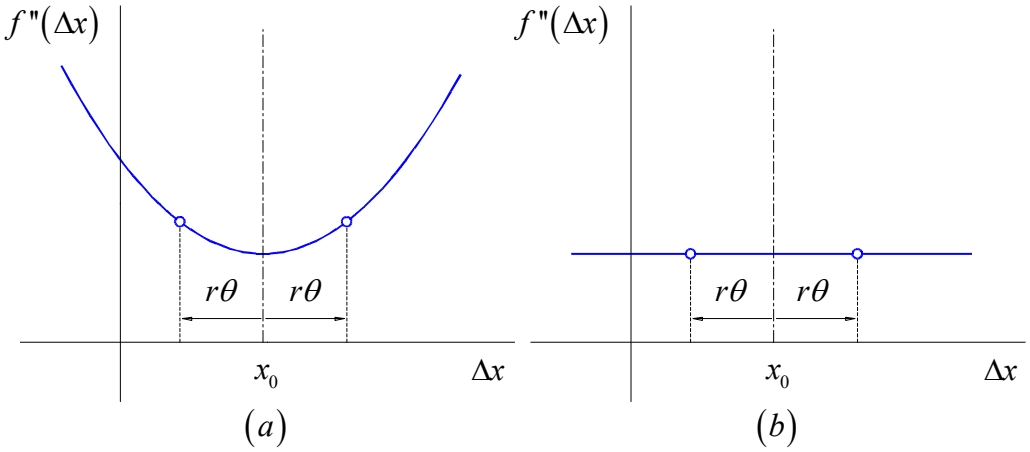

Fig.2.5: Graphical depiction of $f''(\Delta x)$

Then, the only possible f'' function satisfying Equation (2.3) is a constant function (Figure 2.5.b).

Let $f''(\Delta x) = 2A$. Integrating twice,

$$\begin{aligned} &\rightarrow f''(\Delta x) = 2A \\ &\rightarrow f'(\Delta x) = 2A(\Delta x) + B \\ &\rightarrow f(\Delta x) = A(\Delta x)^2 + B(\Delta x) + C \end{aligned} \tag{2.4}$$

Putting Equation (2.4) back into Equation (2.1) and simplifying the result,

$$\begin{aligned} M(\theta) &= r\left[A(x_0 - r\theta)^2 + B(x_0 - r\theta) + C - A(x_0 + r\theta)^2 - B(x_0 + r\theta) - C \right] \\ &= -\underbrace{2r^2\left[2Ax_0 + B\right]}_{k(x_0)}\theta \end{aligned} \tag{2.5}$$

As it is seen $M(\theta)$ turns out to be a linear function of θ and the corresponding stiffness is a function of the pretension x_0. Thus, antagonistically working two quadratic springs set-up is a smart mathematical model that gives adjustable torsion springs with perfect linearity. However this method still suffers from a difficulty because it requires two quadratic translation springs and their commercial

availability is limited. At the below subsections, some mechanically adjustable linear springs appearing in the literature are discussed. All of the following works rely on the antagonistically working two non-linear springs method and they only differ in the way how they obtain a quadratic behavior non-linear spring.

2.1.1 The work of Migliore et. al.

Migliore et al. [20] have described a novel spring mechanism that can be designed to obtain a quadratic spring characteristic and used it at an antagonistically working two quadratic springs set-up. The spring mechanism is based on the motion of rollers rolling on an expanding contour (Figure 2.6). The rollers are attached to each other with some linear helical springs. When a stretching force is applied to the device, the rollers start to get apart and stretch the helical springs (Figure 2.6). That expanding contour can be calculated such that any kind of non-linear spring characteristic can be obtained. After getting a quadratic translation spring by this mechanism, they used it at the antagonistically working two quadratic springs set-up to obtain a mechanically adjustable linear torsion spring (Figure 2.7 – Left). The set-up can adjust the stiffness and the equilibrium position by controlling two position

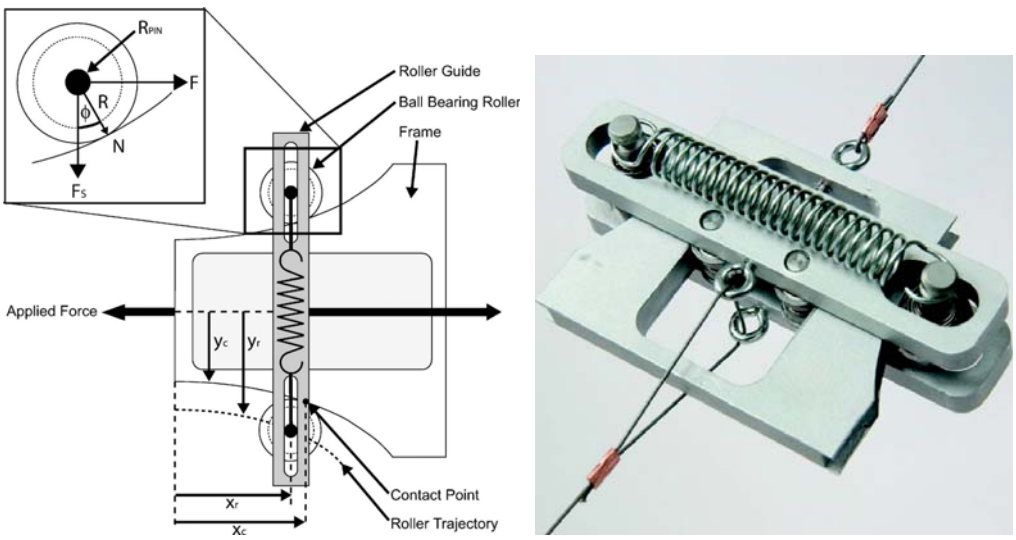

Fig.2.6: The schematic drawing and picture of a quadratic spring device with expanding contour mechanism

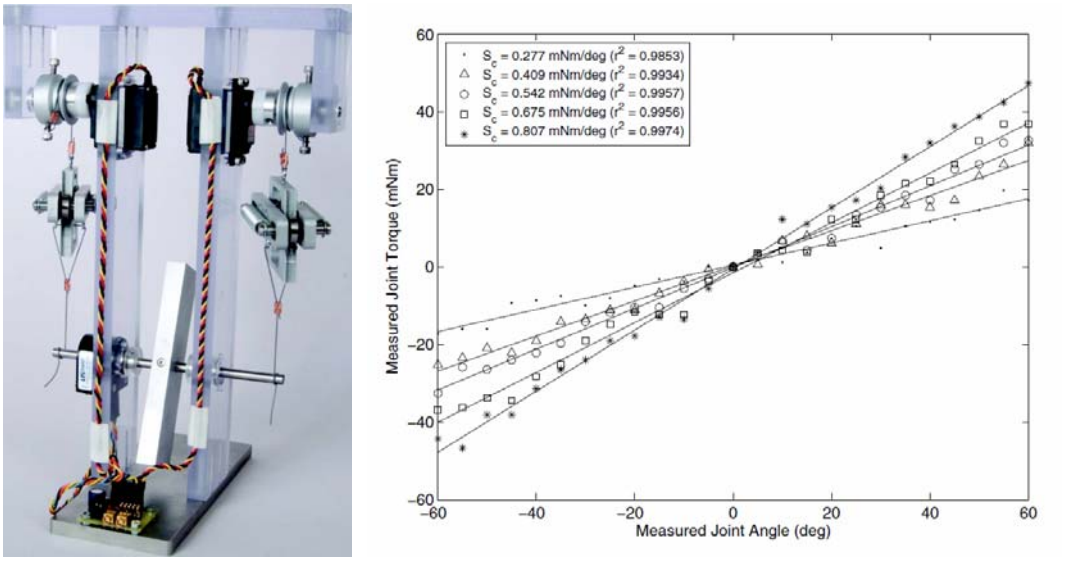

Fig.2.7: The picture of the antagonistically working two quadratic springs set-up using the design given in Figure 2.6 (Left) and the experimental results of the set-up (Right).

controlled servo motors together. The experimental results of the set-up are shown in Figure 2.7 – Right. As it is seen, the experimental data have significant discrepancy from the linear behavior especially at low deflections. It is attributed to the manufacturing errors of the parts and the system friction.

Migliore et al. have also published a second way to obtain non-linear spring characteristics based on a roller rolling on a cam surface [21]. But their work suffers from poor explanations and was not explained here.

2.1.2 The work of Hurst et. al.

Hurst et al. ([22], [23]) designed and manufactured a knee joint called AMASC (Figure 2.9) whose compliance or the spring constant can be adjusted mechanically. Again the stiffness adjustment relies on the antagonistically working two quadratic springs method. Two novel ideas have been embedded in the AMASC and they worth to be mentioned here. First, with a rather complicated mechanism of pulleys and cables, AMASC is able to adjust its stiffness and equilibrium position

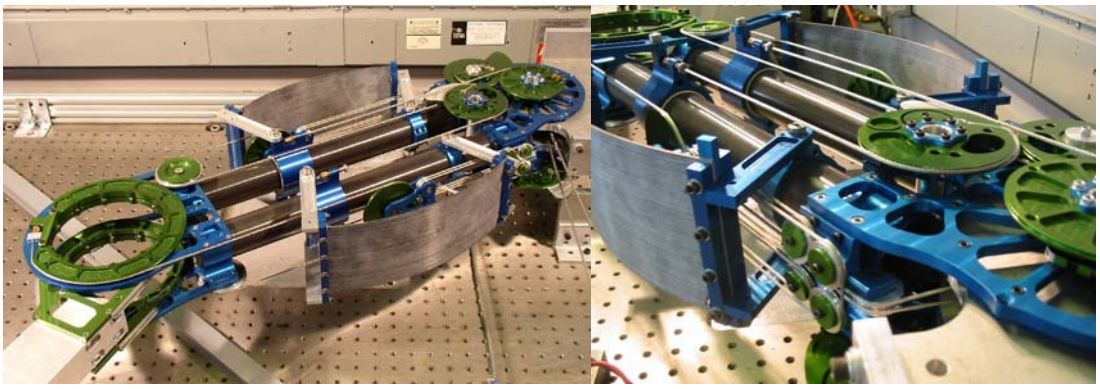

Fig.2.9: AMASC: Actuator with Mechanically Adjustable Series Compliance

independently (Figure 2.10). Their second novel idea is on the acquisition of the quadratic springs. AMASC uses two bending fiberglass plates as energy storage elements (Figure 2.9). These bending plates give a stiffening spring characteristic but not necessarily a quadratic behavior. To convert that stiffening function into a quadratic spring behavior, a spiral pulley mesh is added to the AMASC mechanism (Figure 2.11). The two spiral pulley surfaces can be calculated such that any pulley function, that is, the angular rotation of one pulley as a function of the other's angular rotation, can be calculated. That pulley function must be selected as the one that converts the spring function of the bending plates into a quadratic behavior. This derivation is given in the PhD thesis [23] but less in detail. That thesis guides to [24]

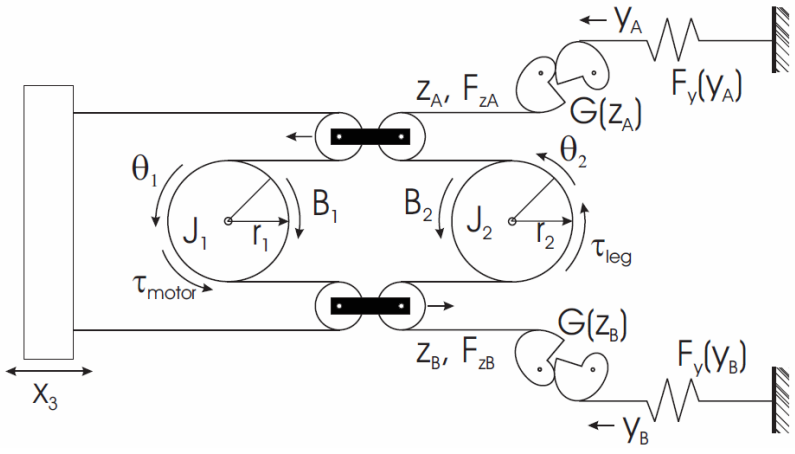

Fig.2.10: The Schematic drawing of AMASC mechanism

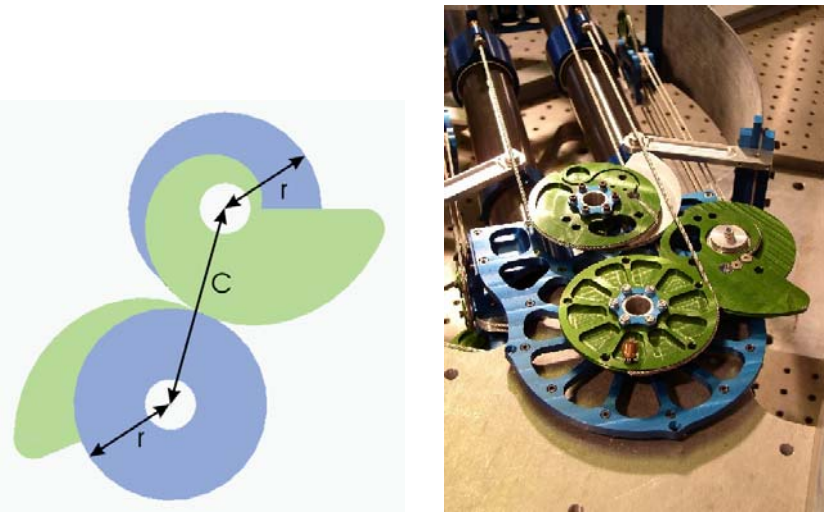

Fig.2.11: The schematic drawing and the picture of the spiral pulleys

for further reference. The best part of these spiral pulleys is that, they just roll on each other without sliding. Therefore, they do not result in extra friction and differ from a spur gear mesh in this sense. It is interesting that Hurst et al. have never made

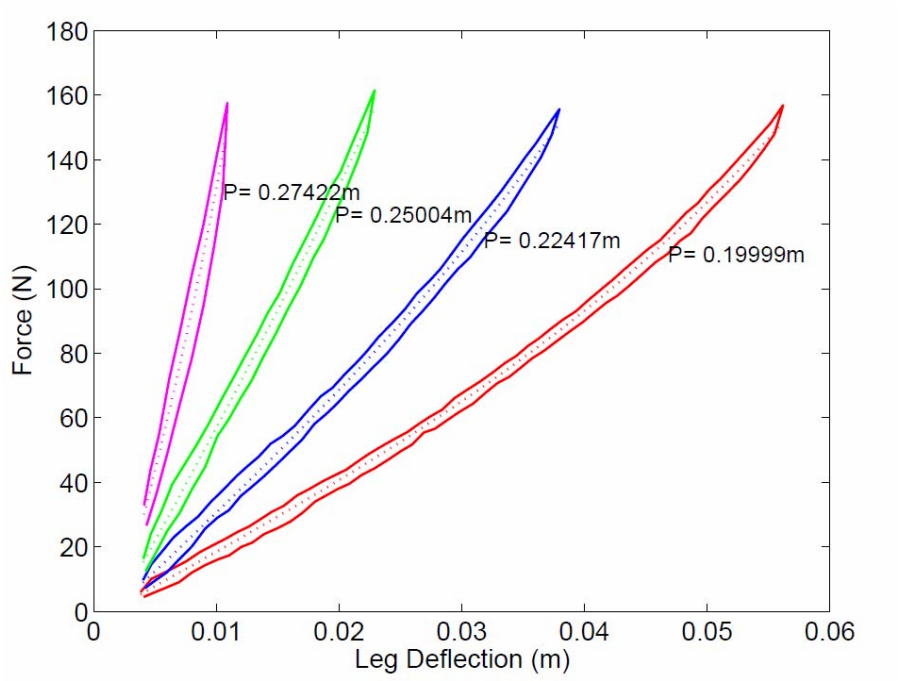

Fig.2.12: Experimental results of AMASC

those calculations although derived them in the PhD thesis. Instead they selected the logarithmic spiral pulleys arbitrarily. So, the spiral pulley mesh bending fiberglass assembly does not give a perfect quadratic behavior but an approximation of it. That is why their experimental results are not able to show perfect linear behaviors (Figure 2.12). Also observe Figure 2.12 that, using many pulleys and cables abundantly returns as significant friction and backlash in the overall performance.

2.1.3 The work of Yamaguchi et. al.

Yamaguchi et al. [25] designed a robot leg whose stiffnesses at its joints are adjustable. They used the antagonistically working two quadratic springs set-up as the stiffness adjustment method in their design (Figure 2.13 – Left). The necessary non-linear springs are obtained with an ingenious combination of two different

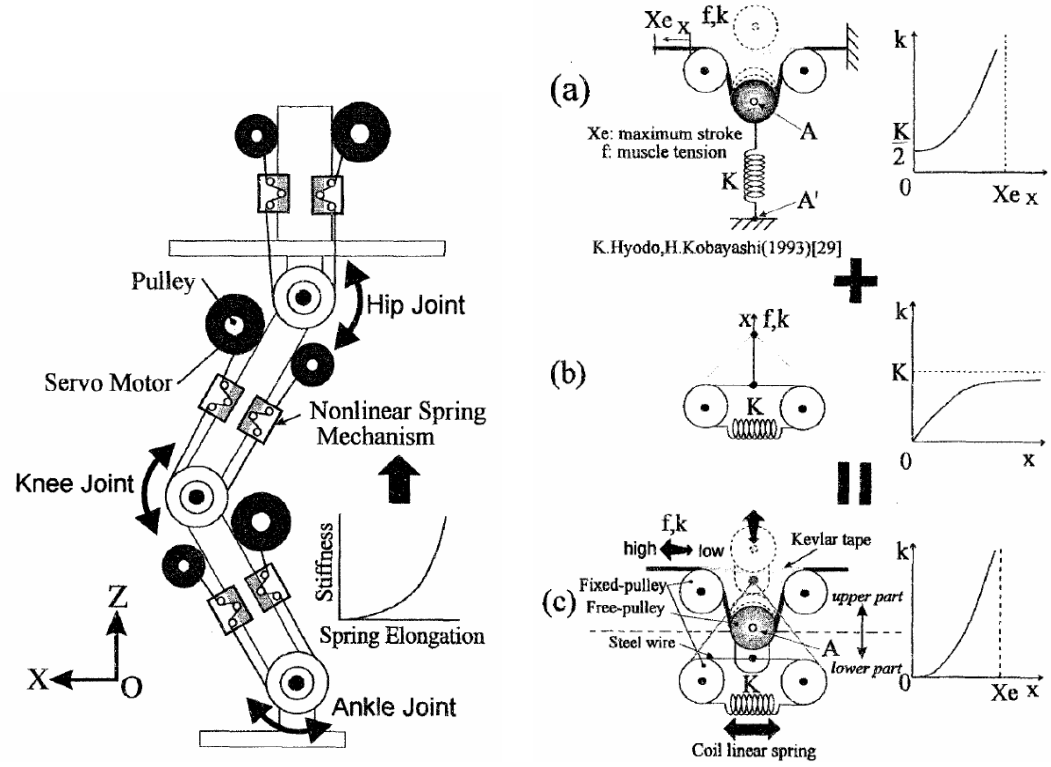

Fig.2.13: Antagonistic driven joint with non-linear spring mechanism (Left). Design of straight type non-linear spring mechanism (Right).

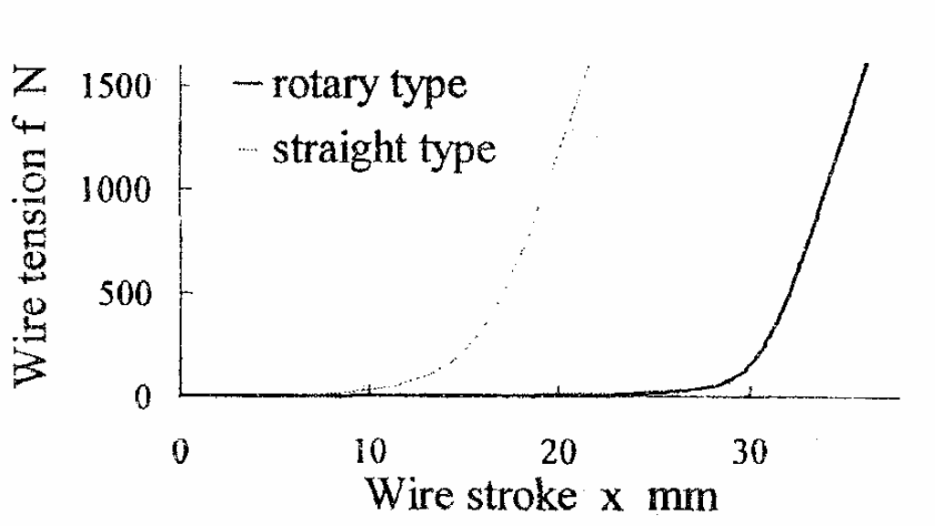

Fig.2.14: Theoretical spring characteristics of the straight type non-linear spring

pulley-cable systems shown in Figure 2.13 – Right. The first pulley-cable system in Figure 2.13.a gives a stiffness between the range $K/2$ and ∞. The second pulley-cable system in Figure 2.13.b gives a stiffness between the range 0 and K. Then the combination of these two mechanisms in Figure 2.13.c also combines these properties and gives a stiffness between the range 0 and ∞. The overall spring characteristic of the final non-linear spring mechanism is shown in Figure 2.14. Observe Figure 2.14 that, the spring characteristic curve is quite dissimilar to a parabola. Then, the antagonistic set-up of these two such springs will not able to give perfect linear behaviors but the springs obtained will still be adjustable. They also designed a rotary type of this non-linear spring but was not mentioned here. The second curve seen in Figure 2.14 is about that mechanism.

2.1.4 The work of Tonietti et. al.

Tonietti et al. [13] have designed and manufactured an adjustable compliant robotic arm called Variable Stiffness Actuator for safe human-robot interaction purposes. Two CAD views of this actuator are shown in Figure 2.15. Three pulleys shown with 1, 2 and 3 in Figure 2.15 are connected to each other with a timing belt and this belt

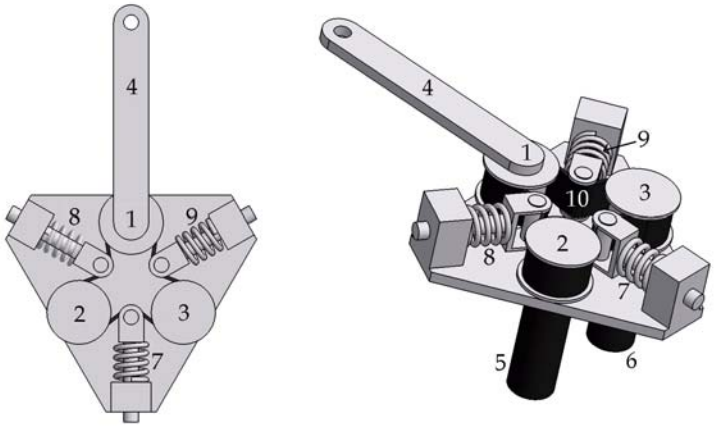

Fig.2.15: Two CAD views of the Variable Stiffness Actuator

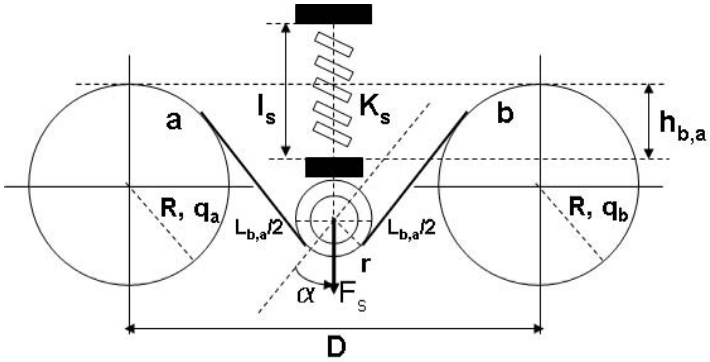

Fig.2.16: The non-linear spring mechanism used in the Variable Stiffness Actuator

is tensioned with three spring systems shown with 7, 8 and 9. Pulley 1 is connected to the robotic arm and the pulleys 2 and 3 are connected to two position controlled servo motors. The two identical pulley-timing belt-spring systems, 1-8-2 and 1-9-3, give a non-linear spring characteristic and actuate pulley 1 antagonistically. When the two servo motors rotate in the same direction, the robotic arm rotates in thatdirection with the same stiffness. Whereas when they rotate in reverse directions, the stiffness of the robotic arm changes. The schematic detail of pulley-timing belt-spring system is shown in Figure 2.16. Notice that this is exactly the same non-linear spring mechanism shown in Figure 2.13.a. So, as for the work of Yamaguchi et al. the Variable Stiffness Actuator is not able to give perfect linear behaviors. However

as the authors argue at the Reference [13], one main achievement of their design is its compactness.

2.1.5 The work of Koganezawa et. al.

Koganezawa et al. [26] have designed and tested a multi-dof forearm prosthesis with adjustable compliance at its joints. They noticed that a conical spring have a stiffening spring characteristic at compression as shown in Figure 2.17 and used it at

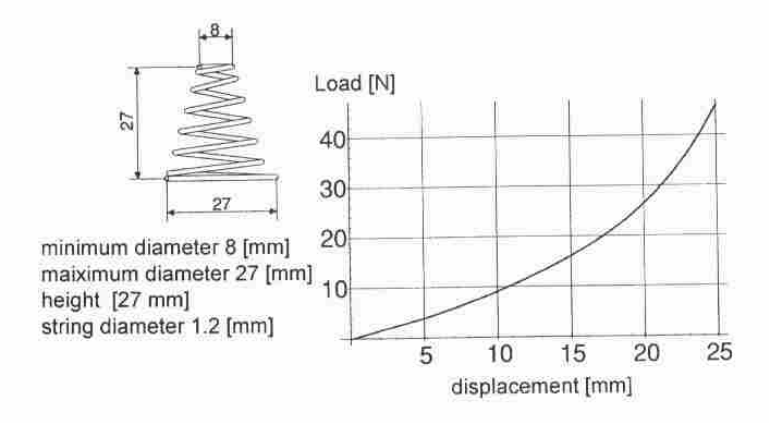

Fig.2.17: Shape and non-linear elasticity of the conical spring

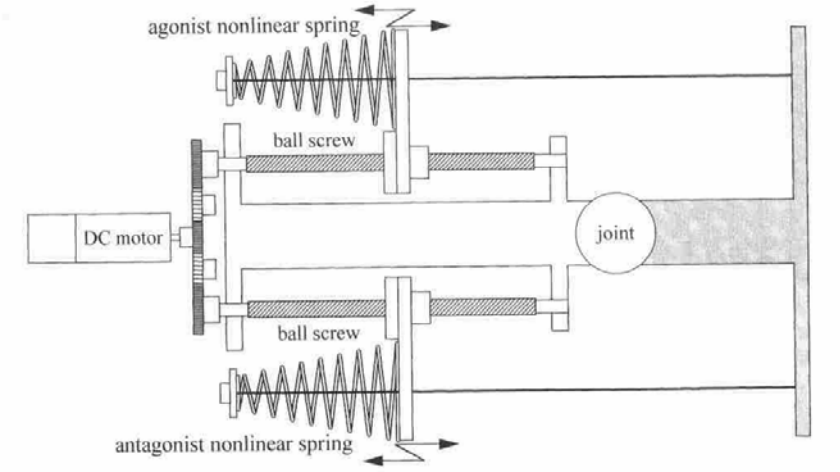

Fig.2.18: Mechanical model of the skeleton-muscular system

an antagonistic set-up shown in Figure 2.18. Note that this antagonistically working non-linear spring set-up is a bit different than the one shown in Figure 2.4; the strings that the springs are attached do not wrap around a pulley but actuates a lever arm instead (Figure 2.18). In summary, the stiffnesses obtained with this set-up are adjustable but does not give perfect linear behaviors.

2.2 The other methods

The works discussed under the previous subsections were all based on the antagonistically working two non-linear springs set-up and required somewhat a complicated mechanical system. Despite this fact, only the works under Sections 2.1.1 and 2.1.2 claimed adjustable springs with perfect linearity but the reaming ones were sill just approximations to linear behavior. To obtain an adjustable spring with a less complicated mechanical system, some different methods were suggested as an alternative to antagonistically working two non-linear springs set-up and they are discussed in the following subsections.

2.2.1 The work of Van Ham et. al.

To use it in a bipedal walking research, Van Ham et al. have introduced the Mechanically Adjustable Compliance and Controllable Equilibrium Position Actuator or simply MACCEPA [27][7]. The schematic drawing of MACCEPA is shown in Figure 2.19. The crank arm AB with length b is able to rotate around point A. Point B of this arm is attached to point C with a linear helical spring. Let the stiffness of this spring be k. A tiny pin at point C guides the string and at the equilibrium position, this spring is pre-tensioned by an amount of p. When the crank arm is rotated by an angle of α, a torsion spring characteristic occurs at the crank arm. After some geometric analysis, the torque on the crank arm is calculated as,

$$T(\alpha) = kbc\sin(\alpha)\left(1 + \frac{p - |c - b|}{\sqrt{b^2 + c^2 - 2bc\cos(\alpha)}}\right) \tag{2.6}$$

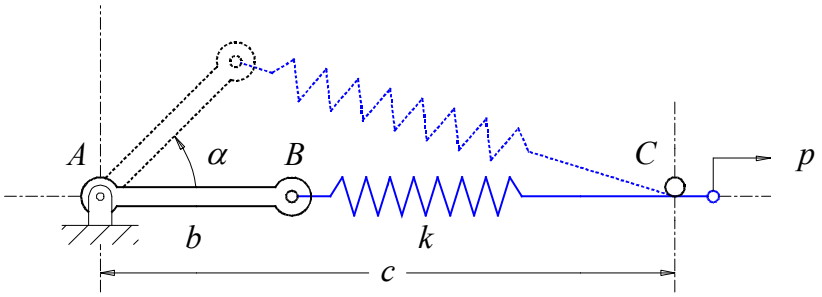

Fig.2.19: The schematic drawing of the MACCEPA

Note that this is quite a complicated equation and it is clear that it will not able to give us prefect linear behaviors. But Van Ham et al. have noticed that this equation in fact gives quite successful linear spring approximations up to $\alpha = \pm 45^0$ and better than that the stiffnesses obtained can be adjusted with changing the pretension p. In Figure 2.19, a numerical simulation is shown. Observe how well the obtained characteristics approximate linear behavior and the stiffnesses change with the initial pretension p. In Figure 2.20, a CAD drawing is given for MACCEPA. The gears seen at the left are for equilibrium position adjustment and at the right a spool is put to adjust the pretension of the spring. So MACCEPA is able to adjust its stiffness and

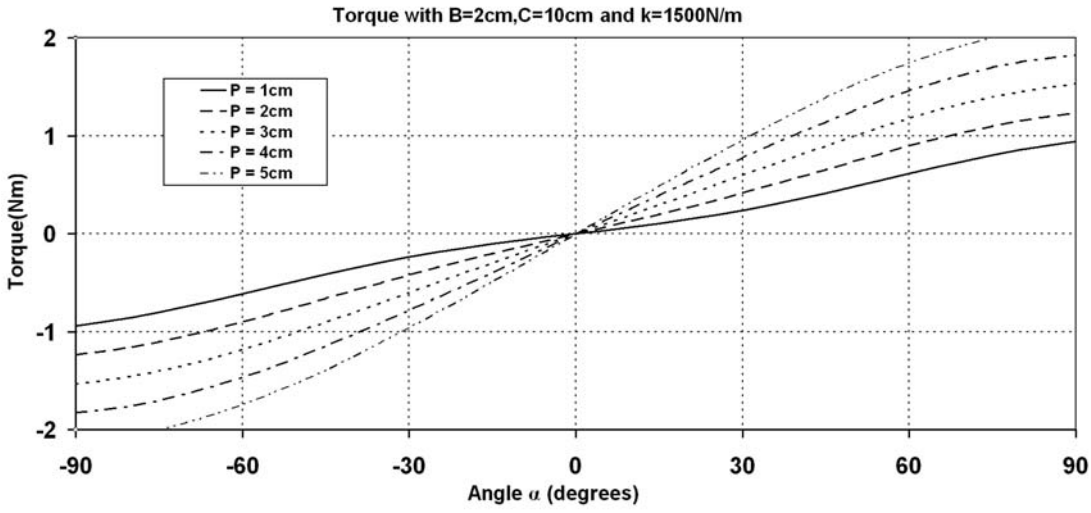

Fig.2.19: Torque as a function of angle α when pretension is altered.

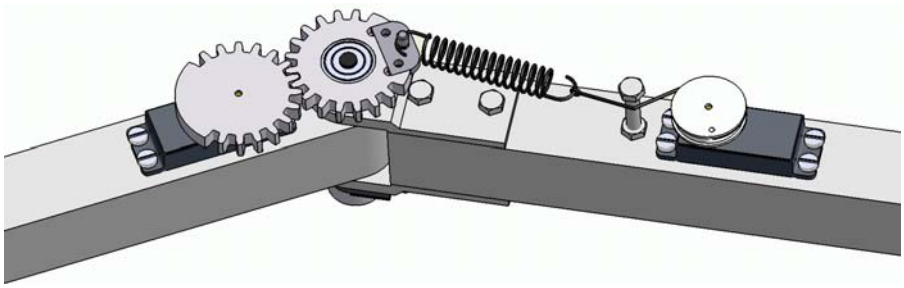

Fig.2.20: CAD drawing of the MACCEPA slimline variant.

equilibrium position independently. MACEPA is distinguished with its simplicity and well enough linear spring approximation. These merits make it one of the best works among the ones cited here.

2.2.2 The work of Morita et. al.

Morita et al. have developed a device called Mechanical Compliance Adjuster to use it at their robotic finger [28]. The spring unit consists of a leaf spring, a slider and a feed screw. The schematic drawing of the Mechanical Compliance Adjuster is shown in Figure 2.21. The leaf spring is bended or deflected with a wire cable then a spring characteristics is obtained at the wire cable. It is observed that the cable pulling direction is in fact parallel to the leaf spring at the equilibrium position. So the leaf spring is not bended as a conventional bending beam. On the other hand, the active leaf spring length is able to be adjusted with the slider position (Figure 2.21). If the active leaf spring length is long, it gives a compliant spring in return and if it is short, it gives a stiff spring. This set-up has experimentally investigated for the spring characteristics acquired (Figure 2.22). Observe successful linear spring approximations up to 40^0 and again see how the stiffness changes with adjusting the slider position. This device is distinguished by one of its aspects; very stiff spring characteristics are possible and even when the slider is at the very left end, it gives in fact a rigid spring. This fact well conforms to the default requirement of a robotic finger; a compliant finger while grasping and a rigid finger when accurate positioning.

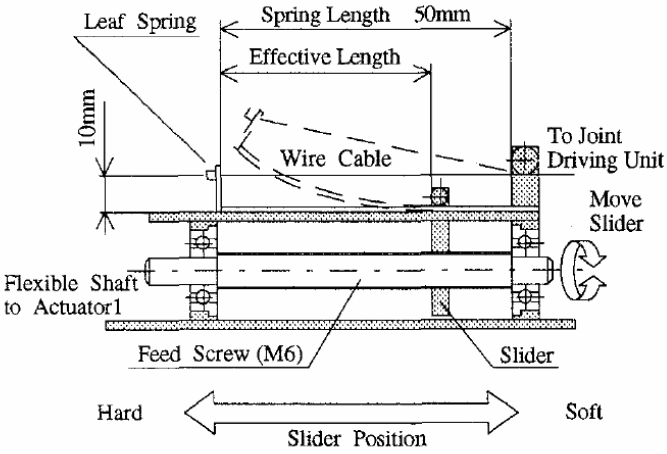

Fig.2.21: The conceptual design of the Mechanical Compliance Adjuster

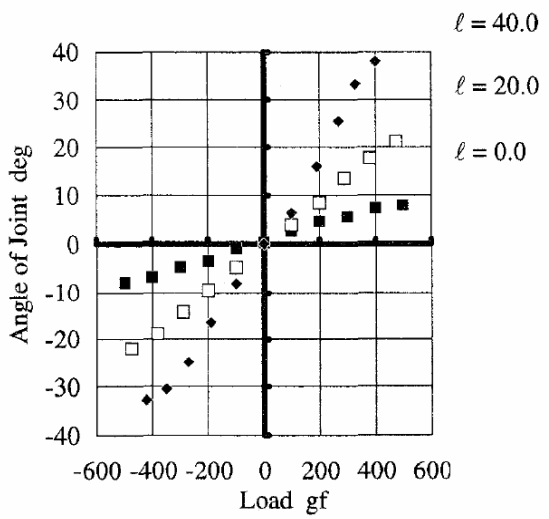

Fig.2.22: Variation of spring constant

2.2.3 The work of Hollander et. al.

The research of Hollander et al. has focused on the mechanics of orthosis, prosthesis and developing new kinds of powered assistance devices for disabled people. They have developed a novel actuator called Jack Spring Actuator to use it at an ankle gait assistance device [11]. The stiffness of a helical spring can be calculated with

Equation (2.7) where D is the coil diameter, d is the wire diameter, n_a is the number of active coils and G is the shear modulus.

$$K = \frac{G \cdot d^4}{8 \cdot D^3 \cdot n_a} \tag{2.7}$$

After this point, the Jack Spring Actuator has a very straight forward idea to change the stiffness; if n_a, the number of the active coils of the helical spring, is controlled, so is the stiffness of the helical spring. The schematic drawing of the Jack Spring Actuator is given in Figure 2.23.

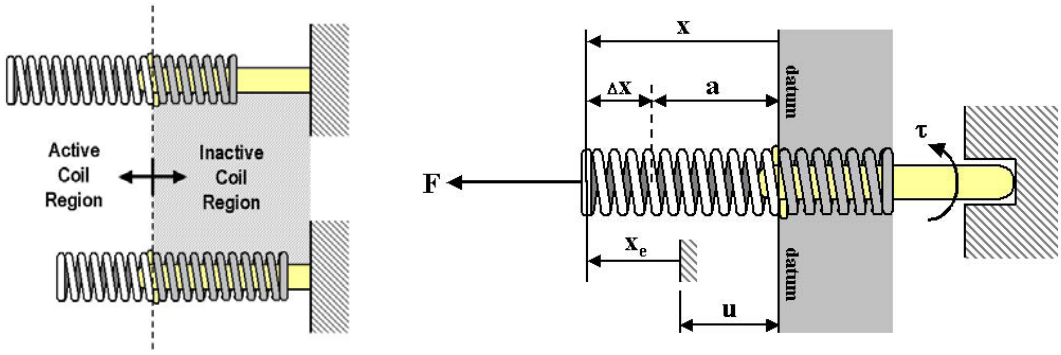

Fig.2.23: The schematic drawing of the Jack Spring Actuator

According to the idea of Hollander et al., the yellow shaft seen in Figure 2.23 works as a lead screw and the helical spring is rotating around it as a nut mesh. Rotating the shaft with respect to the helical spring, new coils are added or subtracted from the active coil region. Hollander et al. have said less about the real design of this mechanism in Reference [11]. However during actuation, some forces will be working on the spring and the mechanism will prone to high friction and deformation. On the other hand, if such problems are overcome, the Jack Spring Actuator offers a compact and easy to implement design.

2.3 Conclusion

In this chapter, the adjustable springs appeared in the literature were first divided into two; the ones that rely on the antagonistically working two non-linear springs and the ones other than these. In Section 2.1, it was first derived that if the antagonistically working two non-linear spring set-up were to give a linear spring characteristic, the non-linear springs must be quadratic springs and this was the only solution. Then, five significant works appeared in the literature that uses this concept were explained. In Section 2.2, three works that do not rely on the antagonistically working two non-linear springs concept but still giving adjustable springs were discussed.

CHAPTER 3

NON-LINEAR TORSION SPRINGS USING CAMS

If you can't explain it simply, you don't understand it well enough.
(Albert Einstein)

3.1 Non-linear springs using mechanisms

Let's say there is a one degree of freedom mechanism and let x be the input variable and y be the output variable (Figure 3.1). Keep in mind that x and y not necessarily be translation variables but can be rotational as well. The mechanism relates these two variables kinematically such that a relation like $y = y(x)$ can be found. These variables are started to be measured from the datum at the initial position, that is, $y = y(0) = 0$. Let's say there is an arbitrary spring with spring characteristic function F. We want to attach this spring to y end of the mechanism.

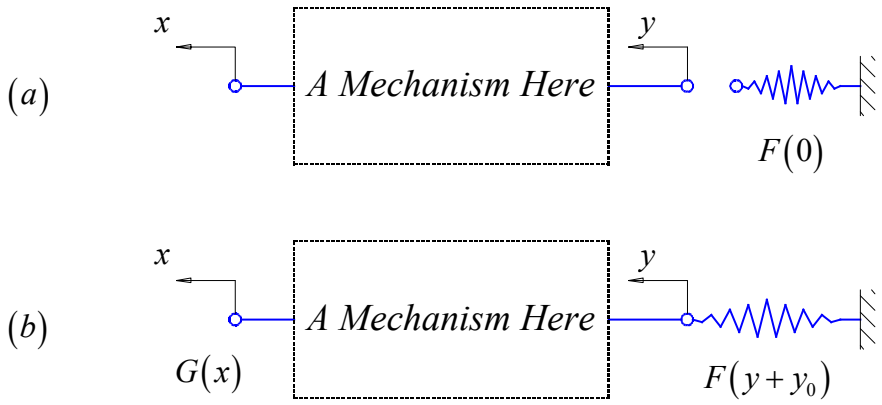

Fig.3.1: A hypothetical mechanism and insertion of a spring to its output end.

With the most general case, this spring is pre-tensioned by an amount of y_0 and is attached to y end (Figure 3.1). Then a spring characteristics function $G(x)$ occurs at the x end of the mechanism. These two springs are in a static equilibrium with the mechanism. Then the virtual works of these two springs must be equal.

$$F(y+y_0)dy = G(x)dx \tag{3.1}$$

Integrating Equation (3.1) by keeping in mind that $y = y(0) = 0$,

$$\int_0^y F(y+y_0)dy = \int_0^x G(x)dx \tag{3.2}$$

Notice that the last equation is nothing but the work expression. It states that the work done by the F function is equal to the work done by the G function.

Three functions appear in Equation (3.2); $F(y)$, $y(x)$ and $G(x)$. If two of these functions are known, the remaining one can be calculated with Equation (3.2). For example, a mechanism and the spring attached to its y end can be given and the spring characteristic occurring at the x end can be asked. That means that, $y(x)$ and $F(y)$ are known and $G(x)$ is going to be calculated. This is a mechanism analysis. Similarly, the two spring characteristics can be given and the required mechanism can be asked. That means that, $F(y)$ and $G(x)$ are known and $y(x)$ is going to be calculated. This is a mechanism synthesis. The second scenario has technical importance, because a mechanism that will transform a given spring characteristic to another required spring characteristic is asked. Thus, by designing a mechanism that makes this transformation, any spring characteristics can be realized in return. But this process is not that straight forward. The critical question here is; are there such mechanisms that can be designed for any $y(x)$ given? Yes there are. Two of them have already appeared in Sections 2.1.1 and 2.1.2. They were reproduced for clarity in Figure 3.2. For the first one, the equation of the rolling surface can be calculate for

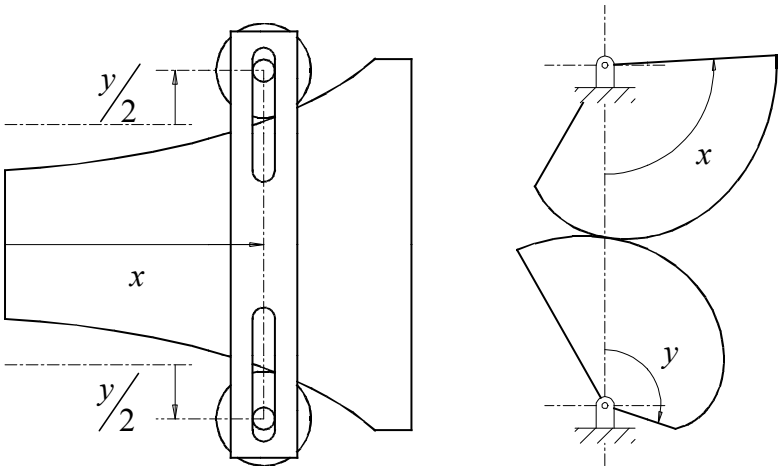

Fig.3.2: The mechanisms appeared in Section 2.1.1 (Left) and Section 2.1.2 (Right).

a given $y(x)$. Note that the path that the center of the rollers follow is directly $y(x)/2$. Then the real paths that the rollers roll on are easily calculated. Similarly for the second one, the spiral pulley surfaces can be calculated for a given $y(x)$. Again an analytic solution to the problem is available and given in the Reference of Section 2.1.2. It will not be reproduced here but the reader should be clarified about a point. Those two spiral pulley surfaces just roll on each other but not slide. The necessary and sufficient condition for pure rolling is that the contact point always lies on the axis passing through the rotation centers. There is also a third mechanism that has this flexibility; the string wrapping around cam mechanism and it is the main topic of the following section.

3.2 String wrapping around cam mechanism

Compound bows use some noncircular pulleys or cams to change the spring characteristic that occurs while drawing an arrow. At a classic bow, this spring characteristic is an increasing function. But at a compound bow, the force on the arrow first increases then takes a maximum value and then decreases. So the archer withstands a lower force at the full draw case, that is, when he is about to aim the target and release the arrow. That is why archers make better shoots with a

compound bow then a classic bow. Although, both the classic bow and compound bow store potential energy in similar structural elements, with a pulley and cam arrangement, the compound bow changes the shape of force draw curve. Being inspired from compound bow cams, the simplest string wrapping around cam mechanism can be constructed as in Figure 3.3.

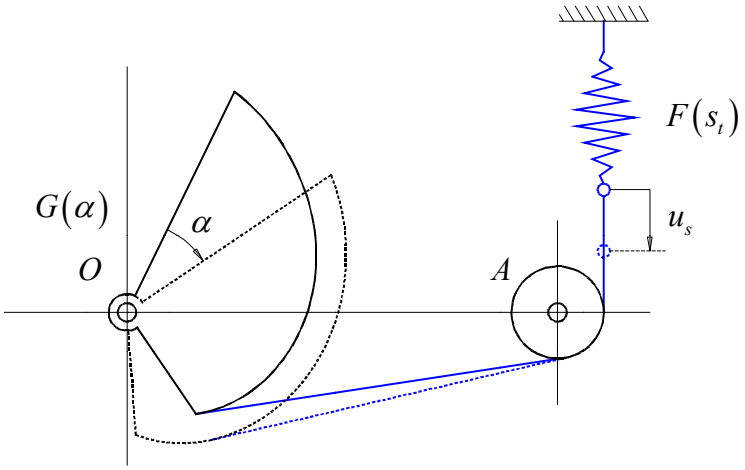

Fig.3.3: String wrapping around cam mechanism.

Take a cam with an arbitrary cam profile turning around point O. While cam makes CW rotation, a string passing around a pulley at A wraps around the cam profile. This mechanism relates the string deflection u_s to the cam rotation α. When a $u_s(\alpha)$ variation is given, the necessary cam profile is hoped to be calculated.

When a translation spring with the spring characteristic $F(\Delta x)$ is attached to the u_s end of the mechanism, a torsion spring characteristic $G(\alpha)$ occurs on the cam. At the initial position, a pretension s_t can be given to the translation spring and attached to u_s end. Then Equations (3.1) and (3.2) reduce to,

$$F(u_s + s_t)du_s = G(\alpha)d\alpha \tag{3.3}$$

or

$$\frac{du_s}{d\alpha} = \frac{G(\alpha)}{F(u_s + s_t)} \tag{3.4}$$

and,

$$\int_0^{u_s} F(u_s + s_t)\, du_s = \int_0^{\alpha} G(\alpha)\, d\alpha \tag{3.5}$$

So, the corresponding $u_s(\alpha)$ variation satisfying the spring characteristics $F(\Delta x)$ and $G(\alpha)$ is found with Equation (3.5). Then the necessary cam profile is calculated as follows.

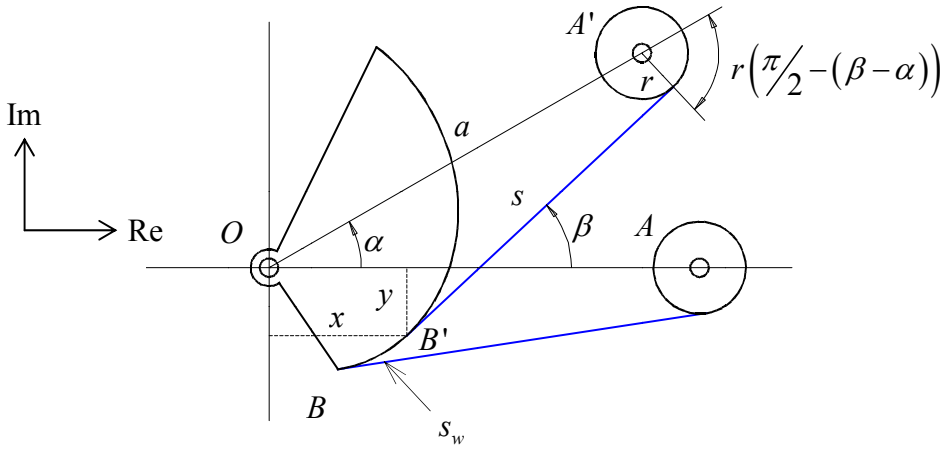

Fig.3.4: The dimensions and the notation.

Let's look at the motion from the cam frame. Instead of different CW cam rotations, now there are CCW rotations of OA (Figure 3.4). Let the tangency point of the string on the cam be B. This point is also the place where the string is attached to the cam. After OA rotates by an angle of α in CCW direction, point A comes to A' and point B comes to B'. During this motion, the string wraps around the cam profile by an amount of s_w. Let the coordinates of the tangency point B' be x and y, the length of the straight part of the string be s, the angle it makes with the horizontal be β, the radius of the pulley be r and the length of OA be a. So for the profile

there are the two unknowns, x and y. The remaining parameters defining the system are s_w, s and β. These total 5 variables are functions of α only and are expected to be calculated for the desired $u_s(\alpha)$ variation.

The length of the string wrapped around the pulley is calculated as $r\left(\pi/2-(\beta-\alpha)\right)$ (observe Figure 3.4). When the cam is rotated by an angle of α, the elongation of the string will be,

$$\rightarrow u_s = s_w + s + r\left(\frac{\pi}{2}-(\beta-\alpha)\right) - s_{w0} - s_0 - r\left(\frac{\pi}{2}-(\beta_0-\alpha_0)\right)$$

$$\rightarrow u_s = s_w + s - r(\beta-\alpha) - s_{w0} - s_0 + r(\beta_0-\alpha_0) \tag{3.6}$$

Due to tangency relation,

$$dx = ds_w \cos(\beta) \tag{3.7}$$

$$dy = ds_w \sin(\beta) \tag{3.8}$$

And the loop closure equation in complex form is,

$$x + iy + (s + ir)e^{i\beta} = ae^{i\alpha} \tag{3.9}$$

There were 5 variables defining the system; x, y, s_w, s and β. And Equations (3.6) to (3.9) are the 5 equations relating these 5 variables to each other (remember that Equation (3.9) includes two relations). But there is a disharmony among these equations; although Equations (3.7) and (3.8) are in the differential form, Equations (3.6) and (3.9) are not. Thus, we take the derivatives of Equations (3.6) and (3.9) respectively,

$$du_s = ds_w + ds - r(d\beta - d\alpha) \tag{3.10}$$

$$dx + idy + (s + ir)e^{i\beta} i\, d\beta + ds\, e^{i\beta} = ae^{i\alpha} i\, d\alpha \tag{3.11}$$

Inserting Equations (3.7) and (3.8) into Equation (3.11) and simplifying the result,

$$\rightarrow ds_w \cos(\beta) + i\, ds_w \sin(\beta) + (s + ir) e^{i\beta} i\, d\beta + ds\, e^{i\beta} = a e^{i\alpha} i\, d\alpha$$

$$\rightarrow ds_w\, e^{i\beta} + (s + ir) e^{i\beta} i\, d\beta + ds\, e^{i\beta} = a e^{i\alpha} i\, d\alpha$$

$$\rightarrow \left(ds_w + ds - r\, d\beta + s\, d\beta\, i\right) e^{i\beta} = a\, d\alpha\, i e^{i\alpha}$$

$$\rightarrow ds_w + ds - r\, d\beta + s\, d\beta\, i = a\, d\alpha\, i e^{i(\alpha-\beta)} \tag{3.12}$$

The real and the imaginary parts of Equation (3.12) give us two identities,

$$ds_w + ds - r d\beta = a \sin(\beta - \alpha) d\alpha \tag{3.13}$$

$$d\beta = \frac{a}{s} \cos(\beta - \alpha) d\alpha \tag{3.14}$$

Using Equations (3.13) and (3.10),

$$du_s = \left(a \sin(\beta - \alpha) + r\right) d\alpha \tag{3.15}$$

Remembering Equation (3.4), β is found as follows,

$$\frac{du_s}{d\alpha} = a \sin(\beta - \alpha) + r = \frac{G(\alpha)}{F(u_s + s_t)} \tag{3.16}$$

or

$$\beta = \sin^{-1}\left(\frac{G(\alpha)}{aF(u_s + s_t)} - \frac{r}{a}\right) + \alpha \tag{3.17}$$

Knowing the analytic solution of β, the analytic solution to s can be found using Equation (3.14). But it requires the derivative of β. The derivative of β can be obtained by taking the derivative of Equation (3.16),

$$a \cos(\beta - \alpha)\left(\frac{d\beta}{d\alpha} - 1\right) = \frac{G'(\alpha) F(u_s + s_t) - G(\alpha) F'(u_s + s_t) \frac{du_s}{d\alpha}}{F(u_s + s_t)^2} \tag{3.18}$$

Inserting Equation (3.16) into Equation (3.18) and simplifying it,

$$\frac{d\beta}{d\alpha}=\frac{G'(\alpha)F(u_s+s_t)^2-G(\alpha)^2F'(u_s+s_t)}{a\cos(\beta-\alpha)F(u_s+s_t)^3}+1 \tag{3.19}$$

Inserting Equation (3.19) into Equation (3.14), the analytic solution to s is found,

$$s=a\cos(\beta-\alpha)\Bigg/\left(\frac{G'(\alpha)F(u_s+s_t)^2-G(\alpha)^2F'(u_s+s_t)}{a\cos(\beta-\alpha)F(u_s+s_t)^3}+1\right) \tag{3.20}$$

Knowing the analytic solutions of β and s, analytic solutions to x and y can now be found by using Equation (3.9),

$$x=a\cos(\alpha)-s\cos(\beta)+r\sin(\beta) \tag{3.21}$$

$$y=a\sin(\alpha)-s\sin(\beta)-r\cos(\beta) \tag{3.22}$$

And if it is needed s_w is found using Equation (3.6),

$$s_w=u_s-\left(s-r(\beta-\alpha)-s_{w0}-s_0+r(\beta_0-\alpha_0)+s_t\right) \tag{3.23}$$

In summary, when a translation spring with spring characteristic $F(\Delta x)$ is given and a torsion spring characteristic $G(\alpha)$ is desired, a string wrapping around cam mechanism can be designed to realize it. A stepwise analytical solution is available to the problem and it is the unique solution. And the corresponding cam profile is obtained by calculating the below equations in the given order.

$$\int_0^{u_s}F(u_s+s_t)\,du_s=\int_0^{\alpha}G(\alpha)\,d\alpha \tag{3.24}$$

$$\beta=\sin^{-1}\left(\frac{G(\alpha)}{aF(u_s+s_t)}-\frac{r}{a}\right)+\alpha \tag{3.25}$$

$$s = a\cos(\beta-\alpha)\Bigg/\left(\frac{G'(\alpha)F(u_s+s_t)^2 - G(\alpha)^2F'(u_s+s_t)}{a\cos(\beta-\alpha)F(u_s+s_t)^3}+1\right) \tag{3.26}$$

$$x = a\cos(\alpha) - s\cos(\beta) + r\sin(\beta) \tag{3.27}$$

$$y = a\sin(\alpha) - s\sin(\beta) - r\cos(\beta) \tag{3.28}$$

$$s_w = u_s - \left(s - r(\beta-\alpha) - s_{w0} - s_0 + r(\beta_0-\alpha_0) + s_t\right) \tag{3.29}$$

Note here that there is less flexibility at the cam design. When the F and G functions are given, the only inherent design flexibility is the initial pretension s_t. However, the coefficients of G function may not be very certain but its behavior may be important. As it will be seen at some examples later, the coefficients of G function are going to offer several valuable design freedoms.

When the equations to calculate the cam profile are observed, it is seen that the first derivative of F and G functions appear at the formulas. So one of the necessary requirements to continue calculation is that F and G functions must be differentiable.

When the calculations are made, sometimes cusps are seen at the cam profiles. Cusps must be avoided by playing the design freedoms.

3.3 State of art examples

Two sate of art examples are given at this subsection. The first one is a cubic spring and the second one is a constant moment spring (Figures 3.5 and 3.6).

Both of these spring characteristics are desired to be obtained from a linear helical spring. Then, with the most general case, a string wrapping around cam mechanism will be designed for $G(\alpha) = A\alpha^3 + B\alpha^2 + C\alpha + D$ and $F(\Delta x) = K\Delta x$. Note here that the given G function can handle both the cubic spring and the constant moment spring together; when A, B and C are taken zero, it expresses the constant moment spring. As it was explained in Section 3.2, the necessary cam profile is calculated

making the calculations given in Equations (3.24) to (3.29) in this order. After selecting a suitable pretension, s_t, the integral in Equation (3.24) is taken as follows.

$$\rightarrow \int_0^{u_s} K\left(u_s + s_t\right) du_s = \int_0^{\alpha} \left(A\alpha^3 + B\alpha^2 + C\alpha + D\right) d\alpha$$

$$\rightarrow \frac{K}{2}\left(u_s + s_t\right)^2 \Big|_0^{u_s} = \frac{A}{4}\alpha^4 + \frac{B}{3}\alpha^3 + \frac{C}{2}\alpha^2 + D\alpha \Big|_0^{\alpha}$$

$$\rightarrow \frac{K}{2}\left(\left(u_s + s_t\right)^2 - s_t^2\right) = \frac{A}{4}\alpha^4 + \frac{B}{3}\alpha^3 + \frac{C}{2}\alpha^2 + D\alpha$$

$$\rightarrow u_s = \sqrt{\frac{2}{K}\left(\frac{A}{4}\alpha^4 + \frac{B}{3}\alpha^3 + \frac{C}{2}\alpha^2 + D\alpha\right) + s_t^2} - s_t \qquad (3.30)$$

Together with Equation (3.30), the remaining equations are calculated for a given α range and the corresponding cam profile is obtained.

At the first example, the cam profile transforms a linear translation spring into a cubic torsion spring (Figure 3.5). Observe that G function first increases then decreases and then increases again. Having such a spring behavior is not easy to get with some other ways.

At the second example, the cam profile transforms a linear translation spring into a constant moment spring (Figure 3.6). It is observed that the cam profile follows a shrinking spiral and compensates for the increasing $F\left(\Delta x\right)$ to hold the resulting moment constant. To obtain a constant moment spring, one of the default solutions is hanging a known weight on a pulley with a string. The solution made here is a smarter solution that can be used instead. The main advantage of this solution is that it does not harness gravity but a linear translation spring. So it also works at zero gravity environments.

The interesting point here is that the two examples use the same linear translation spring but the torsion springs obtained in return have no apparent relation. So, distinct spring characteristics are easily obtained just by changing the cam.

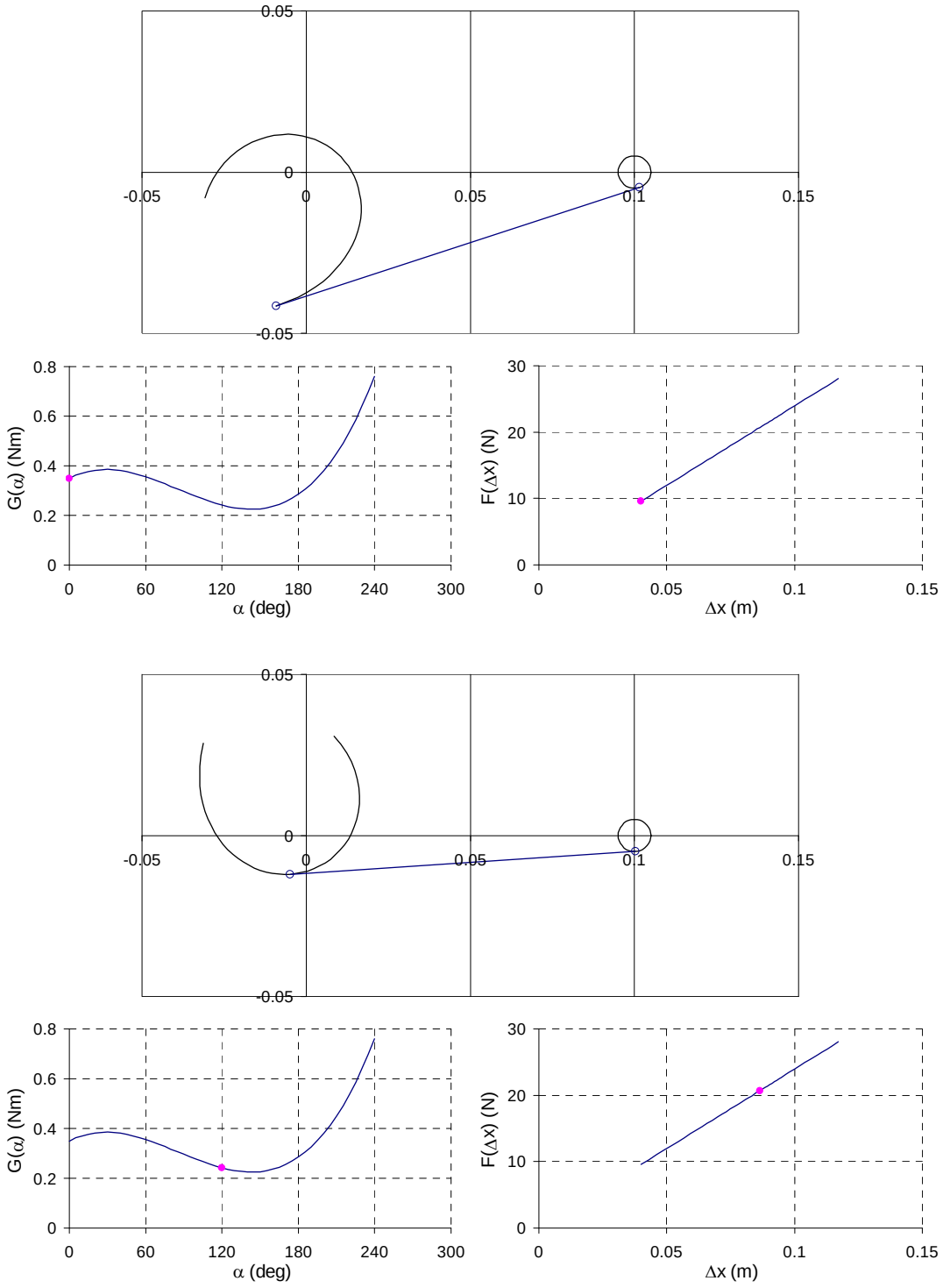

Fig.3.5: State of art calculation for $G(\alpha) = 0.04\alpha^3 - 0.18\alpha^2 + 0.15\alpha + 0.35$, $F(\Delta x) = 239.5\Delta x$ *and* $s_t = 0.04\ m$. *The dimensions are* $a = 0.1\ m$ *and* $r = 0.005\ m$. *The calculations are made for the range* $0 \le \alpha \le 240^0$. *The cam is given at two configurations; when* $\alpha = 0^0$ *and* $\alpha = 120^0$. *The below graphs under each configuration show the corresponding operation points of* F *and* G *functions.*

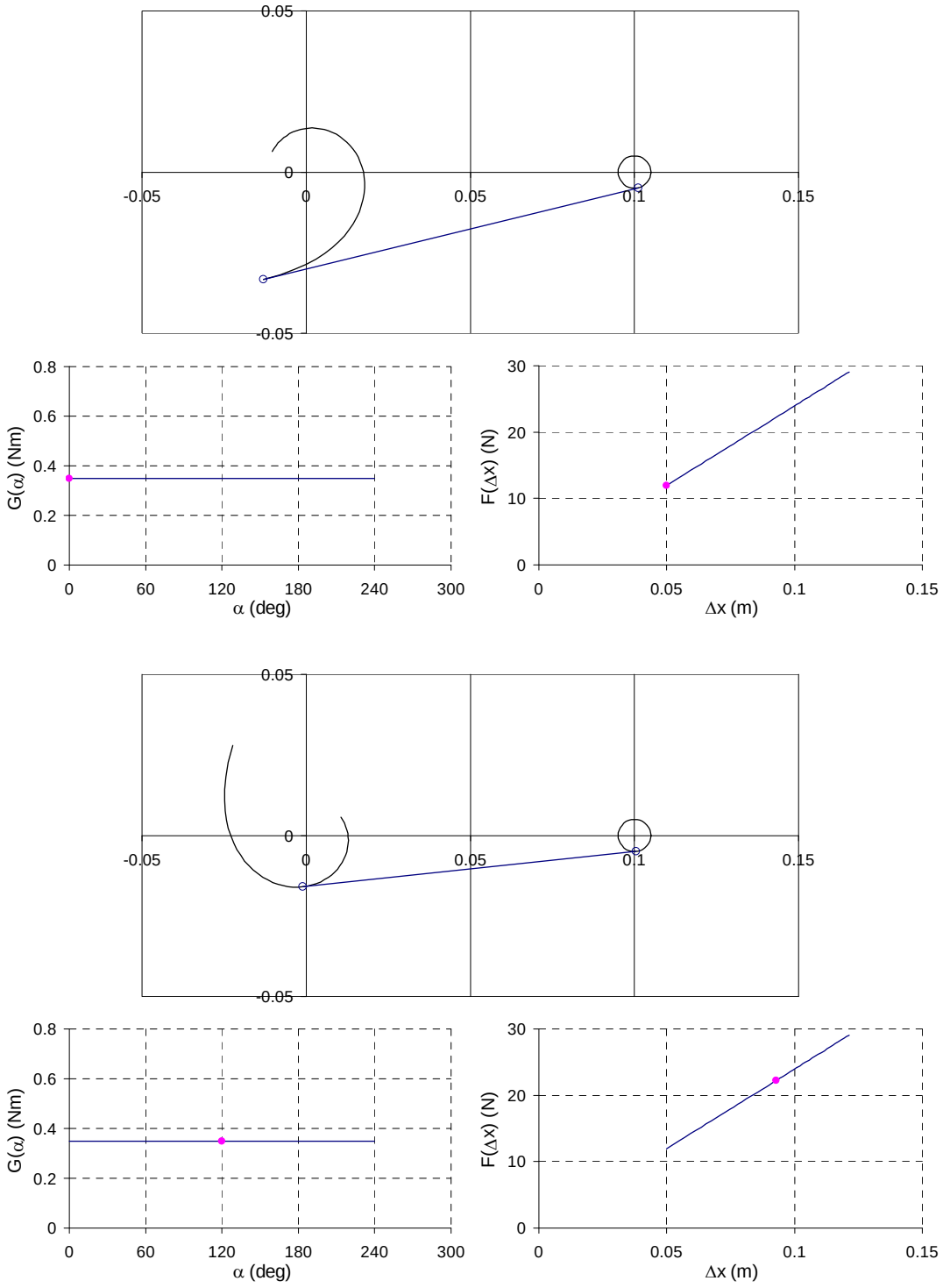

Fig.3.6: State of art calculation for $G(\alpha) = 0.35$, $F(\Delta x) = 239.5\Delta x$ *and* $s_t = 0.05\ m$. *The dimensions are* $a = 0.1\ m$ *and* $r = 0.005\ m$. *The calculations are made for the range* $0 \le \alpha \le 240^0$. *The cam is given at two configurations; when* $\alpha = 0^0$ *and* $\alpha = 120^0$. *The below graphs under each configuration show the corresponding operation points of* F *and* G *functions.*

CHAPTER 4

MECHANICALLY ADJUSTABLE LINEAR TORSION SPRING USING CAMS

Simplicity is the ultimate sophistication.
(Leonardo DaVinci)

In this Chapter, four different methods of obtaining mechanically adjustable linear torsion spring are discussed; with antagonistically working two quadratic springs set-up, with hanging weights, with an exponential characteristic spring and with a linear translation spring. All of them are based on string wrapping around cam mechanism.

4.1 With antagonistically working two quadratic springs set-up

4.1.1 Insertion of cams into antagonistically working two quadratic springs set-up

The antagonistically working non-linear springs set-up used in Chapter 2.1 is given in Figure 4.1.a and 4.1.b again. The pulley was translated by an amount of x_0 in x direction and it was derived in Chapter 2.1 that if $f(\Delta x)$ was a quadratic spring, the corresponding torsion spring behavior occurring at the pulley would become a linear one and its stiffness would be a function of x_0. So translating the pulley is the main motion that enables us to adjust the stiffness. In fact, when the pulley is translated, the two identical quadratic springs are stretched with the same amount of pretension and the equilibrium position of the pulley does not change. There can be several ways to give the same effect to the two springs, but here we will focus on the pulley.

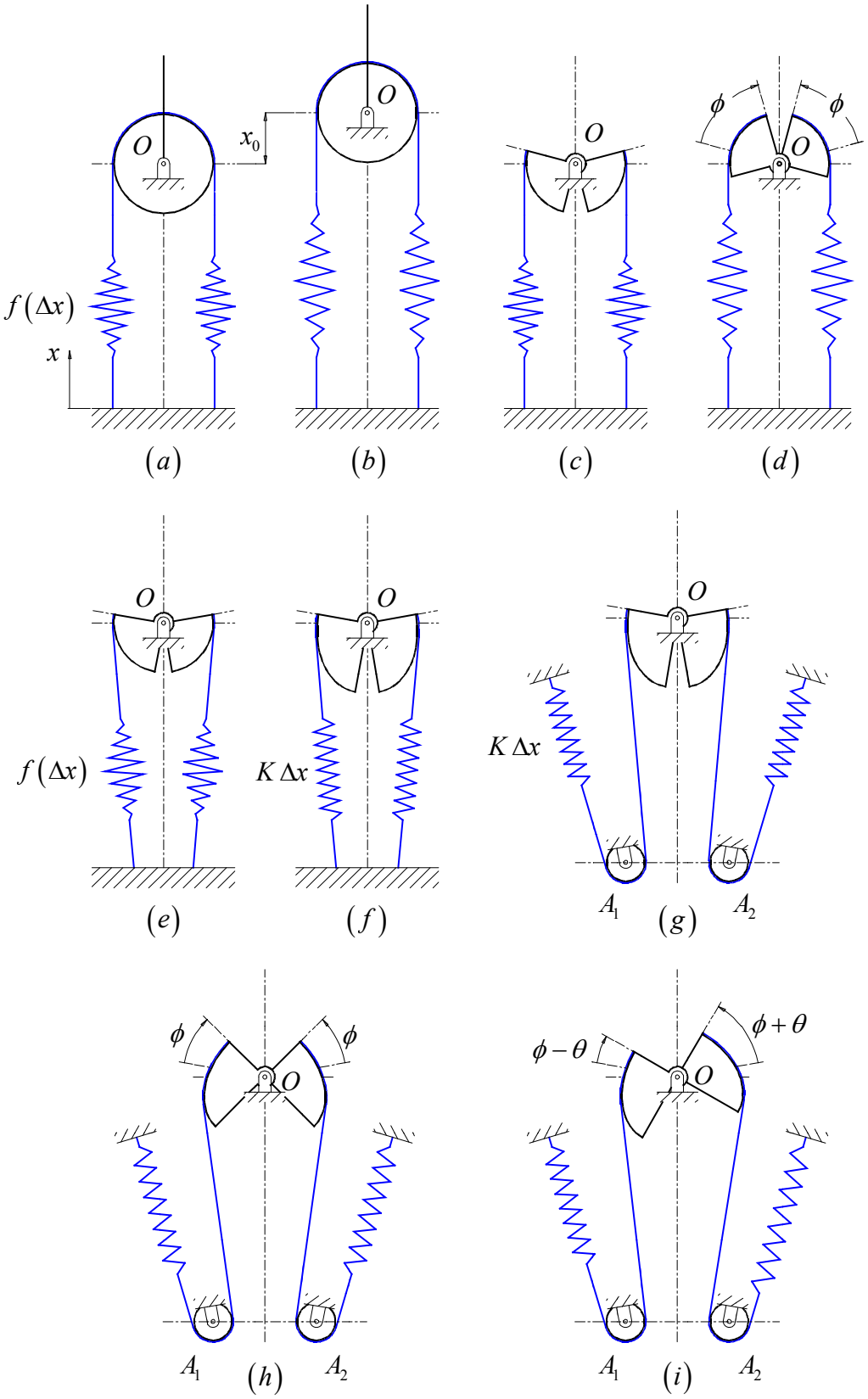

Fig.4.1: The evolution of antagonistically working two quadratic springs set-up.

Let the strings of the springs do not wrap around the same pulley but around two identical concentric pulleys (Figure 4.1.c). Then, instead of translating one pulley by an amount of x_0, now the two identical pulleys will be rotated in reverse directions by an equal amount (Figure 4.1.d) and still the springs are stretched symmetrically and the equilibrium position of the pulley pairs does not change. So both set-ups given at Figures 4.1.a and 4.1.c have the same effect on the springs. The only difference is that at the second set-up the pulleys do not move but turn around a fixed axis. Besides that, the second set-up introduces a new property that the first one does not have. Notice at the first set-up, the two quadratic translation springs must operate parallel to each other. But by decoupling the pulleys of the two quadratic torsion springs, such a requirement is eliminated at the second set-up. The second set-up can be perceived as two quadratic spring-string-pulley units working antagonistically. Such two units can be attached to each other with any angle at point O and it eliminates the parallel orientation requirement of the quadratic springs (Figures 4.1.c and 4.1.e). New ideas can be further build up on the second set-up as follows. The difficulty of the antagonistically working spring set-up is the quadratic spring requirement. Then a very critical question is asked right here; why not the translation springs are linear springs but the surface that the string wraps around is not a pulley but a well calculated cam surface (Figure 4.1.e and 4.1.f). This problem has already been solved in Section 3.2 and it is known how to calculate the cam profile that transforms a linear translation spring into a quadratic torsion spring. Then, the most general case of the string wrapping around cam mechanism given in Figure 3.3 can be applied to our set-up as shown in Figure 4.1.g.

It is better to verify that the set-up give in Figure 4.1.g really gives us a mechanically adjustable linear torsion spring, since it was a long evolution from Figure 4.1.a to 4.1.g. With the teachings of Section 3.2, the cam profile can be calculated such that $G(\alpha) = A\alpha^2 + B\alpha + C$ is satisfied for the given $F(\Delta x) = K\,\Delta x$. First turn the two cams in reverse direction by angle of ϕ (Figure 4.1.h) and fix them to each other. Then turn the two cams in CCW direction by angle of θ (Figure 4.1.i). So the right hand cam has rotated by angle of $\phi + \theta$ in CCW direction and the left hand cam has

rotated by angle of $\phi - \theta$ in CW direction. The resultant moment acting on the pulleys with respect to their rotation axis is,

$$\begin{aligned} M(\theta) &= A(\phi-\theta)^2 + B(\phi-\theta) + C - A(\phi+\theta)^2 - B(\phi+\theta) - C \\ &= -2(2A\phi + B)\theta \end{aligned} \tag{4.1}$$

As expected, the resultant torsion spring behavior is linear and the stiffness of it is a function of the pretension, ϕ.

Using cams instead of pulleys at the antagonistically working two non-linear springs set up has an inherent claim of being compact. In fact, the acquisition of the quadratic springs makes the system complicated and less compact as was seen at the literature examples in Chapter 2. But for our case, the springs that are used are linear springs and can be obtained easily as linear helical springs. The only thing that changes is the shape of the pulleys that the strings wrap around and this does not result in significant complication.

Although complicated quadratic springs were eliminated, another problem appeared; the two cams must be rotated in reverse directions by an equal amount and need a mechanism to do that. Two possible solutions will be given in Section 4.1.4.

The overall picture can be looked at from another point. The main logic of the antagonistically working two non-linear springs set-up is that it transforms two quadratic springs into an adjustable linear spring. There can be two such set-up types. Either two quadratic torsion springs are used and an adjustable linear torsion spring is obtained or two quadratic translation springs are used and an adjustable linear translation spring is obtained. Reverse set-ups can also be built. But, to obtain an adjustable linear torsion spring using quadratic translation springs, first quadratic translation springs must be converted into quadratic torsion springs. In fact, the string and the pulley used at the set-up given in Figure 4.1.a just does that. So the main use of the pulley string pair is a transformation from translation to torsion behavior. In summary, if there were two quadratic torsion springs available as simple as linear

helical springs, they would result in the most compact mechanically adjustable linear torsion spring.

4.1.2 Notes on cam design for quadratic torsion springs

To construct a mechanically adjustable linear torsion spring, one must first have two quadratic torsion springs and as it was pointed out in Section 4.1.1, they can be realized by designing string wrapping around cam mechanism. So with the most general case, $F(\Delta x) = K\,\Delta x$ and $G(\alpha) = A\alpha^2 + B\alpha + C$ will be satisfied. There are several notes on designing the cam profile for parabolic characteristic torsion spring.

Note 1: $B = 0$ can be selected beforehand. Because the selection of the cam orientation where α is zero is quite arbitrary. To understand how, observe Figure 4.2. The same cam string set-up is given at two different positions in Figures 4.2.a and 4.2.b. If the cam rotations are started to be measured from these positions, the parabolic spring characteristics shown at the right hand graphs are obtained respectively. The only difference is that the same pink parabola shifts to the left. Although the cam string set-ups are the same, two different torsion spring behaviors are obtained. To overcome the obscurity, the vertical $G(\alpha)$ axis can be selected congruent with the axis of the parabola and that means $B = 0$ (Figure 4.2.c).

Note 2: Not K, A and C but $\frac{A}{K}$ and $\frac{C}{K}$ are important. Remember Equation (3.3). When $F(\Delta x) = K\,\Delta x$ and $G(\alpha) = A\alpha^2 + C$ are inserted into it,

$$K \cdot (u_s + s_t)\,du_s = \left(A\alpha^2 + C\right)d\alpha \tag{4.2}$$

Dividing both sides with K,

$$(u_s + s_t)\,du_s = \left(\frac{A}{K}\alpha^2 + \frac{C}{K}\right)d\alpha \tag{4.3}$$

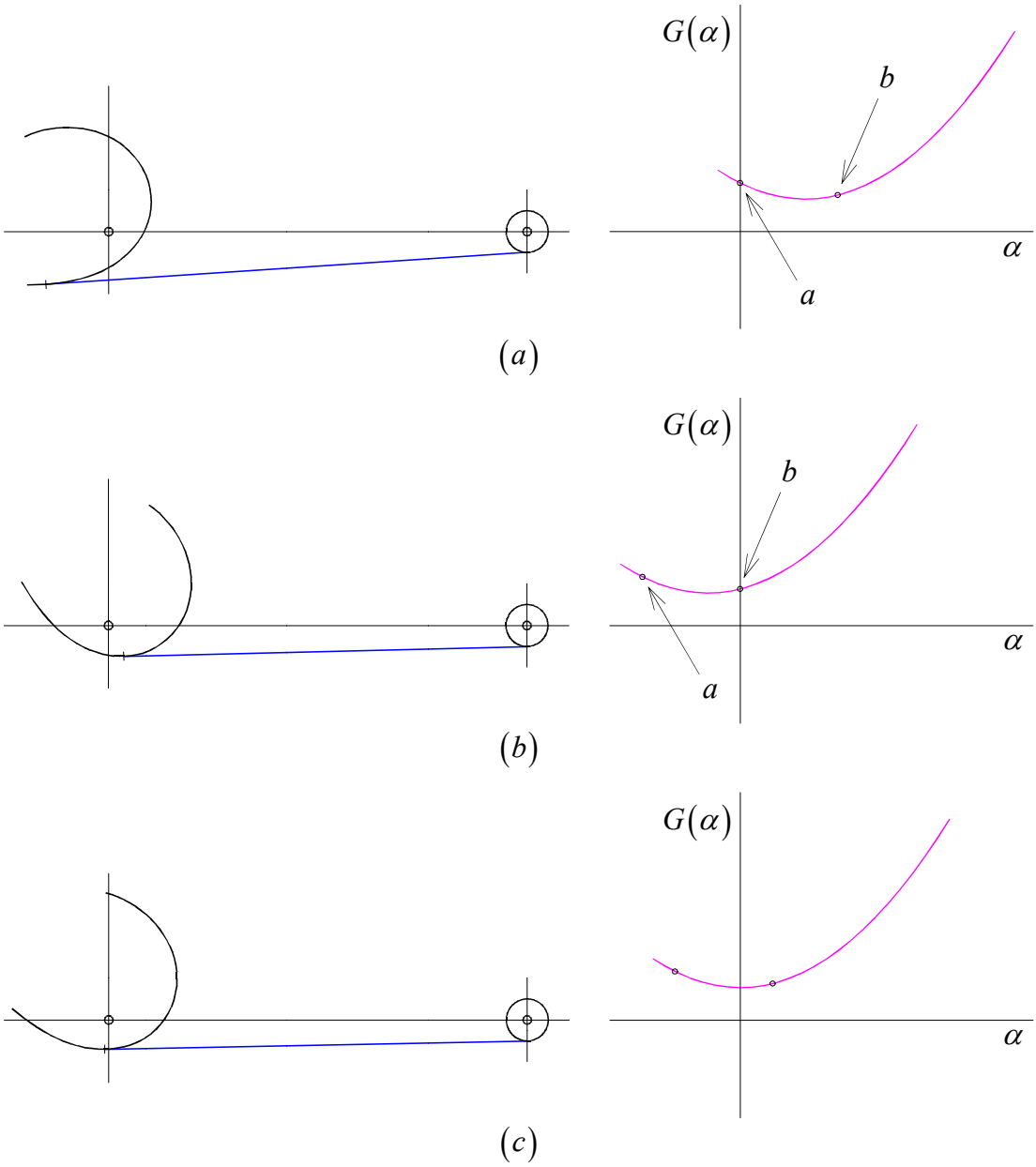

Fig.4.2: Different selection of the cam orientations where $\alpha = 0$.

So, K just scales Equation (4.2). When $\frac{A}{K}$ and $\frac{C}{K}$ are assigned, $u_s(\alpha)$ variation is obtained by integrating Equation (4.3) and the corresponding cam is calculated as explained in Section 3.2. It was stated at the end of Section 3.2 that, the only inherent design freedom was the initial pretension s_t and was wished that the G function would offer other design freedoms. For the problem concerned here, G function

introduces two further design freedoms. In summary, to obtain a quadratic torsion spring using cams, there are in total three design freedoms, namely; s_t, $\frac{A}{K}$ and $\frac{C}{K}$.

Note 3: The left hand branch of the parabola, $G(\alpha) = A\alpha^2 + C$, is shorter than the right hand branch. A sample calculation is given in Figure 4.3 to show it. Notice that the left hand branch of the cam grows faster than the right hand branch. The reason is, although $F(\Delta x) = K\,\Delta x$ decreases here, $G(\alpha) = A\alpha^2 + C$ insist on increasing. So the cam prefers to increase the effective moment arm faster to compensate the decreasing F function and catch up with the increasing G function. This situation on the cam results in a shorter left hand branch of $G(\alpha) = A\alpha^2 + C$ than the right hand branch.

Note 4: C must be non-zero or new design problems are ahead. A sample cam design for a negative C is given in Figure 4.4. Since C is negative, G function is able to become zero at two different positions. At these two positions, the straight part of the string points to the rotation axis of the cam. When G function is positive, the straight part of the string lies above the rotation axis and when G function is negative, it lies below the rotation axis. So during the operation, the string sweeps the rotation axis and it means that the string will pass inside a shaft that the cam is rotating around. The problem can be solved as in the case of the crank shaft of the internal combustion engine, but this solution complicates the design and manufacturing. To facilitate the design, it is better to work with positive C values.

Although positive C is fostered here, negative C has also some merits. Compare the cam designs given in Figures 4.3 and 4.4. The two calculations are made for the same design parameters except the C values. When the F function graphs are compared, the maximum deflection decreases which is quite important when the limits of linear translation springs are concerned. Another merit is that the size of the cam decreases.

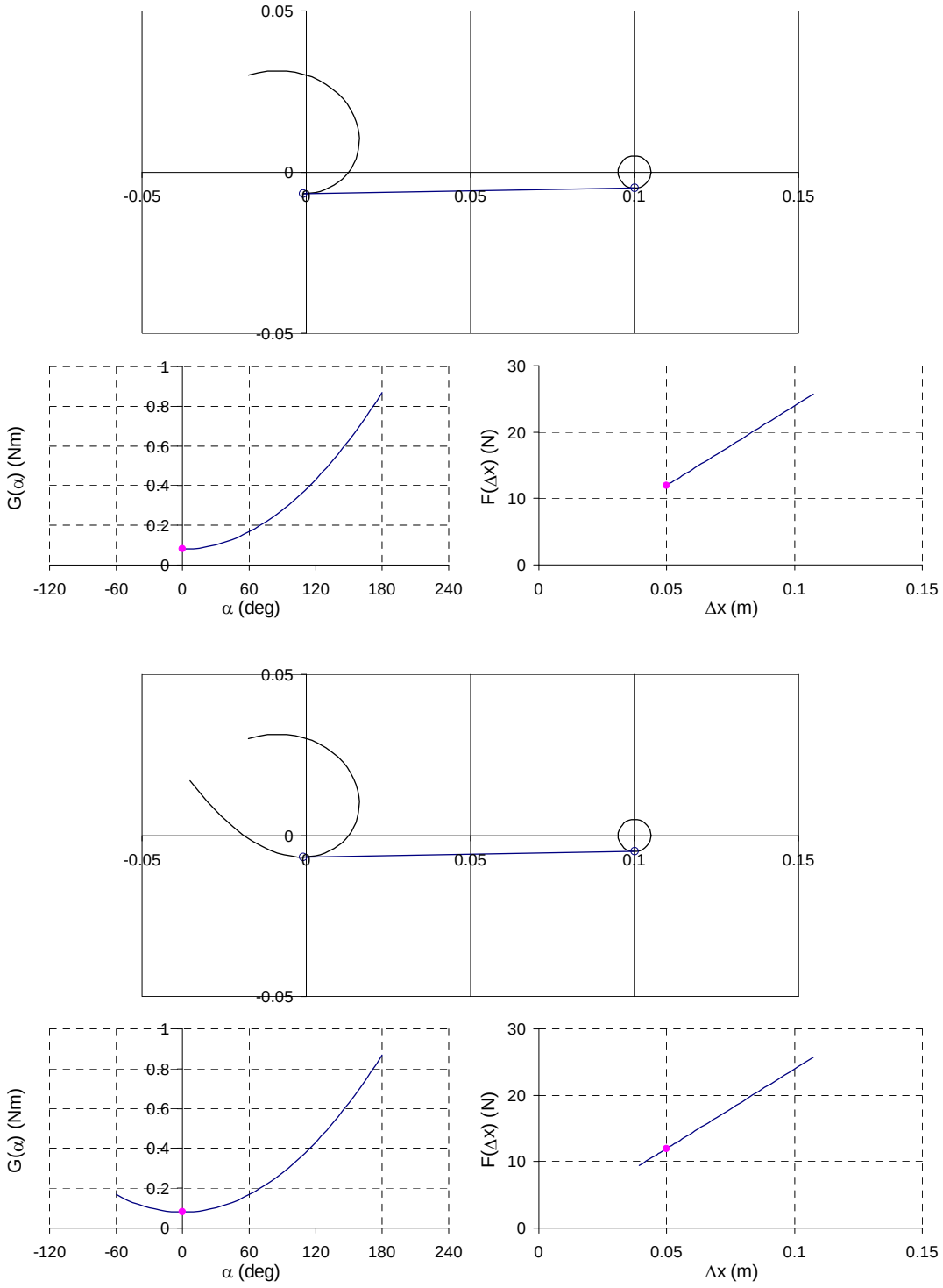

Fig.4.3: Demonstration of the left hand branch of the cam. $G(\alpha) = 0.08\alpha^2 + 0.08$, $F(\Delta x) = 239.5\Delta x$ *and* $s_t = 0.05\ m$. *The dimensions are* $a = 0.1\ m$ *and* $r = 0.005\ m$. *The upper figure shows the solution for* $0 \le \alpha \le 180^0$. *The lower figure shows the solution for* $-60 \le \alpha \le 180^0$. *The below graphs under each configuration show the corresponding operation points of* F *and* G *functions.*

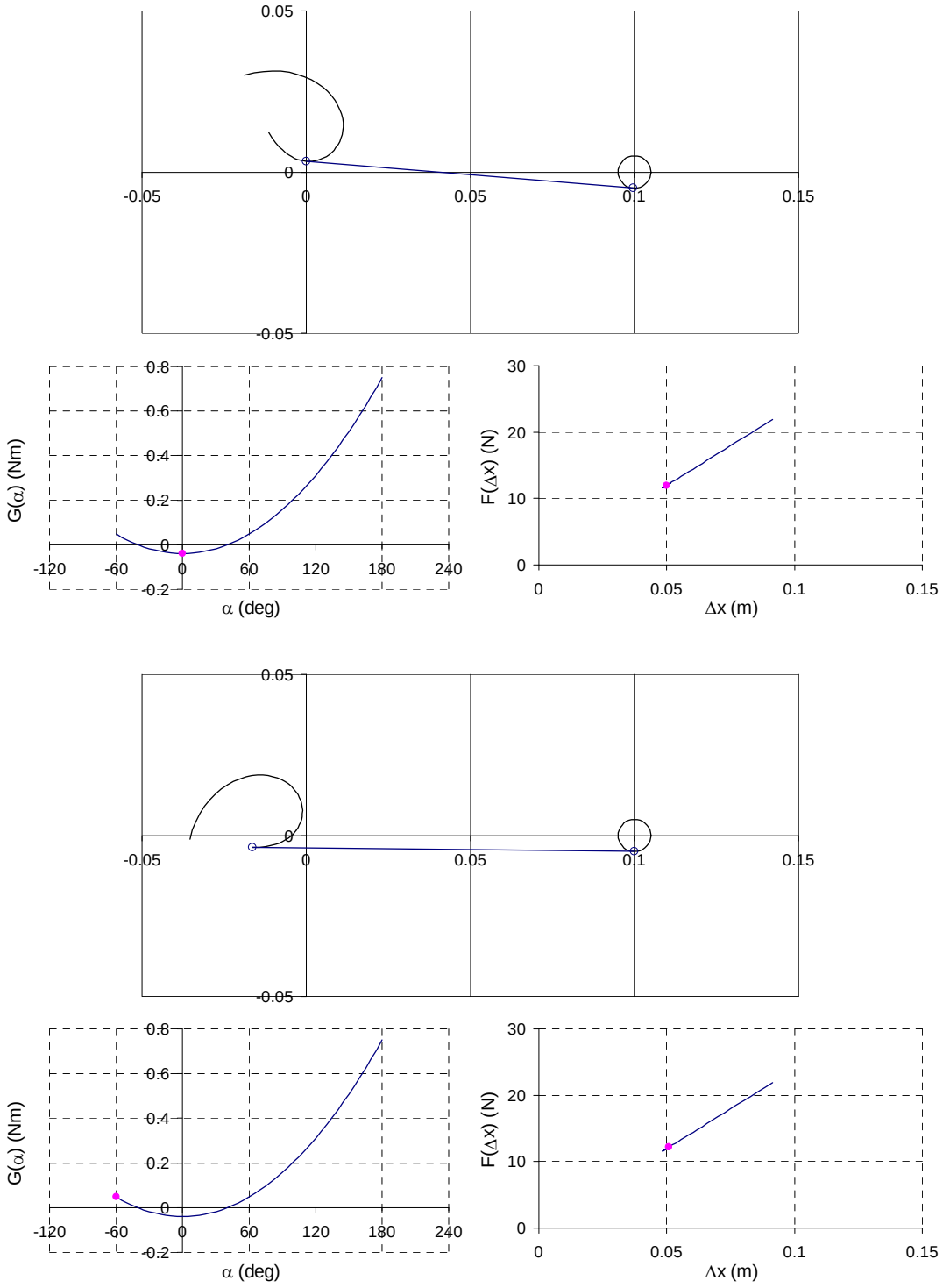

Fig.4.4: A case when C is negative. $G(\alpha) = 0.08\alpha^2 - 0.04$, $F(\Delta x) = 239.5\Delta x$ and $s_t = 0.05\,m$. The dimensions are $a = 0.1\,m$ and $r = 0.005\,m$. The cam profile was calculated for $-60^0 \le \alpha \le 180^0$. The cam is give at two configurations; when $\alpha = 0^0$ and $\alpha = -60^0$. The below graphs under each configuration show the corresponding operation points of F and G functions.

Note 5: r can be selected zero to eliminate pulleys and to reduce friction. The main goal of the pulley at the string wrapping around cam mechanism was guiding the string so that the translation spring would be put anywhere suitable (Figure 3.3). But the pulleys add to the friction with their revolute joints. They can be eliminated to reduce the friction; however the solution comes with the price of increased a value. Remember that if the pulley is eliminated, at the most tensed position, the length of the straight part of the string must be higher than the released length of the translation spring plus the maximum deflection of it. Eliminating the pulley at the calculations is quite easy; just assign zero to r. Also notice that r can be assigned negative. This time the string rolls around the pulley not from below but from above.

Note 6: The string thickness can be taken into account in the calculations. The equations were derived for a string with zero thickness but in real life it will always have a finite thickness. It can be assumed that the string's neutral axis is at its center. Then the cam profile calculated here is for the neutral axis. The real cam surface will then be half the string thickness below. This can be adapted to the calculations easily because β is calculated at each step.

4.1.3 The operation region

There is an operation region for the adjustable linear torsion spring. Since the cams will have limits, so will the adjustable linear torsion spring that uses them. Before going further, Equation (4.1) must be updated first, since B was selected zero at Section 4.1.2 – *Note 1*. Then, Equation (4.1) becomes,

$$M(\theta) = -4A\phi\theta \tag{4.4}$$

See how simple the Equation (4.4) is. The stiffness of the adjustable linear torsion spring is linearly related to A and ϕ. It could be a complex function of ϕ either. It facilitates the effort if the real adjustable linear torsion spring is needed to be calibrated experimentally.

Remember that the cams were calculated for an α range like $\alpha_{\min} \le \alpha \le \alpha_{\max}$. If the cam is rotated with the pretension ϕ in CW direction, then it will able to rotate at most by an angle of $\alpha_{\max} - \phi$ in CW direction and $\phi - \alpha_{\min}$ in CCW direction. The mechanically adjustable linear torsion spring using cams uses two mirror image cams that work antagonistically (Figure 4.1.g). That is, when they are rotated together in one direction, one cam rotates towards its $\alpha_{\max}$ edge and the other rotates towards its $\alpha_{\min}$ edge. So the mirror image cam couple can rotate at most either by an angle of $\alpha_{\max} - \phi$ or $\phi - \alpha_{\min}$. The smaller one rules.

$$\theta_{\max} = Min\left[\alpha_{\max} - \phi\,;\, \phi - \alpha_{\min}\right] \tag{4.5}$$

Equation (4.5) can be restated as follows,

For $\alpha_{\min} \le \phi \le \dfrac{\alpha_{\max} + \alpha_{\min}}{2}$, $\qquad \theta_{\max} = \phi - \alpha_{\min}$ (4.6)

For $\dfrac{\alpha_{\max} + \alpha_{\min}}{2} \le \phi \le \alpha_{\max}$, $\qquad \theta_{\max} = \alpha_{\max} - \phi$ (4.7)

A representative sketch is given in Figure 4.5 for the cam calculated in Figure 4.3. Observe how different edges of the cam constrain the maximum deflection, the $\theta_{\max}$.

Inserting Equations (4.6)and (4.7) into Equation (4.4), the moment limits are found (negative sign is eliminated).

For $\alpha_{\min} \le \phi \le \dfrac{\alpha_{\max} + \alpha_{\min}}{2}$,

$$M\left(\theta_{\max}\right) = 4A\phi\theta_{\max} = 4A\left(\alpha_{\min} + \theta_{\max}\right)\theta_{\max} \tag{4.8}$$

For $\dfrac{\alpha_{\max} + \alpha_{\min}}{2} \le \phi \le \alpha_{\max}$,

$$M\left(\theta_{\max}\right) = 4A\phi\theta_{\max} = 4A\left(\alpha_{\max} - \theta_{\max}\right)\theta_{\max} \tag{4.9}$$

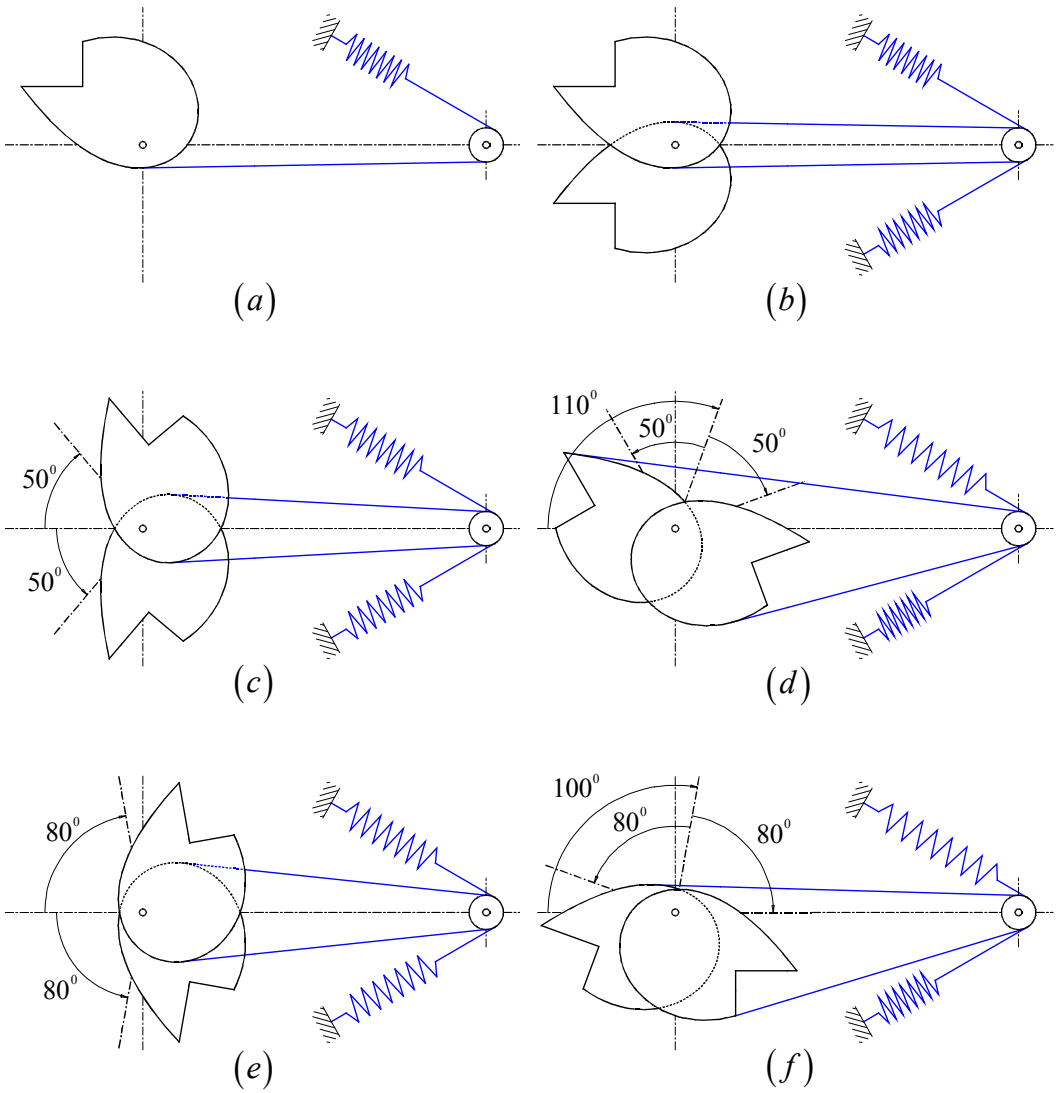

Fig.4.5: (a) The quadratic torsion spring using cam himself. This is the one given in Figure 4.3 and calculated for $-60 \le \alpha \le 180^0$. *(b) Two such quadratic torsion springs are working antagonistically. (c) The cams are rotated by* $\phi = 50^0$ *in reverse directions at the equilibrium position. (d) Cam pairs can be rotated at most by* $\theta_{max} = 110^0$. α_{min} *edge of the cam constrain* θ_{max}. *(e) The cams are rotated by* $\phi = 80^0$ *in reverse directions at the equilibrium position. (f) Cam pairs can be rotated at most by* $\theta_{max} = 100^0$. α_{max} *edge of the cam constrain* θ_{max}.

Equations (4.8) and (4.9) represent two parabolas that constitute the borders of the operation region of the mechanically adjustable linear torsion spring using cams. The operation region graph for the cases given in Figure 4.5 is shown in Figure 4.6.

Observe how the two obtained linear torsion springs are limited by two different parabolas expressed with Equations (4.8) and (4.9).

The possible stiffness range is $4A\alpha_{\min} \le k \le 4A\alpha_{\max}$. Yet, the springs with stiffnesses $4A\alpha_{\min}$ and $4A\alpha_{\max}$ can not be deflected since they have the maximum deflection $\theta_{\max} = 0$. The maximum deflectable spring is obtained when $\phi = \dfrac{\alpha_{\max} + \alpha_{\min}}{2}$. The stiffness obtained for this case is $k = 2A(\alpha_{\max} + \alpha_{\min})$ and that spring can be deflected at most $\theta_{\max} = \dfrac{\alpha_{\max} - \alpha_{\min}}{2}$.

Observe that negative stiffnesses can be obtained if $\alpha_{\min}$ is negative (Figure 4.6). The negative stiffness may not have a practical use, but in our case, negative $\alpha_{\min}$ widens the operation region of the soft springs (Figure 4.6). Remember that negative $\alpha_{\min}$ is harder to obtain than $\alpha_{\max}$ as explained in Section 4.1.2 – *Note 3*.

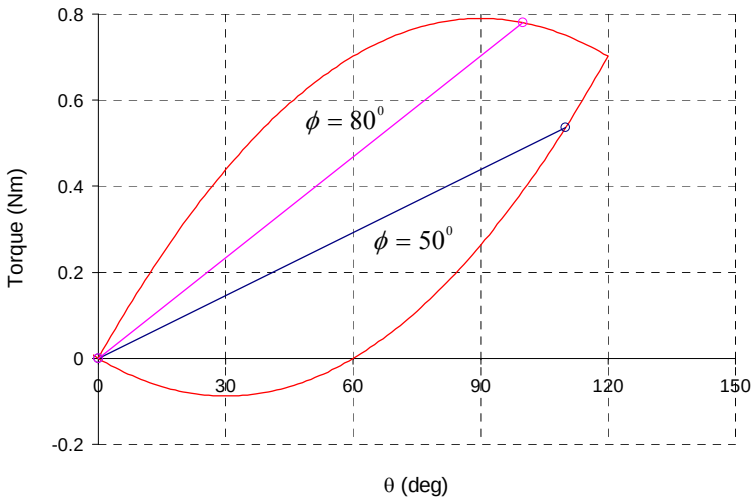

Fig.4.6: The operation region of the antagonistically working two quadratic torsion springs set-up given in Figure 4.5. $A = 0.08$, $\alpha_{\min} = -60^0$ *and* $\alpha_{\max} = 180^0$. *The pink and the blue straight lines show the linear torsion springs obtained when* $\phi = 50^0$ *and* $\phi = 80^0$ *respectively.*

4.1.4 Mechanical details of the prototypes

After calculating the necessary cam profile satisfying the operation region requirements of the mechanically adjustable linear torsion spring, there remains some other mechanical problems that must be solved. A good mechanical design is quite crucial because a reliable, light, low inertia and low friction machine is deeply affected from the quality of the design and manufacturing. Since our prototypes will be just for demonstration purposes, there is no apparent requirement like fitting the whole system into a confined space. Here, making the prototypes as compact as possible was adopted. Two different prototypes were manufactured for this purpose. At the first prototype, the manufacturing skills were tested and the nature of the prototype was perceived better. The second prototype was manufactured to overcome the problems seen at the first prototype and the ideal design was tried to be reached.

When it is settled to manufacture a prototype of the mechanically adjustable linear torsion spring, the first thing it must be thought about is the stiffness tuning mechanism. Nothing has been said about it up to now, but it is not as straight forward as it is first thought. First of all, it needs a non-back drivable mechanism element since stiffness must not change during the adjustable spring operates. Two possible non-back drivable mechanisms can be the screw-nut mesh and the worm-gear mesh. Secondly, the cams must rotate in reverse directions by an equal amount. One solution can be realized using symmetrically operating slider crank mechanisms. Crank arms rotate the cams in reverse directions by an equal amount and the stiffness is tuned with translating their common slider. When the slider is translated with screw-nut mesh, a non-back drivable stiffness tuning mechanism is obtained. This method is applied at the first prototype. The second and in fact the default solution to the problem is to use two bevel gears which are driven by the same pinion gear. Two bevel gears rotate the cams in reverse directions equal amount and their common pinion gear can be rotated with a worm gear. Again a non-back drivable stiffness tuning mechanism is obtained and this method is used at the second prototype.

Prototype #1

Basic components of the Prototype #1 are shown in Figure 4.7. The cams were calculated for $G(\alpha) = 0.05\alpha^2 + 0.034875$, $F(\Delta x) = 232.5\Delta x$ and $s_t = 0.03\,m$. The cam calculations are made for the range $-40^0 \le \alpha \le 200^0$. The dimensions are $a = 0.08\,m$ and $r = 0.005\,m$. As it is seen in Figure 4.7, the string wraps around a second pulley so that the linear helical spring used is placed horizontally just below the cams. For this set-up, a long dimension is unavoidable. The free length of the helical spring is $5.9\,cm$ and it elongates $9\,cm$ at the most loaded position. So it requires a $14.9\,cm$ long space to operate. Here a second pulley was quite crucial to save space but it comes with the price of friction of a new element. Initial pretension, s_t, of this spring is given with the pretension adjustment handle.

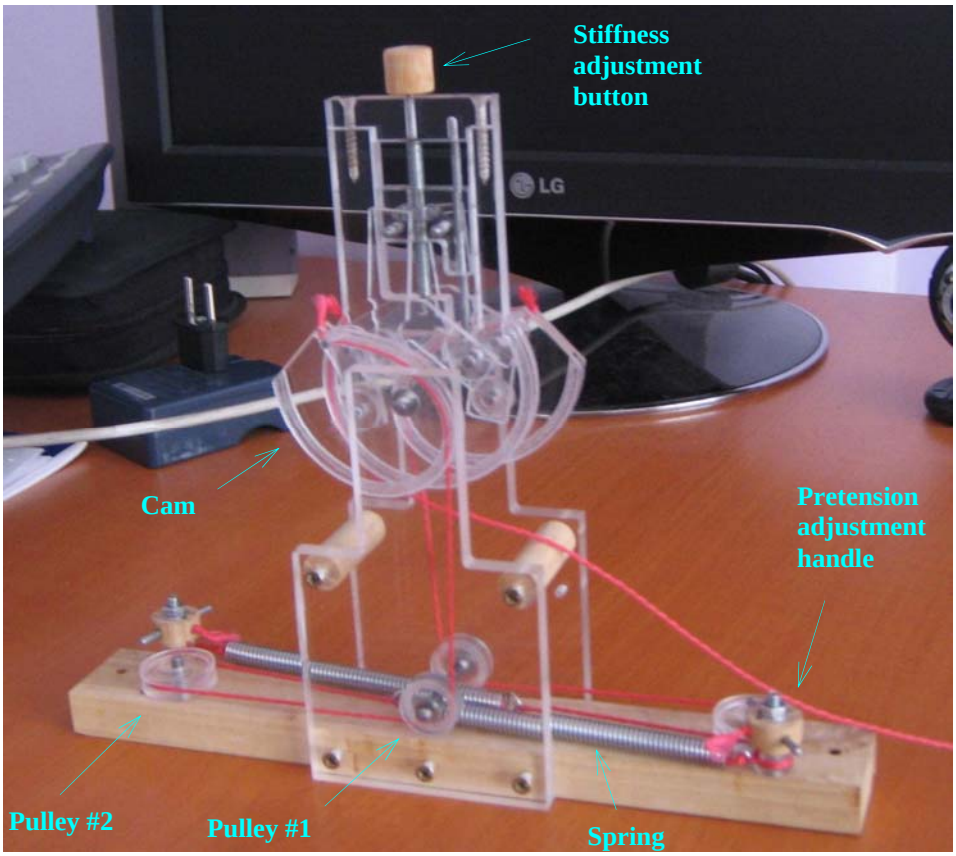

Fig.4.7: Basic components of Prototype #1.

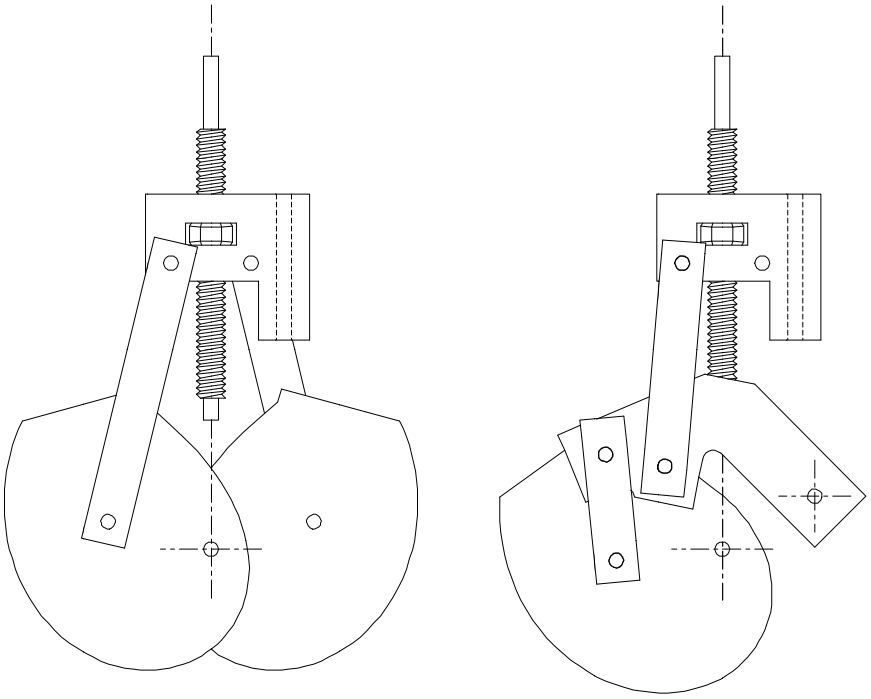

Fig.4.8: Symmetrically operating slider crank mechanisms powered by a nut-screw mesh (Left). Symmetrically operating slider crank mechanism plus a four bar mechanism powered by a nut-screw mesh (Right). The symmetric portion was eliminated for clarity.

At prototype #1, stiffness tuning is made with symmetrically operating slider crank mechanisms powered by a nut-screw mesh (Figure 4.8 – Left). At the design stage, the cams were asked to rotate 120^0 in reverse directions and this angular deflection is quite high for a slider crank mechanism that does not suffer from transmission angle problem. So, a four bar mechanism added serially to the slider crank mechanism (Figure 4.8 – Right). Slider crank mechanism rotate its crank 60^0 meanwhile the rocker arm of the four bar mechanism rotates 120^0. These two mechanisms were designed for keeping the torque transmissions as constant as possible. That is, approximating the gear meshes.

The performance of the prototype #1 was quite unsatisfactory so no experiments were conducted on it to verify linear behavior. The major problem was the friction of the system. Dry friction resulted in significant backlash and thus a useless spring yet

it is still adjustable. No roller bearings were used at the revolute joints and worse than that, the pulleys and the adjustable torsion spring handle itself rotate around $3\,mm$ thick shafts whereas $2\,mm$ shafts were possible.

The main material used for manufacturing the cams and other parts for the first prototype was Plexiglas. It is thought that, since Plexiglas was a transparent material, it would show the details inside of the mechanism and since it was a soft material, it could be machined easily. However, making most of the parts transparent did not make the inside details visible but everything invisible and at high cutting speeds Plexiglas tended to melt and resulted in low surface quality. With the teachings of the first prototype, the second prototype was manufactured from aluminum, which is a light and heat conductive material.

Prototype #2

The general view of the Prototype #2 is shown in Figure 4.9. The cams were calculated for $G(\alpha) = 0.08\alpha^2 + 0.02514$, $F(\Delta x) = 239.5\Delta x$ and $s_t = 0.05\,m$. The cam calculations are made for the range of $-70^0 \le \alpha \le 180^0$. The dimensions are $a = 0.18\,m$ and $r = 0\,m$. As it seen in Figure 4.9, the string does not wrap around any pulley so that the system is free of pulley friction. The free length of the spring is $6\,cm$ and it elongates $10\,cm$ at the most loaded position. So it requires a $16\,cm$ long space to operate. This space was acquired by making $a = 0.18\,m$.

The stiffness adjustment mechanism is shown in Figure 4.10. Two bevel gears connected to the two cams are driven by the same pinion gear. The cams are able to rotate in reverse directions with equal amounts. The pinion gear is driven by a non-back drivable worm-gear mesh. While the adjustable spring operates under load, the bevel gears-pinion mesh was not able to keep its contact. It is due to the pressure angle of the teeth since it creates an axial force on the bevel gears. The problem was solved by introducing gear holders (Figure 4.10). They imposed a kinematic constrain on the bevel gears-pinion contact.

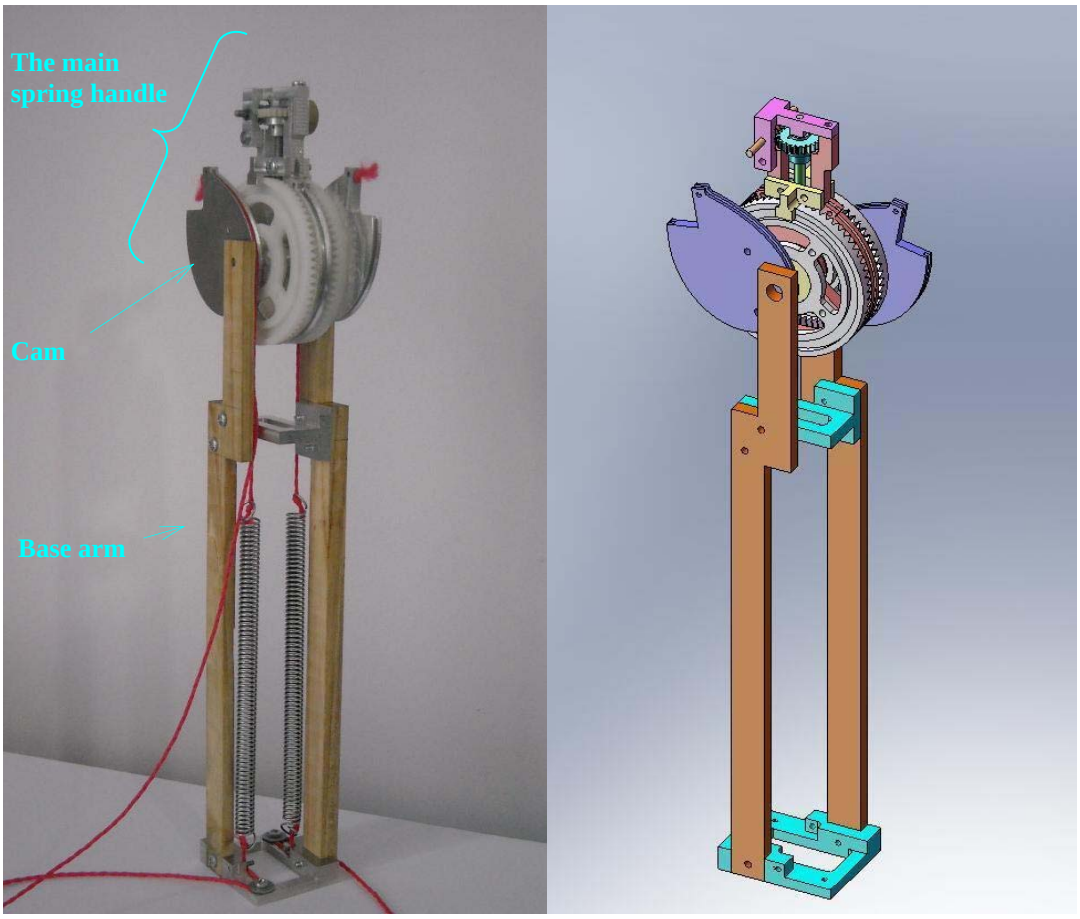

Fig.4.9: The picture of the prototype (Left) and the CAD model (Right).

On the main spring handle, a half pulley was added for experimental measurements (Figure 4.10 – lower right). So, during the experiments, not the angular deflection but the deflection of the string that wraps around it was measured. A half pulley was enough because the spring handle can rotate at most $\pm 125^0$ (Refer to Section 4.1.3).

At the first prototype, the base arms were connected to each other by two cylindrical parts that pass outside the string operation region (Figure 4.7). Since the main objective of the prototypes was the compactness, a better way to separate the base arms were found and applied at the second prototype. Observe how the middle part seen at Figure 4.11 – Left connects the base arms by passing between the strings .So the second prototype was able become thinner and more compact (Compare Figures 4.7 and 4.9).

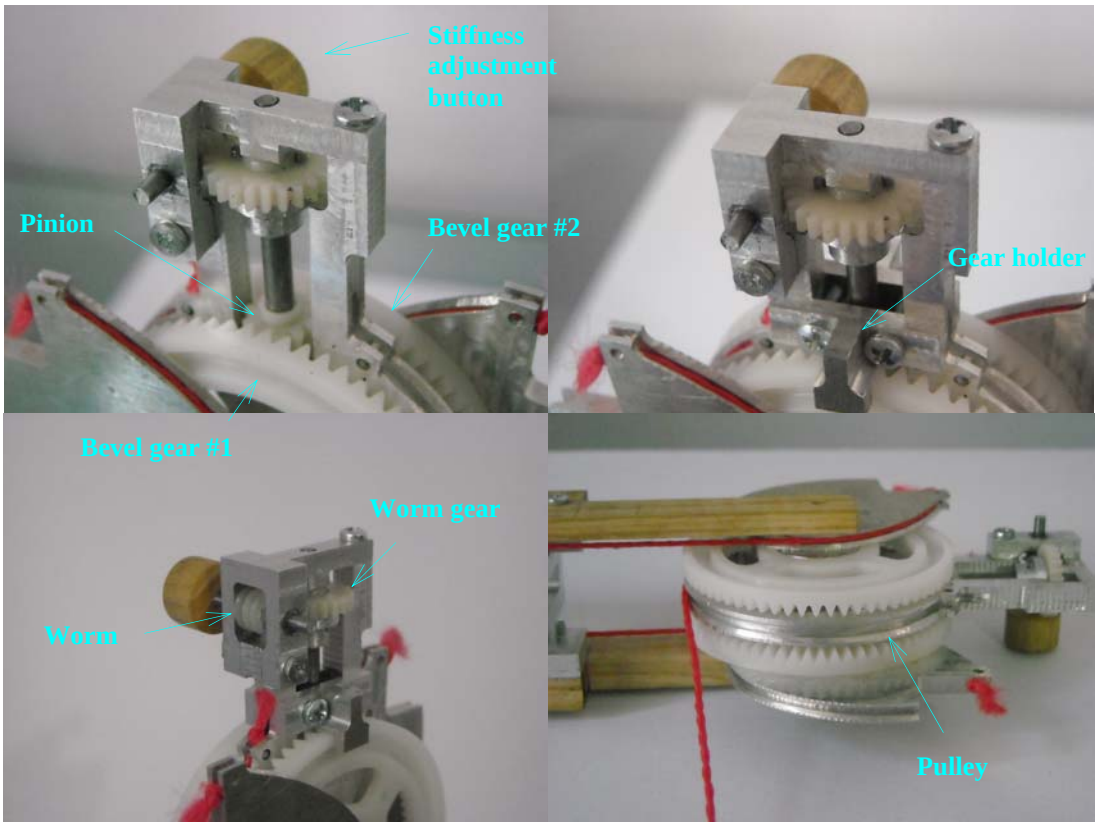

Fig.4.10: The stiffness adjustment mechanism.

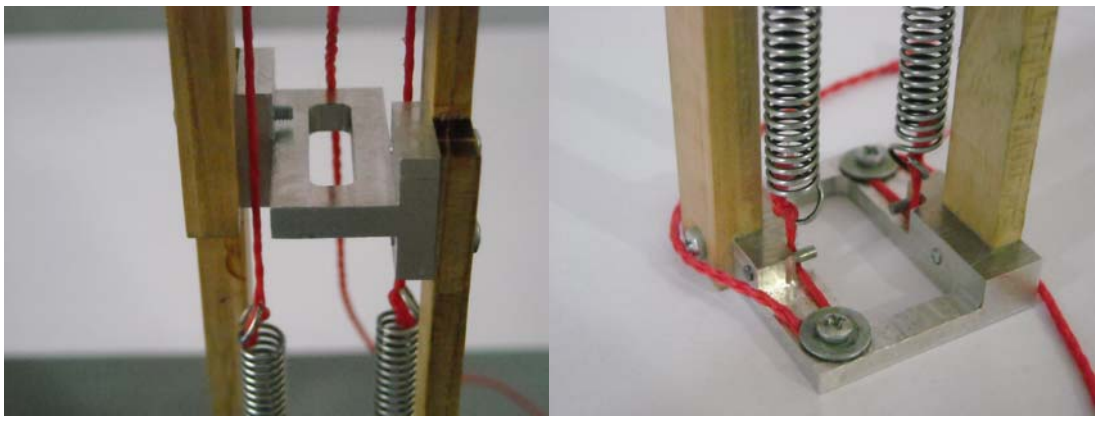

Fig.4.11: Close views of the part that separates the two base arms (Left) and the pretension adjustment tool (Right).

Initial pretension, s_t, is given to the two helical springs used in the second prototype with the pretension adjustment system shown in Figure 4.11 – Right. As it is

observed, a more effective and smaller system is introduced for spring pretension adjustment at the second prototype than the first prototype.

To decrease the effects of the friction on the system performance, roller bearings were used at the rotational joints. Since there are no pulleys in the second prototype, the only revolute joint used is at the main spring handle. The roller bearings are not visible in Figure 4.9 because they are embedded inside the base arms.

Notice an important thing here. The cams are connected to the bevel gears rigidly. Then, while the adjustable spring operates, they are the teeth of the bevel gears that will transfer the force created at the cams to the main spring handle. So the weak chain of this design is the strength of the teeth. It is better to manufacture them from a metal, but for our case they are made up of plastic.

4.1.5 Experimental verification of the linearity

As it was noted before, the first prototype was quite unsatisfactory and was suffering from significant backlash, thus no experiments were conducted on it, and instead the second prototype was designed and manufactured. This time the performance of the prototype was satisfactory and experiments were conducted on it. The results are given in this section.

The pictures of the experimental set-up are shown in Figure 4.12. As it was expressed before, on the main spring handle, a half pulley was added for experimental measurements (Figure 4.10 – lower right). A string that wraps around this half pulley is loaded with some known weights at the other end and the mechanically adjustable linear torsion spring is loaded by this way. A black spot was made on this string and its deflections were measured with a ruler of 0.5 mm accuracy (Figure 4.12). Knowing the radius of the half pulley and the deflections of the string, the torsion spring behavior was obtained.

When the experiments started, a striking problem was encountered. The first results spilled over the operation region which was an impossible conclusion. Then it was

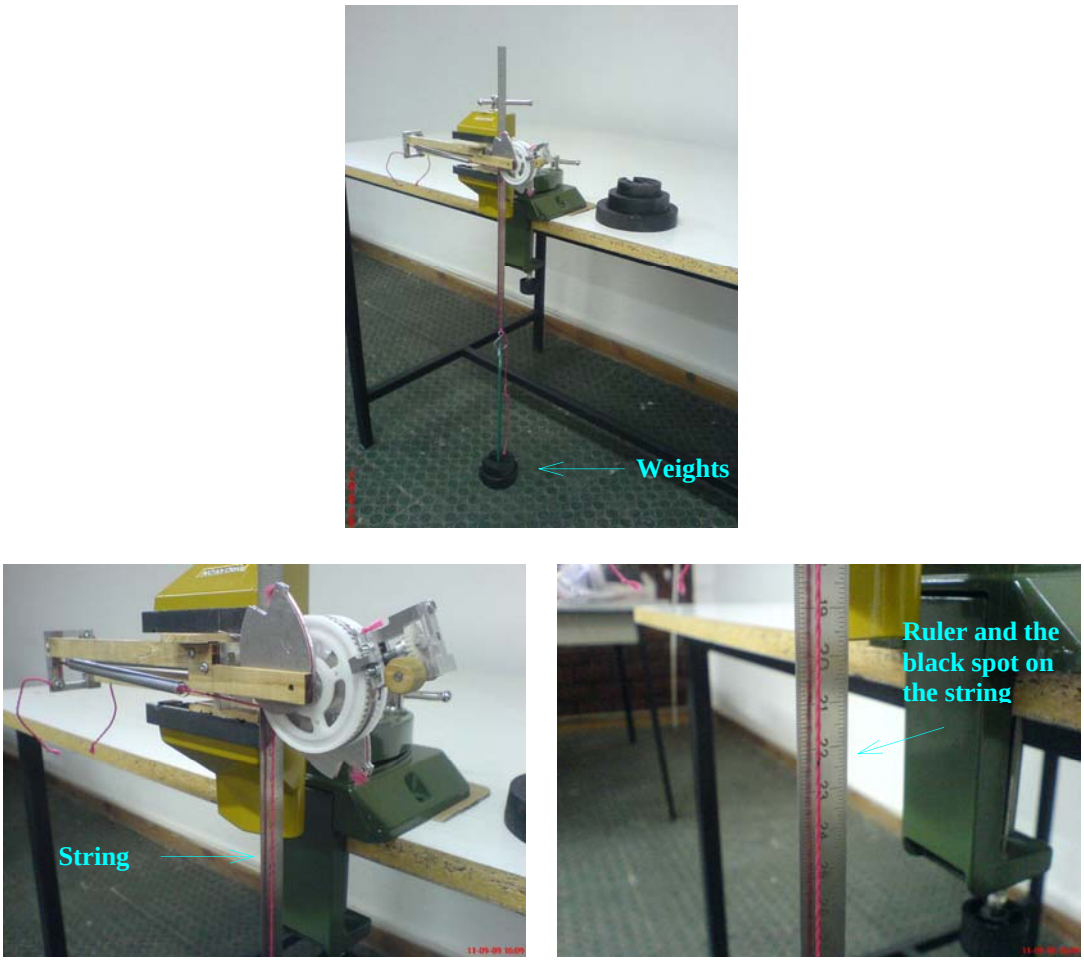

Fig.4.12: Experimental set-up

realized that the strings that were used had significant elasticity. The work done up to that time was questioned and noticed that some critical calculation values were even wrong. For example, the stiffness of the helical spring used at the quadratic spring calculations was not correct because the experiments made to find its stiffness also included that string. Thanks to the merits of the set-up that all the work up to the experiments was not thrown to the dustbin, although the second prototype had already been manufactured with rigid string assumption.

The strings come into the picture at two points. Firstly, the helical springs are attached to the cams with these springs. So their finite stiffness must be added to the stiffness of the helical spring and the stiffness appearing at $F(\Delta x) = K\,\Delta x$ must be

refined like that. Of course, the string must have a linear spring behavior. As it was noted in Section 4.1.2 – *Note 2,* the value K himself was not an important parameter for the cam profile calculations. As long as $F(\Delta x)$ has a linear spring behavior and it is pre-tensioned correctly as s_t much, the antagonistically working two quadratic springs set-up will continue to give adjustable linear springs. Secondly, the adjustable linear torsion spring is experimented by hanging weights to the pulley on the main spring handle with such a string. Then the string works as a spring attached serially to the adjustable linear torsion spring. So the experimental data must be corrected for its stiffness.

First the spring behavior of the string was measured. It was a quite slow responding spring. When a weight is hanged on its one end, it takes some time to come to an equilibrium. So it was waited approximately 1 minute at every loading and the elongation was noted.

As observed in Figure 4.13, the string shows strong linear behavior. Then the stiffness of the helical spring was measured (Figure 4.14). Again it showed strong linear behavior. But the stiffness that is obtained in Figure 4.14 is spoiled by a 10 cm

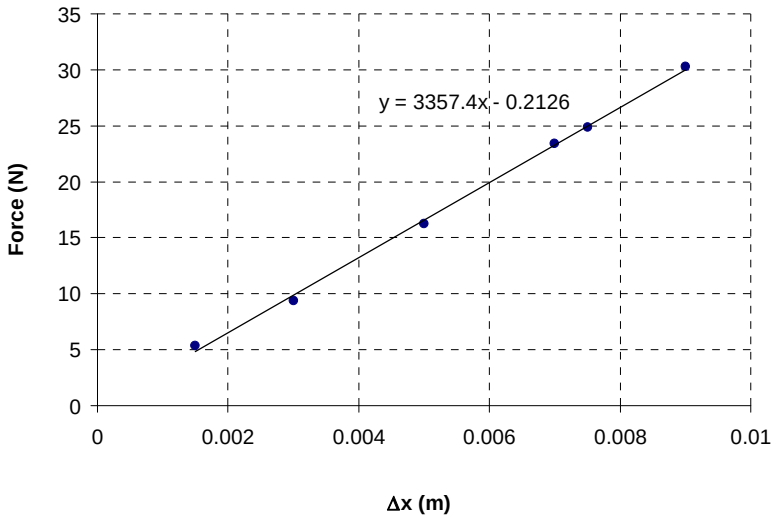

Fig.4.13: Spring characteristic of 30.6 cm long string.

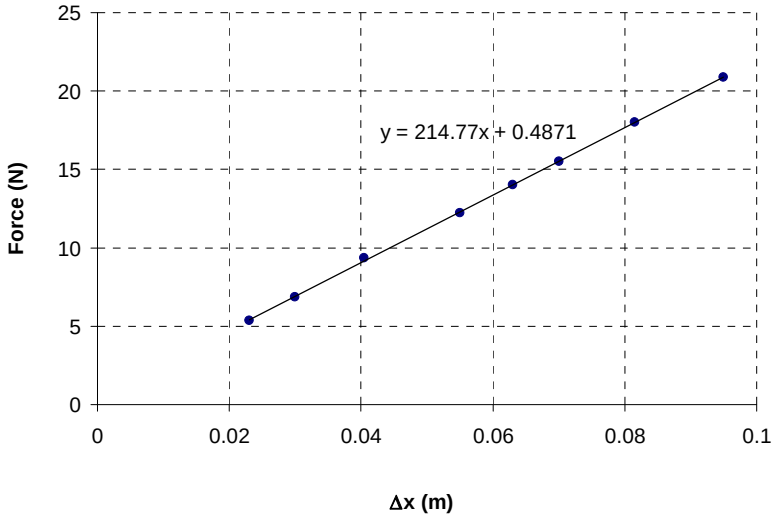

Fig.4.14: Spring characteristic of 5.9 cm long helical spring with 10 cm long string.

long string. When the result is refined, the stiffness of the helical spring is found as $219.36\ N/m$. At the quadratic torsion spring, this helical spring is attached to the cam with 16 cm long string. Then effective F function is found as $F(\Delta x) = 212.11\Delta x$. The F function was noted in Section 4.1.4 as $F(\Delta x) = 239.5\Delta x$. So the spring coefficients given in Section 4.1.4 are totally wrong and must be corrected with $F(\Delta x) = 212.11\Delta x$ and $G(\alpha) = 0.07085\alpha^2 + 0.02227$.

The second prototype was tested for three different stiffnesses (Figure 4.15). It is observed that the springs showed strong linear behavior as it is expected.

The experimental procedure followed like this. The stiffness tuning button was rotated 12 times and the first linear spring was obtained. It was rotated for another 12 times and the second linear spring was obtained. Likewise, it was rotated for another 12 times and the third linear spring was obtained. Since the numbers of teeth of the gears are known (bevel gears have 66 teeth, pinion has 10 teeth and worm gear has24 teeth), the ϕ values are calculated as 27.27^0, 54.55^0 and 81.82^0 respectively. By using Equation (4.4), the stiffnesses of the linear springs are calculated as

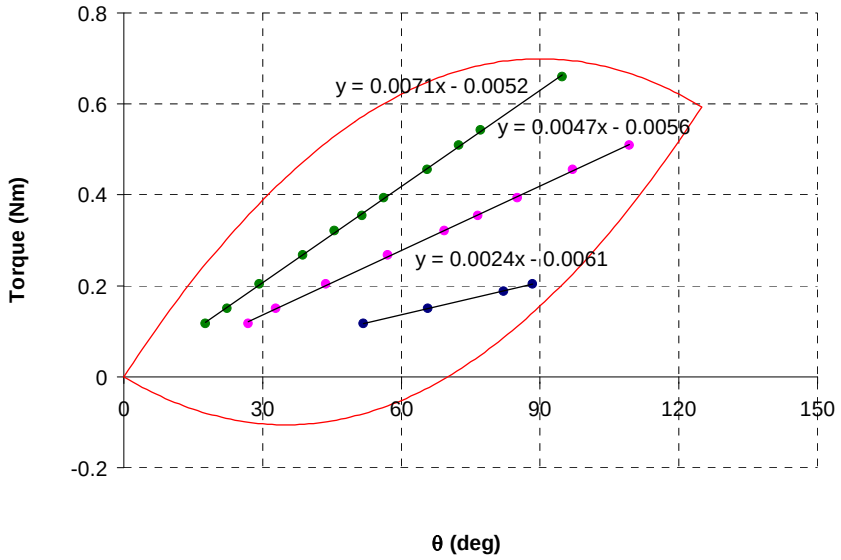

Fig.4.15: Experimental results of the mechanically adjustable linear torsion spring using cams for three different stiffnesses.

$0.002354\ Nm/\text{deg}$, $0.004709\ Nm/\text{deg}$ and $0.007063\ Nm/\text{deg}$ respectively. It is observed that these values are in good agreement with the experimental results (Figure 4.15). Manufacturing quality of the prototype is proven by these results.

4.2 With hanging weights

Remember that cam design starts with integrating Equation (3.3). Equations (3.3) can also be written in the following form;

$$\frac{du_s}{d\alpha} F\left(u_s + s_t\right) = G\left(\alpha\right) \tag{4.10}$$

As long as Equation (4.10) stays the same, the integration of it will give the same $u_s\left(\alpha\right)$ variation, and remember from Section 3.2 that after this point the calculations will result in a unique cam profile. For example, scaling Equation (4.10) with a constant does not change the $u_s\left(\alpha\right)$ variation obtained so the cam that is designed for it stays the same. This idea has already been stated in Section 4.1.2 – *Note 2*.

Remember that the K value there was just scaling Equation (4.10). That is, if another linear spring with a different spring constant is used, the same cam will again give a quadratic torsion spring but with the coefficients scaled this time. Similarly adjusting something at F function and keeping Equation (4.10) the same, adjustable G functions can be obtained by using the same cam. This is the idea that the works at this section and at the following two sections are going to rely on.

Let's F and G functions be $F(\Delta x) = W$ and $G(\alpha) = A\alpha$. That is, the designed cam will transform a constant force function to a linear torsion spring. Keep in mind that a constant force function can be obtained with hanging weights. Inserting these two functions into Equation (4.10),

$$\frac{du_s}{d\alpha} W = A\alpha \tag{4.11}$$

or

$$\frac{du_s}{d\alpha} = \frac{A}{W}\alpha = \eta\alpha \tag{4.12}$$

where η is a constant. Solving the cam profile problem stated in Equation (4.12) with η is a constant, a specific cam profile is obtained. That cam profile will then have the following torsion spring behavior,

$$G(\alpha) = A\alpha = W\eta\alpha \tag{4.13}$$

Note that, the stiffness obtained includes W as a multiplier. Then, changing the weight that hangs down the string will have a tuning effect on the linear torsion spring obtained at the cam. The schematic of a sample design is given at Figure 4.16.

The cusp on the cam profile in Figure 4.16.a has a technical importance because the string must be attached to the cam at that cusp. And again observe how the string wraps around the upper part and the lower part of the cam when α is positive and negative respectively (Figures 4.16.b and 4.16.c).

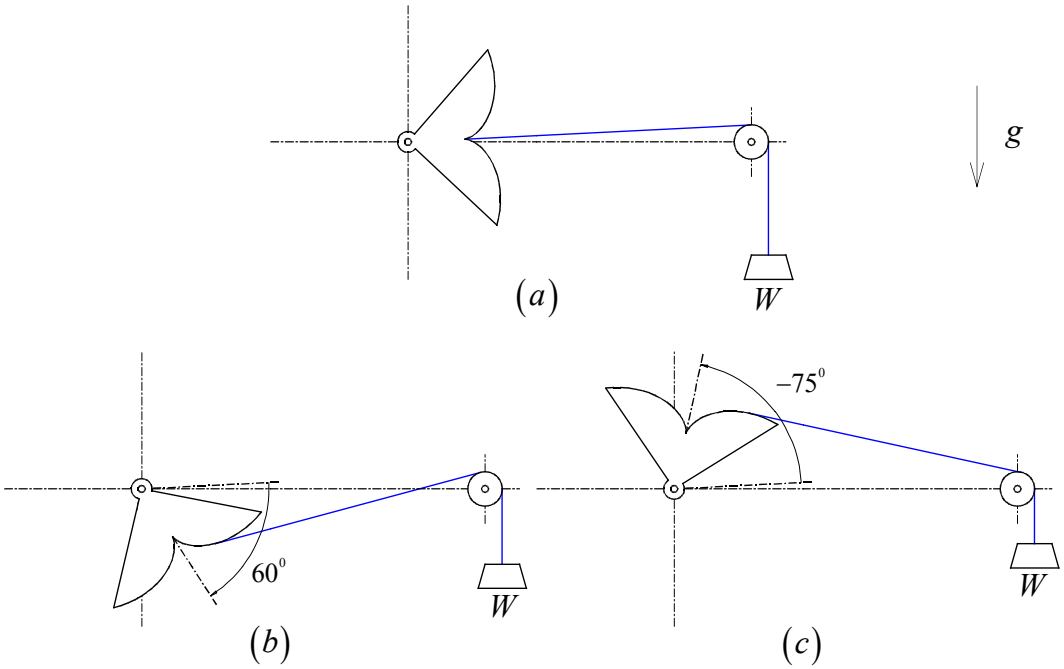

Fig.4.16: Mechanically adjustable linear torsion spring with hanging weights. The dimensions are $a = 0.1\,m$ *and* $r = -0.005\,m$. *The cam profile was calculated for* $\eta = 0.02$ *and with the limits* $-90^0 \le \alpha \le 90^0$. *Then, the corresponding torsion spring behavior is* $G(\alpha) = 0.02\,W\,\alpha$. *The cam is given at three configurations; (a) when* $\alpha = 0^0$, *(b) when* $\alpha = 60^0$ *and (c) when* $\alpha = -75^0$.

4.3 With an exponential characteristic spring

Let's turn back to Equation (4.10) again;

$$\frac{du_s}{d\alpha} F(u_s + s_t) = G(\alpha) \tag{4.10}$$

It was seen in Section 4.2 that if F function were a constant function, Equation (4.10) could be scaled and the scaling factor (it was the weight W there) turned out to be a tuning tool for the obtained linear torsion spring. The same idea can also work if the F function satisfies the identity given in Equation (4.14).

$$F(u_s + s_t) = h(s_t) \cdot F(u_s) \tag{4.14}$$

Remember that the exponential function satisfies this identity. Let's F and G functions be $F(\Delta x) = Ke^{L\cdot\Delta x}$ and $G(\alpha) = A\alpha$. Inserting these two functions into Equation (4.10),

$$\frac{du_s}{d\alpha} Ke^{L\cdot(u_s+s_t)} = A\alpha \tag{4.15}$$

or

$$\frac{du_s}{d\alpha} Ke^{L\cdot u_s} = \frac{A}{e^{L\cdot s_t}}\alpha = \eta\alpha \tag{4.16}$$

where η is a constant. Solving the cam profile problem stated in Equation (4.16) with η is a constant, a specific cam profile is obtained. That cam profile will then have the following torsion spring behavior,

$$G(\alpha) = A\alpha = e^{L\cdot s_t}\eta\alpha \tag{4.17}$$

Note that, the stiffness obtained includes $e^{L\cdot s_t}$ as a multiplier. Then, changing the pretension of the F function, "s_t", will have a tuning effect on the linear torsion spring obtained at the cam.

The mathematics is fine up to now. But is there a translation spring with an exponential spring characteristic? Not yet, but a string wrapping around cam mechanism can easily be design to realize it. In short, two cams will be designed through out the way. The design of mechanically adjustable linear torsion spring with an exponential characteristic spring is explained step by step as follows.

Step 1: First, an exponential characteristic torsion spring will be designed using string wrapping around cam mechanism. A sample design is given in Figure 4.17.

If the cam rotations are started to be measured from the horizontal axis, the cam will have the following torsion spring behavior (Figures 4.17.a and 4.17.b),

$$G_1(\alpha_1) = A_1 \times e^{B_1\alpha_1} \tag{4.18}$$

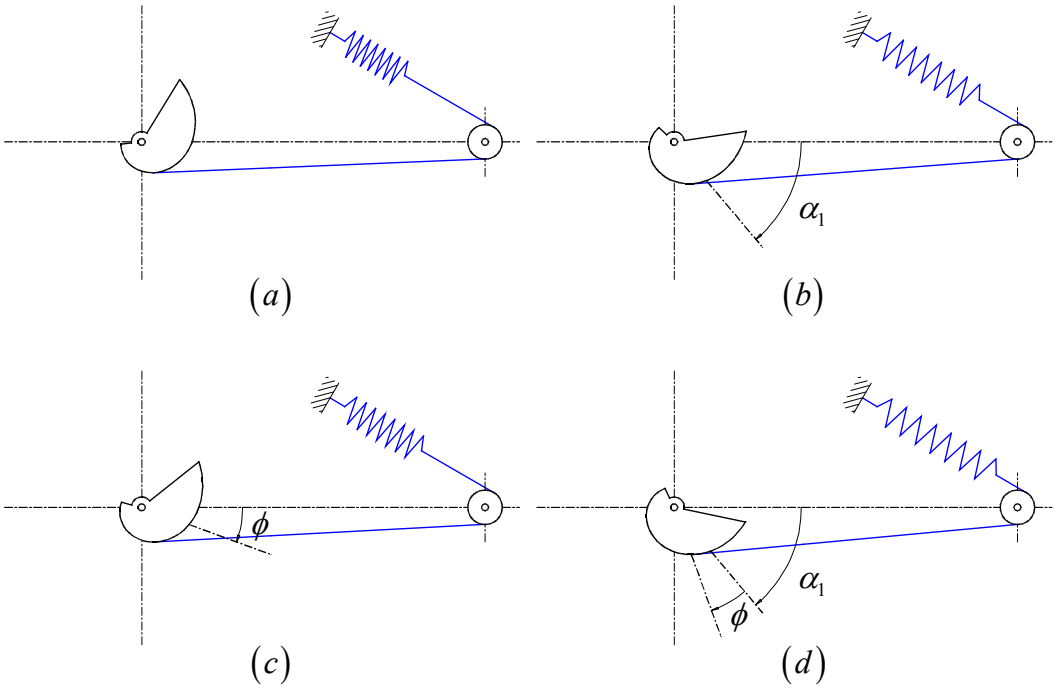

Fig.4.17: 1st cam design; exponential characteristic torsion spring. The dimensions are $a_1 = 0.1\,m$ *and* $r_1 = 0.005\,m$. *The cam profile was calculated for* $G_1(\alpha_1) = 0.04\,e^{0.8\alpha_1}$, $F_1(\Delta x_1) = 219.36\Delta x_1$ *and* $s_{t1} = 0.02\,m$. *The calculation limits are* $-90^0 \le \alpha_1 \le 120^0$. *The cam is given at four configurations; (a) when* $\alpha_1 = 0^0$, *(b) when* $\alpha_1 = 50^0$, *(c) when* $\phi = 20^0$ *and (d) when* $\phi = 20^0$ *and* $\alpha_1 = 50^0$.

If the cam is rotated by an angle of ϕ and the cam rotations are started to be measured from that new configuration, the cam is going to have the following torsion spring behavior (Figures 4.16.c and 4.16.d),

$$G_1(\alpha_1) = A_1 \times e^{B_1(\phi+\alpha_1)} = A_1\, e^{B_1\phi} \times e^{B_1\alpha_1} \tag{4.19}$$

Thus, the same spring characteristic behavior appears again, "$e^{B_1\alpha_1}$", but it is scaled with "$e^{B_1\phi}$" this time. In summary, exponential characteristic torsion spring is scaled with pre-tensioning its cam some amount and starting to measure the α_1 from that configuration. This property is in its nature.

Step 2: If this exponential characteristic torsion spring is desired to be used at a second cam design, it must be converted into a translational one first. That conversion can easily be made via a pulley attached to it (Figure 4.18). A string attached to that pulley will then have a translation spring characteristic as derived below.

$$\Delta s_2 = r_2 \alpha_1 \tag{4.20}$$

$$F_2\left(\Delta x_2\right) = \frac{G_1\left(\alpha_1\right)}{r_2} = \frac{A_1}{r_2} e^{B_1 \phi} \times e^{\frac{B_1}{r_2}\Delta x_2} \tag{4.21}$$

It is observed in Equation (4.21) that $e^{B_1\phi}$ still stays as a scaling factor.

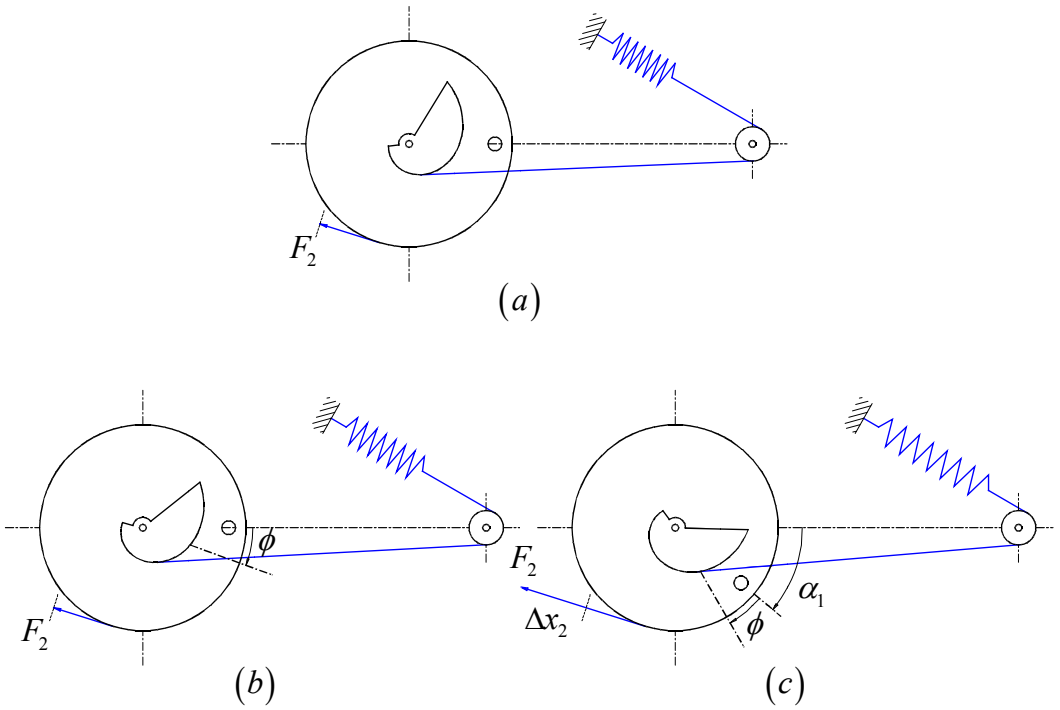

Fig.4.18: Exponential characteristic translation spring. It is obtained by attaching a $r_2 = 0.03\,m$ *radius pulley to the exponential characteristic torsion spring given in Figure 4.17. The system is given at there configurations; (a) when* $\phi = 0^0$ *and* $\alpha_1 = 0^0$*, (b) when the cam is rotated by* $\phi = 20^0$ *with respect the pulley and (c) when the cam-pulley assembly is rotated* $\alpha_1 = 40^0$*. The string attached to the pulley gives us the following translation spring characteristic;* $F_2\left(\Delta x_2\right) = 1.33\, e^{0.8\phi} \times e^{26.67\Delta x_2}$.

Step 3: Since an exponential characteristic translation spring in now available, it can readily be used in the second cam design. Let the F function be the $F(\Delta x_2)$ function given in Equation (4.21) and the G function that will be obtained be $G_2(\alpha_2) = A_2\alpha_2$. Inserting these two functions into Equation (4.10),

$$\frac{du_{s2}}{d\alpha_2}\frac{A_1}{r_2}e^{B_1\phi}\times e^{\frac{B_1}{r_2}u_{s2}} = A_2\alpha_2 \tag{4.22}$$

or

$$\frac{du_{s2}}{d\alpha_2}e^{\frac{B_1}{r_2}u_{s2}} = \frac{A_2}{\frac{A_1}{r_2}e^{B_1\phi}}\alpha_2 = \eta\alpha_2 \tag{4.23}$$

where η is a constant. Solving the cam profile problem stated in Equation (4.23) with η is a constant, a specific cam profile is obtained. That cam profile will then have the following torsion spring behavior,

$$G_2(\alpha_2) = A_2\alpha_2 = \frac{A_1}{r_2}e^{B_1\phi}\eta\,\alpha_2 \tag{4.24}$$

Then, adjusting the orientation of the first cam with respect to the second pulley, that is, "ϕ", will have a tuning effect on the linear torsion spring obtained at the cam as expressed in Equation (4.24). A sample design is given in Figure 4.19.

The logic of mechanically adjustable linear torsion spring using an exponential characteristic spring can be expressed in a different manner. As it was already expressed in *Step 1*, the exponential characteristic torsion spring is self-adjustable in nature, but with an exponential characteristic which does not have an apparent use. Then this spring can be converted into a linear torsion spring with a second string cam arrangement and the obtained linear torsion spring becomes an adjustable one just as the exponential torsion spring was.

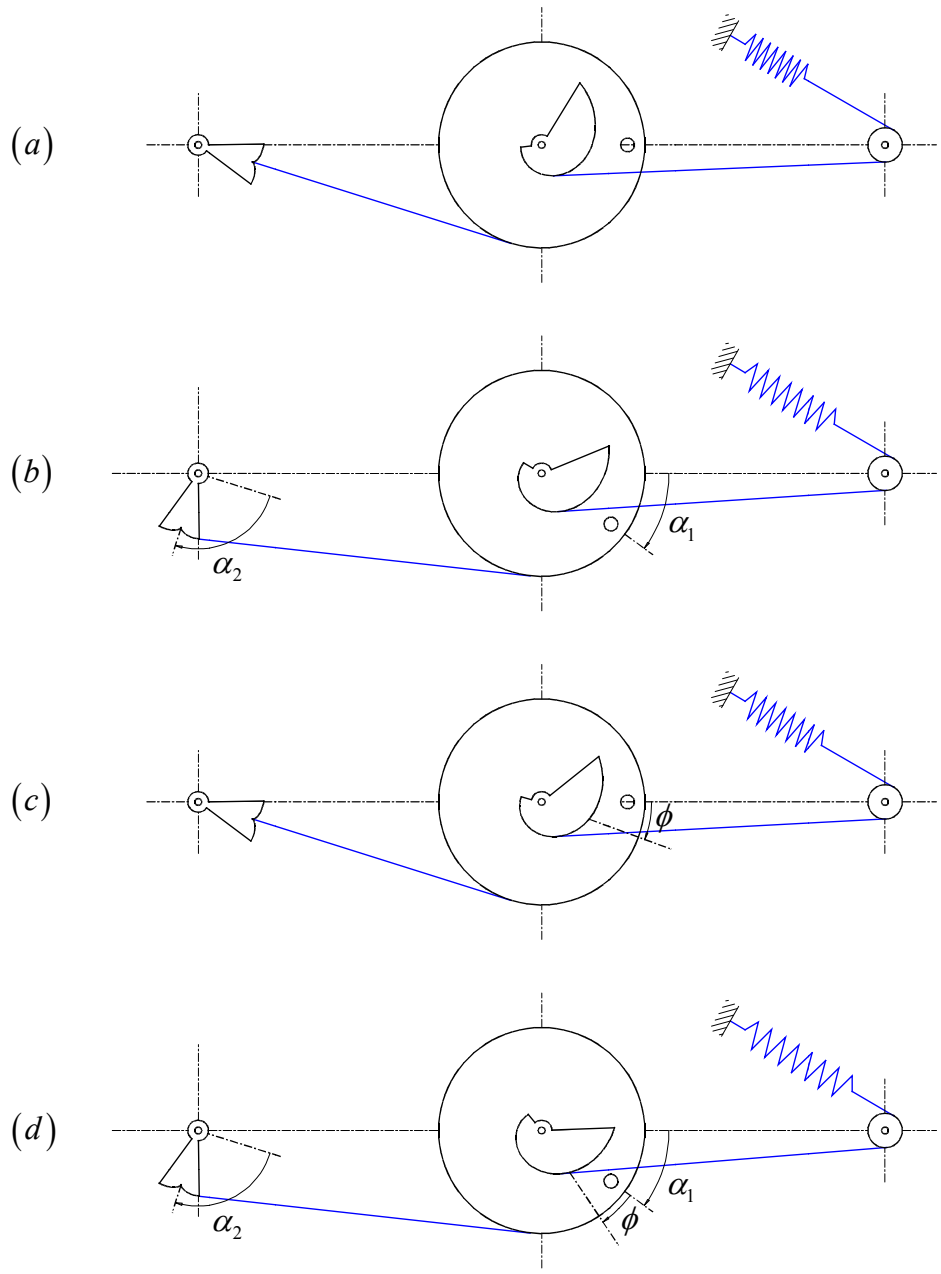

Fig.4.19: Mechanically adjustable linear torsion spring using an exponential characteristic translation spring. The exponential characteristic translation spring is the one given in figure 4.18. The remaining dimensions are $a_2 = 0.1\,m$ *and* $r_2 = 0.03\,m$. *The second cam profile was calculated for* $\eta = 0.02$. *Then, the corresponding torsion spring behavior is* $G_2(\alpha_2) = 0.02667\, e^{0.8\phi} \times \alpha_2$. *The calculation limits of the second cam are* $-90^0 \le \alpha_2 \le 90^0$. *The cam system is given at four configurations; (a) at the equilibrium position when* $\phi = 0^0$, *it corresponds to* $G_2(\alpha_2) = 0.02667 \times \alpha_2$ *(b) when the second cam is rotated* $\alpha_2 = 90^0$, *meanwhile the first cam rotates by an angle of* $\alpha_1 = 36.21^0$ *(c) at the equilibrium position when*

$\phi = 20^0$, it corresponds to $G_2(\alpha_2) = 0.03526 \times \alpha_2$ (d) when the second cam is rotated $\alpha_2 = 90^0$, meanwhile the first cam rotates by an angle of $\alpha_1 = 36.21^0$.

Note that the second pulley, the bigger one seen in Figure 4.18, never makes a full rotation. So, it can be made a pulley portion to make the whole system lighter and compact.

4.4 With a linear translation spring

Say, it has been calculated a cam profile for the given $G(\alpha)$, $F(\Delta x)$ and s_t. Then the question is; what is the new torsion spring characteristic that this cam profile will give if the F function is pre-tensioned differently then s_t? No doubt that the new spring characteristic changes with s_t, but can not it be calculated beforehand, that is, before calculating the cam profile himself? The answer is as follows.

Remember Equation (4.10) here again,

$$\frac{du_s}{d\alpha} F(u_s + s_t) = G(\alpha) \tag{4.10}$$

First integrate Equation (4.10) for the given $G(\alpha)$, $F(\Delta x)$ and s_t and find u_s. Note that, u_s function is quite specific to the cam geometry and does not change unless the cam surface changes. Then put the u_s function and the new pretension value into Equation (4.10) and find the new $G(\alpha)$ function.

Now it is clear how to calculate the new torsion spring characteristic occurring at the cam when the pretension is changed from the cam calculation values. So the new s_t value somehow makes the torsion spring characteristic obtained at the cam adjustable. Then the second critical question is; can not it be controlled? Can not it be made to give an adjustable linear spring for example? The answer is yes. But a

revolutionary move must be made first. Up to here, always u_s was calculated for the given $G(\alpha)$, $F(\Delta x)$ and s_t. What about calculating $G(\alpha)$ for the given u_s, $F(\Delta x)$ and s_t?

To see the adjustment effect of s_t on $G(\alpha)$ barely at the calculations, it is better u_s and s_t separable at $F(u_s + s_t)$ in Equation (4.10). The linear F function meets this requirement and Equation (4.10) becomes,

$$\frac{du_s}{d\alpha} K \cdot (u_s + s_t) = G(\alpha) \tag{4.25}$$

or

$$\frac{du_s}{d\alpha} K \cdot u_s + \frac{du_s}{d\alpha} K \cdot s_t = G(\alpha) \tag{4.26}$$

If an adjustable linear spring is desired,

$$\frac{du_s}{d\alpha} = \eta \cdot \alpha \tag{4.27}$$

where η is a constant.

Then integrate Equation (4.27) to find u_s. Keep in mind that $u_s(0) = 0$.

$$u_s = \frac{\eta}{2} \cdot \alpha^2 \tag{4.28}$$

Inserting Equations (4.27) and (4.28) into Equation (4.26)

$$K \frac{\eta^2}{2} \cdot \alpha^3 + s_t K \eta \cdot \alpha = G(\alpha) \tag{4.29}$$

So the adjustment effect of s_t on $G(\alpha)$ became linear but with the price of an excess cubic function. Fortunately it will not make a significant problem because

there is a very trivial routine to eliminate it. A second cam can easily be designed with the following spring characteristic,

$$-K\frac{\eta^2}{2}\cdot\alpha^3 = G_2(\alpha) \tag{4.30}$$

and can be used together with the cam of Equation (4.29). So the cubic terms cancel out and only the linear term remains.

$$s_t K\eta\cdot\alpha = G(\alpha) + G_2(\alpha) \tag{4.31}$$

For the cam profile that will have the torsion spring characteristic given in Equation (4.29), the cam problem must be solved for $G(\alpha) = K\frac{\eta^2}{2}\cdot\alpha^3$, $F(\Delta x) = K\Delta x$ and $s_t = 0$. It is interesting that the cam profile problem for $G(\alpha) = \eta\cdot\alpha$ and $F(\Delta x) = 1$ can also be calculated instead of it by observing Equation (4.27). Both equations result in the same u_s expressed in Equation (4.28) so will result in the same cam profile. In summary, the cam profile that converts a constant force function to a linear torsion spring also converts a linear translation spring to a cubic spring. Remember here that this problem have already been solved in Section 4.2. So exactly the same cam profile given in Figure 4.16 is going to be get if the η values are selected the same. A sample design is given in Figure 4.20.

A sample design for minus cubic behavior is shown in Figure 4.21.a. The cam profile has a cusp on it as had the cam profile given in Figure 4.20. That cam profile was easily actuated with one string only, but it is not possible for this case. A solution with two translation springs is shown in Figure 4.21.b. Observe how the strings wrap around two separate branches of the cam surface and also observe that when one of the strings produces a moment on the cam, the other produces zero moment.

The combination of the cam systems shown in Figures 4.20 and 4.21 is given in Figure 4.22.a. Since those cam surfaces are fixed to each other here, a one piece cam is obtained in return, yet it is actuated by three strings. Then the overall torsion

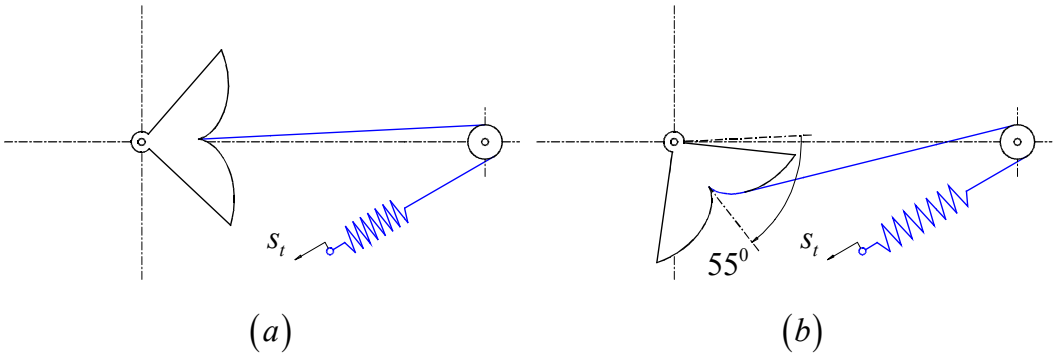

Fig.4.20: The cam profile was calculated for $G(\alpha)=K\frac{\eta^2}{2}\cdot\alpha^3$, $F(\Delta x)=K\,\Delta x$ *and* $s_t=0$ *where* $\eta=0.02$ *and* $K=219.36\ N/m$. *The remaining dimensions are* $a=0.1\,m$ *and* $r=-0.005\,m$. *The calculation limits are* $-90^0\le\alpha\le 90^0$. *The cam is given at two configurations; (a) at the equilibrium position (b) when* $\alpha=55^0$.

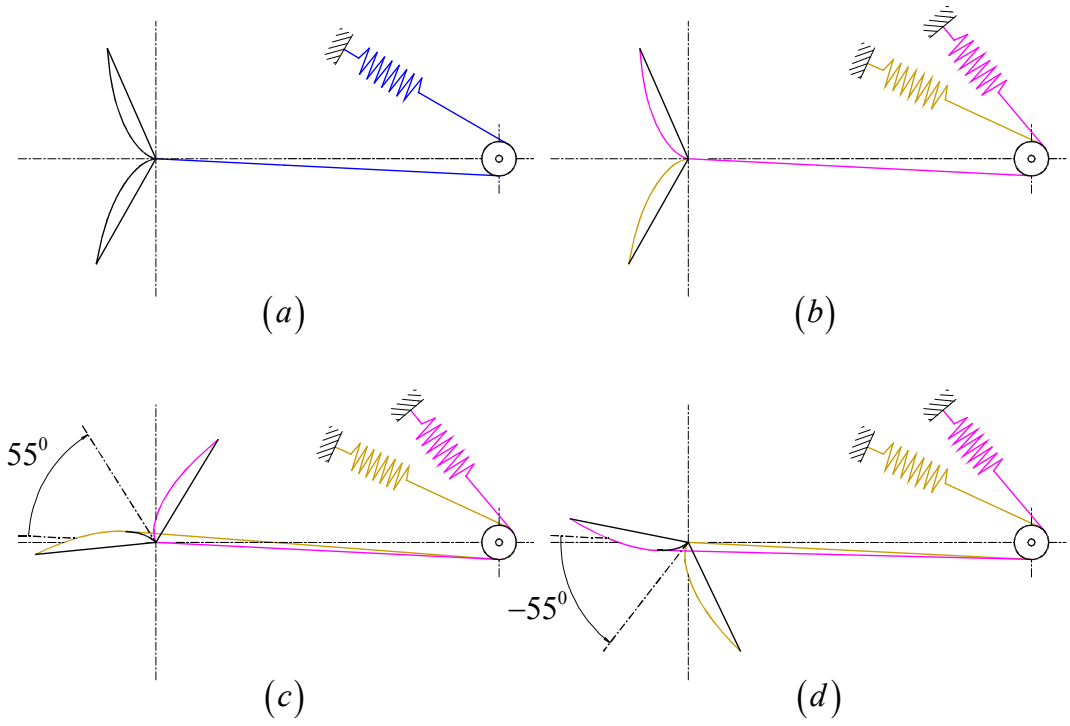

Fig.4.21: The cam profile was calculated for $G(\alpha)=-K\frac{\eta^2}{2}\cdot\alpha^3$, $F(\Delta x)=K\,\Delta x$ *and* $s_t=0.07$ *where* $\eta=0.02$ *and* $K=219.36\ N/m$. *The remaining dimensions are* $a=0.1\,m$ *and* $r=0.005\,m$. *The calculation limits are* $-90^0\le\alpha\le 90^0$. *(a) the cam profile himself (b) at the equilibrium position (c) when* $\alpha=55^0$ *(d) when* $\alpha=-55^0$.

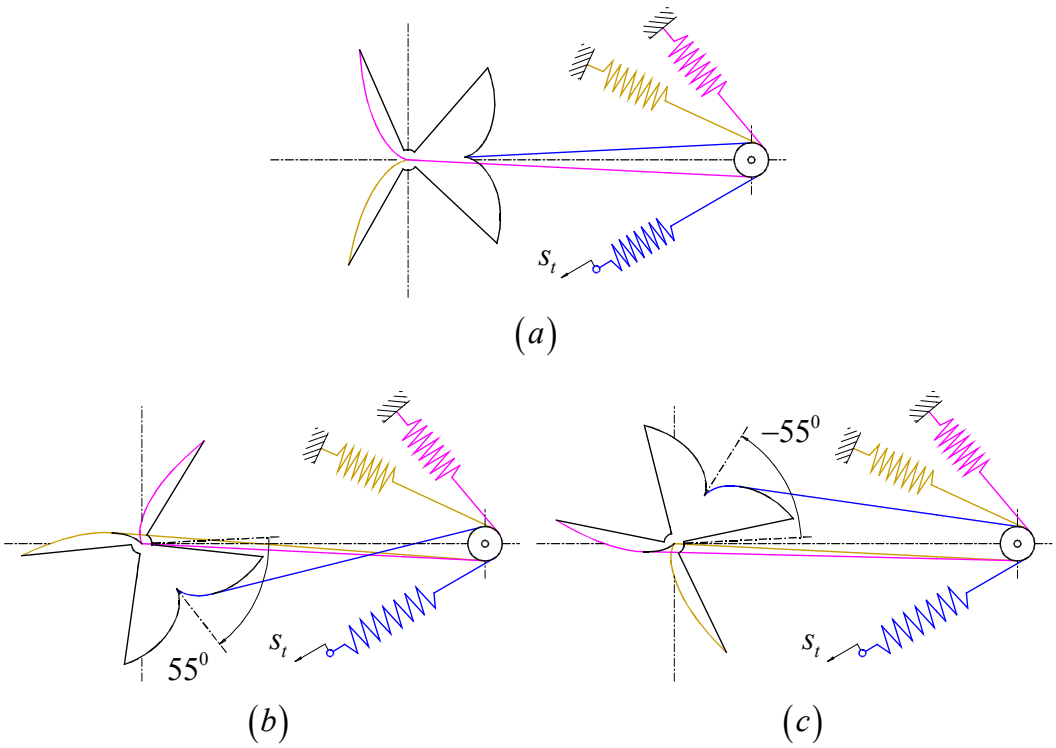

Fig.4.22: The cam profiles in Figures 4.20 and 4.21 together. The cam assembly has the linear spring characteristic $G(\alpha) = s_t K\eta \cdot \alpha$ *in total where* $\eta = 0.02$ *and* $K = 219.36\ N/m$. *The cam assembly is given at three configurations, (a) at the equilibrium position (b) when* $\alpha = 55^0$ *(c) when* $\alpha = -55^0$.

spring behavior occurring on this cam assembly becomes the one that is expressed in Equation (4.31). s_t appears as an apparent adjustment parameter. It is interesting to note here that, if s_t is selected zero, the overall moment that occurs on the cam assembly will be zero regardless of the orientation of that strange looking cam assembly. The cam assembly system is shown in two different deflected positions in Figures 4.22.b and 4.22.c.

4.5 General discussions

Four different ways of obtaining a mechanically adjustable linear torsion spring was explained in this chapter. They were obtained with the antagonistically working two quadratic springs, with hanging weights, with an exponential characteristic spring

and with a linear translation spring respectively. The main actors in action were always the string wrapping around cam mechanisms and they made it possible to get some critical non-linear spring characteristics with a striking simplicity.

The last three ways to obtain mechanically adjustable linear springs are distinguished from the first one in a very important sense. The antagonistically working two quadratic springs set-up can only be used to get adjustable linear spring characteristics. But the last three methods can also be designed to give us any adjustable characteristics wanted. At the hanging weights method, the G function can easily be selected as any other function than the linear function selected in Equation (4.11). At the exponential characteristic spring method, similarly the G_2 function can easily be selected as any other function than the linear function selected in Equation (4.22). Note here that, for this case, the designs made in *Step 1* and *Step 2* remain the same and only the cam designed in *Step 3* changes in Section 4.3. Finally, at the fourth method, the linear function selected in Equation (4.27) can easily be selected as different function and again an adjustable version of that different function can be obtained.

In this Chapter, all the mechanically adjustable linear torsion springs were realized designing string wrapping around cam mechanisms. It was stated in Section 3.2 that for the antagonistically working two quadratic springs method, some other mechanisms like the ones given in Figure 3.2 can be used to get quadratic springs. Similarly, the remaining three methods do not have to use string wrapping around cam mechanisms. Although the sample designs were always made using string wrapping around cam mechanisms, the mechanisms given in Figure 3.2 can also be used instead.

What about the stiffness adjustment capabilities of these 4 different mechanically adjustable linear spring methods? As it was mentioned in Section 4.1.3, the method with antagonistically working two quadratic springs can adjust the stiffneses even for negative values. Hanging weights method can give us stiffness at least zero or higher. The exponential spring method can not give us zero stiffness because $e^{B_1\phi}$ in

Equation (4.24) can never ever be zero or negative. So the lower and higher bounds of the stiffness are positive. The fourth method is similar to the hanging weights method, at least zero or higher but not negative stiffnesses.

The stiffness tuning mechanisms possible for the antagonistic set-up of two quadratic springs have already been discussed in Section 4.1.4. For the second method, such a mechanism is not required because the stiffness tuning is made by changing the weights. For the third case, the cam and the pulley shown in Figure 4.18 must be rotated with respect to each other to tune the stiffness. The mechanisms discussed for the antagonistic set-up of two quadratic springs can readily be used. For the last method, the stiffness is tuned by adjusting the pretension of a linear translation spring. It can be realized by the method of MACCEPA (Section 2.2.1), that is, a spool that the string attached to the linear translation spring rolls up.

At these four different methods, the equilibrium positions do not change with the stiffness adjustment. But, at the first case, if the two cams are not manufactured identical or the pretensions of the strings are not given the same, the equilibrium position will surely shift slightly. But for the remaining 3 methods, this is not a case. Even if the cams that were manufactured are unsatisfactory, the equilibrium positions would not be affected by that. Because the equilibrium positions are forced kinematically and not rely on the manufacturing quality.

Then the question is; which method is the best to obtain mechanically adjustable linear springs? Basically, it changes from application to application. For example, the second method does not suit to robotic applications but may be to physical therapy activities. But an important thing should be here. For robotic applications, the fourth method gives the least complicated mechanism although it uses a strange looking cam assembly. Because, there are less number of moving parts.

CHAPTER 5

CONCLUSIONS

At this thesis work, mechanically adjustable linear springs were discussed in detail. There are essentially three reasons why a reader will consult this thesis. The first one is the derivation made in Section 2.1 for the necessity of quadratic springs at antagonistically working two non-linear springs set-up. It was derived there that it was only when the non-linear springs were quadratic ones; the antagonistic set-up would give mechanically adjustable springs with perfect linearity in return and this was the unique solution. The second reason is the string wrapping around cam mechanism discussed in Section 3.2. The string wrapping around cam mechanism can be designed to get any non-linear spring characteristics and it provides this astonishing task with a very simple mechanical system. Remember that there were only two rotating parts; the cam and an optional pulley to guide the string. And may be this is our chance that there is a stepwise anlytical solution for the cam profile calculations. The third reason is the three new mechanically adjustable spring philosophies introduced in Sections 4.2, 4.3 and 4.4. These novel methods have a revolutionary importance; in the past, there were only the antagonistically working two quadratic springs set-up that can give adjustable springs with perfect linearity. Now there are three more. And they can easily be implemented designing string wrapping around cam mechanisms. As it was argued before, the author thinks that they are in fact the most important contribution to the subject cited at this thesis.

The objective of this thesis work was just presenting the design details of mechanically adjustable springs but not designing one of them for a specific task. But still, a prototype based on the antagonistically working two quadratic springs set-up was designed, manufactured and tested for adjustable linear spring behavior. The

nature of the mechanical system was perceived better and important rule of thumbs were given on the topic in Section 4.1.

REFERENCES

[1] Honda Motor Company, Ltd., http://world.honda.com/ASIMO/, last visited on August 2009.

[2] Sony Corporation, http://www.sony.net/SonyInfo/QRIO/, last visited on August 2009.

[3] McGeer, "Passive Dynamic Walking", *Int. J. Rob. Res*., Vol. 9, no.2 April 1990. pp. 62-82.

[4] Fujimoto Laboratory, Sano Laboratory, Nagoya Institute of Technology, http://drei.mech.nitech.ac.jp/~fujimoto/sano/walk_eng.html, last visited on August 2009.

[5] M. Garcia, A. Chatterjee, A. Ruina, and M. J. Coleman, "The simplest walking model: Stability, complexity, and scaling", *ASME J. Biomech. Eng.*, 120(2), pp. 281–288, April 1998.

[6] J.W. Hurst, J. Chestnutt and A. Rizzi, "Design and Philosophy of the BiMASC, a Highly Dynamic Biped", in *Proceedings of the IEEE International Conference on Robotics and Automation, April, 2007.*

[7] R.V. Ham, "Compliant Actuation for Biologically Inspired Bipedal Walking Robots", *Ph.D. Thesis*, Department of Mechanical Engineering, Vrije University, Brussels, Belgium, 2006.

[8] B. Vanderborgh, "Dynamic stabilization of the biped Lucy powered by actuators with controllable stiffness", *Ph.D. Thesis*, Department of Mechanical Engineering, Vrije University, Brussels, Belgium, 2007.

[9] Össur, http://www.ossur.com/prosthetics/feet/Vari-Flex-with-EVO, last visited on August 2009.

[10] S.K. Au, H. Herr, J. Weber and E.C. Martinez-Villapando, "Powered Ankle–Foot Prosthesis for the Improvement of Amputee Ambulation", *Proceedings of the 29th Annual International Conference of the IEEE EMBS*.

[11] K. W. Hollander, T. G. Sugar and D. E. Herring, "Adjustable Robotic Tendon using a 'Jack Spring'", *Proceedings of the 2005 IEEE, 9th International Conference on Rehabilitation Robotics*, June 28 - July 1, 2005, Chicago, IL, USA

[12] Department of Mechanical Engineering, Vrije University Brussel, http:// mech.vub.ac.be/multibody/publications/full_texts/clawar.pdf

[13] G. Tonietti, R. Schiavi and A. Bicchi, "Design and Control of a Variable Stiffness Actuator for Safe and Fast Physical Human/Robot Interaction", in *Proceedings of the 2005 IEEE, International Conference on Robotics and Automation*, Barcelona, Spain, April 2005.

[14] Arrow Vale Community High School, http://www.arrowvale.worcs.sch.uk/ sportscollege/muscles.htm, last visited on May 2009.

[15] The New York Times, http://www.nytimes.com/imagepages/2007/08/01/health/ adam/19089Tendonv-sligament.html, last visited on May 2009.

[16] N. Hogan, "Adaptive control of mechanical impedance by coactivation of antagonist muscles", *IEEE Trans. Automat. Control*, vol. 28, no. 8, pp. 681–690, August 1984.

[17] D. P. Ferris, M. Louie, and C. T. Farley, "Running in the real world: adjusting leg stiffness for different surfaces", in *Proc. R. Soc. Lond.*, vol. 265, January 1998, pp. 989–993.

[18] David Hawkins and Micheal Bey, "Muscle and tendon force-length properties and their interactions in vivo", in *J. Biomechanics*, Vol. 30, No. 1, pp. 63-70, 1997.

[19] R. Kirsch, D. Boskov and W. Rymer, "Muscle stiffness during transient and continuous movements of cat muscle: Perturbation characteristics and physiological relevance", *IEEE Trans. Biomed. Eng.*, vol. 41, no. 8, pp. 758–770, August 1994.

[20] S. A. Migliore, E. A. Brown and S. P. DeWeerth, “Biologically Inspired Joint Stiffness Control”, in *Proceedings of the 2005 IEEE, International Conference on Robotics and Automation*, Barcelona, Spain, April 2005.

[21] S. A. Migliore, E. A. Brown and S. P. DeWeerth, “Novel Nonlinear Elastic Actuators for Passively Controlling Robotic Joint Compliance”, *Journal of Mechanical Design*, Vol. 129, April 2007.

[22] J.W. Hurst, J.E. Chestnutt and A. Rizzi, “An Actuator with Physically Variable Stiffness for Highly Dynamic Legged Locomotion”, in *Proceedings of the 2004 International Conference on Robotics and Automation*, May, 2004.

[23] J.W. Hurst, “The Role and Implementation of Compliance in Legged Locomotion”, *Ph.D. Thesis*, The Robotics Institute, Carnegie Mellon University, Pittsburgh, Pennsylvania, USA, 2008.

[24] Nicholas P. Chironis, “Mechanisms, Linkages, and Mechanical Controls”, chapter Types of Noncircular Gears, pages 241–244. *McGraw Hill*, 1965.

[25] J. Yamaguchi and A. Takanishi, “Design of biped walking robots having antagonistic driven joints using nonlinear spring mechanism”, in *Proceedings of the 1997 IEEE/RSJ International Conference on Intelligent Robots and Systems*, vol. 1, Grenoble, France, September 1997, pp. 251–259.

[26] K. Koganezawa, Y. Watanabe and N. Shimizu, “Antagonistic muscle-like actuator and its application to multi-d.o.f. forearm prosthesis”, *Adv. Robotics*, vol. 12, no. 7,8, pp. 771–789, 1999.

[27] R. V. Ham, B. Vanderborght, B. Verrelst, M. V. Damme and D. Lefeber, “MACCEPA: the Mechanically Adjustable Compliance and Controllable Equilibrium Position Actuator used in the Controlled Passive Walking Biped Veronica”, in *Proceedings of the 15th International Symposium on Measurement and Control in Robotics*, 2005.

[28] T. Morita and S. Sugano, “Design and Development of a new Robot Joint using a Mechanical Impedance Adjuster”, *IEEE International Conference on Robotics and Automation*, 1995.